Aus der Klinik für Gynäkologie mit
Schwerpunkt gynäkologische Onkologie
der Medizinischen Fakultät Charité - Universitätsmedizin Berlin

DISSERTATION

Investigation of ALDH^{bright} Cancer Stem (-like) Cell-targeted Treatment by Cisplatin and all-trans Retinoic Acid in Cervical Cancer Cell Lines

Zur Erlangung des akademischen Grades
Doctor medicinae (Dr. med.)
vorgelegt der Medizinischen Fakultät
Charité - Universitätsmedizin Berlin
von

Jinfeng Xu
aus Anhui, China

Datum der Promotion: 20.10.2020

CONTENTS

LIST OF TABLES

LIST OF FIGURES

ABSTRACT

Background: As the mainstay of chemotherapy, cisplatin has been increasingly adopted in cervical cancer treatment. However, cisplatin is not sufficient to eradicate all cancer cells, due to the existence of cancer stem (-like) cells (CSCs). ALDH is a marker of CSCs, as well as the speed-limiting enzyme in the cellular metabolism of ATRA. The impacts of cisplatin or/and ATRA on ALDH might offer useful information for the treatment of cervical cancer.

Methods: A 3-dimensional cell culture method was employed to generate spheroid- derived cells (SDCs) from three cervical cancer cell lines (HeLa, MRIH186, and SiHa). An Aldefluor kit was used for sorting of $ALDH^{bright}$ and $ALDH^{low}$ cells. Furthermore, the frequency of $ALDH^{bright}$ cells was determined by this assay in SDCs after treatment with cisplatin or/and ATRA. The mRNA profile of CSC-related markers was concomitantly observed by quantitative real-time PCR. The stemness, apoptosis ratio, invasiveness, and motility of cells were assessed by colony formation assay, Annexin-*V*/Propidium iodide assay, invasion assay, and scratching assay, respectively.

Results: This study confirmed that $ALDH^{bright}$ cells possess enhanced CSC-related properties compared to $ALDH^{low}$ cells, especially in drug resistance. SDCs contained an increased proportion of $ALDH^{bright}$ cells compared to traditional monolayer-derived cells (1.85 to 5.12-fold; $p < 0.05$). The $ALDH^{bright}$ population of SDCs responded to serial titrated concentration of cisplatin in a bi-phasic manner. Low-dose cisplatin (lower than 1 μM in HeLa and SiHa, and 3 μM in MRIH186) augmented the proportion of $ALDH^{bright}$ cells to 30.32 % in HeLa, to 62.44% in MRIH186, and to 55.21% in SiHa, which was about 1.83-fold, 1.67-fold, and 2.04-fold of their untreated control (all, $p < 0.05$), respectively. An increase of cisplatin concentration led a reduced proportion of $ALDH^{bright}$ cells. The $ALDH^{bright}$ population was inhibited by ATRA in a dose-dependent way. ATRA overcame the increased $ALDH^{bright}$ population in SDCs derived from HeLa, MRIH186 and SiHa. Additionally, ATRA partially counteracted other adverse effects caused by low-dose cisplatin, such as the augments in stemness, invasiveness, and cellular motility.

Conclusions: Consistently, low-dose cisplatin increases the $ALDH^{bright}$ population in SDCs derived from cervical cancer cell lines. ATRA presents the ability to reverse the increased $ALDH^{bright}$ population and the concomitant CSC-related effects caused by cisplatin. Inhibition of ALDH activity by ATRA might be beneficial for cervical cancer treatment by cisplatin.

ZUSAMMENFASSUNG

Hintergrund: Als Hauptstütze der Chemotherapie wurde Cisplatin zunehmend in der Behandlung von Gebärmutterhalskrebs eingesetzt. Cisplatin reicht jedoch nicht aus, um alle Krebszellen zu vernichten, da es Krebsstammzell (-ähnliche) gibt (CSC). ALDH ist ein Marker für CSCs sowie das geschwindigkeitsbegrenzte Enzym im Zellstoffwechsel von ATRA. Die Auswirkungen von Cisplatin oder/und ATRA auf ALDH könnten nützliche Informationen für die Behandlung von Gebärmutterhalskrebs liefern.

Methoden: Eine 3-dimensionale Zellkulturmethode wurde eingesetzt, um aus drei zervikalen Krebszelllinien (HeLa, MRIH186 und SiHa) sphäroid-abgeleitete Zellen (SDCs) zu erzeugen. Das Aldefluor-Kit wurde für die Sortierung von $ALDH^{bright}$- und $ALDH^{low}$-Zellen verwendet. Darüber hinaus wurde die Häufigkeit der $ALDH^{bright}$-Zellen durch diesen Assay in SDCs nach der Behandlung mit Cisplatin oder/und ATRA bestimmt. Das mRNA-Profil von CSC-spezifischen Markern wurde gleichzeitig durch quantitative real time-PCR untersucht. Der Stammzellcharaktor Steifheit, das Apoptose verhalten, die Invasivität und die Motilität der Zellen wurden durch Koloniebildungs-assay, Annexin-*V*/Propidiumiodid-assay, Invasions-assay, und Scratch-assay bewertet.

Ergebnisse: Diese Studie bestätigte, dass $ALDH^{bright}$-Zellen verbesserte CSC-spezifische Eigenschaften aufweisen als $ALDH^{low}$-Zellen, insbesondere bei Resistanzen gegen Therapeutika. Die SDCs enthielten einen erhöhten Anteil an $ALDH^{bright}$-Zellen im Vergleich zu herkömmlichen ,,monolayer‘‘-abgeleiteten Zellen (1,85 bis 5,12-fach; $p < 0,05$). Die $ALDH^{bright}$-Population der SDCs reagierte auf die seriell titrierte Konzentration von Cisplatin in zweiphasiger Weise. Niedrig dosiertes Cisplatin (niedriger als 1 µM in HeLa, und SiHa und 3 µM in MRIH186) erhöhte den Anteil der $ALDH^{bright}$-Zellen auf 30,32 % in HeLa, 62,44 % in MRIH186 und 55,21 % was in SiHa, das etwa 1,83-fach, 1,67-fach und 2,40-fach ihrer unbehandelten Kontrolle war (alle, $p < 0,05$). Eine Erhöhung der Cisplatin Konzentration führte zu einem reduzierten Anteil an $ALDH^{bright}$-Zellen. Die $ALDH^{bright}$ Zellpopulation wurde durch ATRA in einer dosisabhängigen Weise gehemmt. ATRA Behandlung verringerte die erhöhte $ALDH^{bright}$-Zellpopulation in SDCs, die von HeLa, MRIH186 und SiHa stammten. Darüber hinaus wirkte ATRA teilweise auch

anderen Nebenwirkungen entgegen, die durch niedrig dosiertes Cisplatin verursacht wurden, wie z.B. die Erhöhung der Stammzelleigenschaften, Invasivität und zellulären Beweglichkeit.

Schlussfolgerungen: Durchgängig erhöht niedrig dosiertes Cisplatin die $ALDH^{bright}$-Zellpopulation in SDCs, die aus Gebärmutterhalskrebs-Zelllinien stammen. ATRA bietet die Möglichkeit, die erhöhte $ALDH^{bright}$-Population und die damit verbundenen CSC-bezogenen Effekte, die durch Cisplatin verursacht werden, umzukehren. Die Hemmung der ALDH-Aktivität durch ATRA könnte für die Behandlung von Gebärmutterhalskrebs von Vorteil sein.

ABBREVIATIONS AND ACRONYMS

Units

bp	Base pair
cm^2	Square centimeter
g	Gram
h	Hour
kb	Kilo base-pair
mg	Milligram
min	Minute
ml	Milliliter
nM	Nanomolar
rpm	Rotations per minute
sec	Second
U	Unit
µL	Microliter
µM	Micromolar
µm	Micrometer
%	Percent
℃	Degree Celsius

Others

2-D	2-dimensional
3-D	3-dimensional
9-cis RA	9-cis retinoic acid
ABC	ATP-binding cassette transporter
ALDH	Aldehyde dehydrogenase
ATRA	All-trans retinoic acid
BAAA	BODIPY amino-acetaldehyde
bFGF	Basic fibroblast growth factor

BSA	Bovine serum albumin
CD	Cluster of differentiation
C/EBPb	CCAAT/enhancer-binding protein
CFE	Colony formation efficiency
CI	Combination Index
CIN	Cervical intraepithelial neoplasia
CO_2	Carbon dioxide
CSC	Cancer stem (-like) cell
DEAB	Diethylaminobenzaldehyde
DMEM	Dulbecco's modified Eagled medium
DNA	deoxyribonucleic acid
EC_{50}	Half maximal effective concentration
ECM	Extracellular matrix
EDTA	Ethylene diaminetetra acetic acid
e.g.	exempli gratia
EGF	Epidermal growth factor
EGFR	Epidermal growth factor receptor
et al.	et aliae
FACS	Fluorescence activated cell sorter
FBS	Fetal bovine serum
FIGO	International Federation of Gynecologists and Obstetricians
FITC	Fluorescein isothiocyanate
FL	Fluorescence channel
FSC	Forward scatter
GADD	growth arrest- and DNA damage-inducible gene 153
GAP-DH	Glyceraldehyde-3-phosphate dehydrogenase
HPV	Human papillomavirus
IC_{50}	Half maximal inhibitory concentration

i.e.	id est
IHC	immunohistochemistry
MDCs	Monolayer derived cells
MFI	Mean fluorescence intensity
NACT	Neoadjuvant chemotherapy
NAD	Nicotinamide adenine dinucleotide
NADPH	Nicotinamide adenine dinucleotide phosphate
Oct3/4	Octamer-binding transcription factor 4
PBS	Phosphate buffered saline
PCR	Hematopoietic stem cells
PI	Propidium iodide
RA	Retinoic acid
RAR	Retinoic acid receptor
RARE	Retinoic acid response element
RNA	Ribonucleic acid
ROS	Radical oxygen species
SD	Standard deviation
SDCs	Spheroids derived cells
SFE	Spheroids formation efficiency
Sox2	Sex-determining region-box2
SSC	Side scatter
TE	Trypsin/EDTA
TFs	Transcription factors
TSC	Tissue stem cells
TZ	Transformation zone
vs.	versus

1. Introduction

Despite many outstanding methods, such as cytological screening and HPV detection, which have been dedicated to reducing the disease burden, cervical cancer remains a major cause of mortality in women worldwide [1]. The failure of cervical cancer treatment might be due to the existence of cancer stem (-like) cells (CSCs) which are cancer initiating, sustaining, and therapy resistant (e.g. chemo- and radiotherapy) [2]. Cisplatin is currently used in therapeutic approaches for cervical cancer in neoadjuvant, concomitant (chemo-radiotherapy), or adjuvant chemotherapy. Given the increasing application of cisplatin in cervical cancer treatment, the response of cervical cancer cells and cervical CSCs to cisplatin should be deciphered in more detail.

Aldehyde dehydrogenase (ALDH) is a group of evolutionarily conserve enzymes, which are capable of oxygenizing aldehyde to its corresponding acid. Accumulation of ALDH activity has been highlighted by its roles in resistance to chemotherapy and in the enrichment of CSCs [3, 4]. ALDH-targeting approaches might represent a promising direction for cancer treatment [5]. All-trans retinoic acid (ATRA), a downstream product of ALDH, has been reported as a potential ALDH inhibitor [1, 3, 6-8]. Moreover, ATRA has been tested in numerous malignancies for its anti-cancer effects. Therefore, the present study intends to describe ALDH activity in cervical cancer cells and their potential responses to cisplatin or/and ATRA treatment. The background of this study can be further introduced by addressing the following questions: (1) what is the recurrent understanding of cervical CSCs? ; (2) What is the function of ALDH and ATRA in stem cells or in CSCs? ; (3) Why is cisplatin getting increasingly important for cervical cancer treatment? ; (4) What is the implication of CSCs for cervical cancer therapy?

1.1 Introduction to current knowledge on cervical CSCs

1.1.1 Cervical CSCs and their unique properties

CSCs share important features with normal tissue stem cells (TSCs), including the capacity of self-renewal and asymmetric division [9, 10]. However, it is still controversially discussed whether CSCs are the direct descendants of mutated TSCs, or developed from more differentiated cells that reacquire stem cell properties during tumorigenesis [9]. Cervical cancer might be an exception to this argument. It has been established that human papillomavirus (HPV) is the

etiologic agent for cervical cancer development [11, 12]. According to the strict tissue tropism of the HPV life cycle, the basal or reserve cells (i.e. TSCs) in the cervical epithelium were identified as the target of HPV infection and the origin of cervical cancer [13]. Although HPV is also the etiologic agent of many other tumors derived from different epithelia, HPV preferably induces carcinogenesis at the cervix with an approximately 20-fold higher risk than in other tissues [14]. The incidental discrepancy has been proven by Herfs et al. to be attributable to some reserve cells exhibiting multi-potency as the residual of embryonic cells located in the transformation zone (TZ) (Figure 1) [15, 16]. These immature cells possess a self-renewal ability by asymmetric division that is a property of stem cells. Therefore, the embryonic reserve cells infected by HPV may directly give rise to CSCs [15].

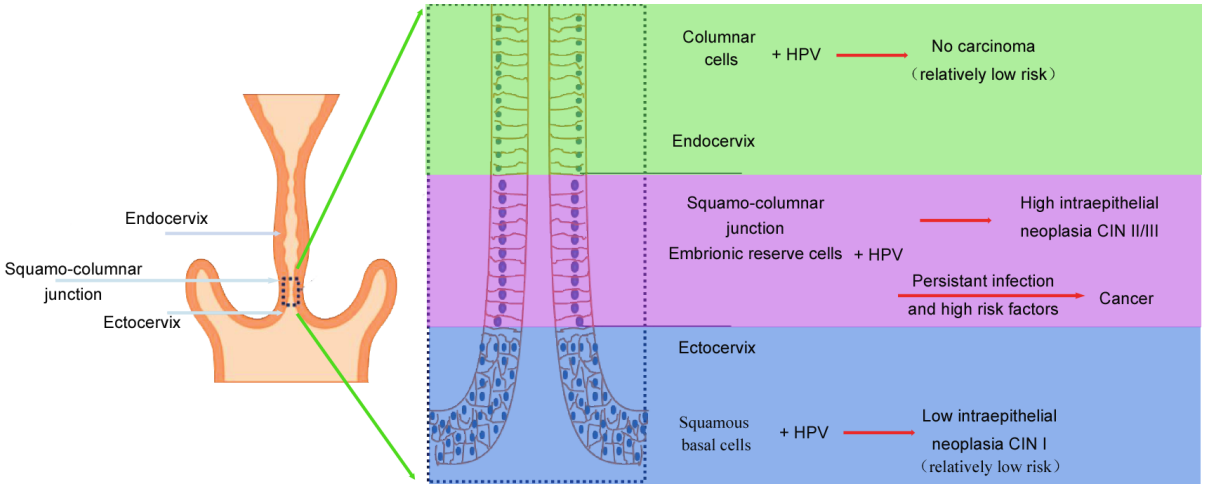

Figure 1: Illustration of cervical carcinogenesis and cells of of cervical cancer origin. *High-grade cervical intraepithelial neoplasia (CIN) and cervical carcinomas are usually generated within a specific cell population that is located in the squamo-columnar junction of the cervix. They are typically not generated in the columnar cells in the endo-cervix and squamous cells in the ecto-cervix. HPV-related CINs and cervical cancers maintain the genetic profile of the junction cells, indicating their cellular hierarchy. Reserve cells located in the TZ infected with carcinogenic HPV form pre-malignant neoplastic stem cells that can progress to CSCs, which reproduce cervical carcinoma clones.*

1.1.2 Embryonic transcription factors (TFs) are important CSC-related markers

The similarities shared between TSCs and CSCs include shared gene expression regulation, in

particular the encoding transcription factors (TFs) [17]. Previous studies highlighted a group of TFs, i.e. Sox2, Oct3/4, and Nanog, which maintain the pluripotency and self-renewal capacity of embryonic stem cells [18]. In the embryonic stem cells, reduction of Sox2 expression is linked to loss of the pluripotent state [19]. Some early events in carcinogenesis are under the control of Sox2 in the cervix. Sox2 regulates the HPV life cycle by the interaction with the target gene sequences located in the HPV genome [20, 21]. Over-expression of Sox2 is found in the stem cell-like cells situated in the TZ, and Sox2 can cooperate with HPV oncoproteins by retarding cellular damage which allows viral persistence [21]. Cervical cancer with high Sox2 expression is more poorly differentiated, indicating that Sox2 is a marker of undifferentiated cells [17, 22]. Sox2 also plays a role as a protector, as it shields cells from apoptosis with the help of Oct3/4 and Nanog [23, 24]. Oct3/4 is involved in the E7 oncoprotein pathway, and its expression is negatively related to prognosis in cervical cancer [17, 25]. The Nanog level is higher in cervical cancer compared to normal cervical epithelium [26]. One possibility is that Nanog is suppressed by p53, which is inactivated by E6 in cervical cancer. As a consequence of HPV infection, the stemness of reserve cells may be restrained by HPV oncoproteins in the process of cancer development. In fact, these TFs are CSC-related biomarkers (CSC-markers) and play a role in maintaining the biological behavior of cervical CSCs [2, 17].

1.2 The function of ALDH and ATRA in stem cells and in CSCs

Research focusing on CSC-markers has been expanded from the study of TFs to signaling pathways and the functional features shared between embryonic stem cells and CSCs. ALDH is a group of evolutionarily conserved enzymes which play important roles in embryonic development [27, 28]. The distribution of ALDH subtypes contributes to gradients of Retinoic acids (RA) in tissues, which is essential for mammals, especially in the control of embryonic development. The natural form *in vivo* is essentially all-trans RA (ATRA) and negligible levels of 9-cis RA. Among numerous subtypes of ALDH enzymes, ALDH1 and ALDH8 mainly play a role in ATRA and 9-cis retinoic acid biosynthesis, respectively [29, 30]. Lack of vitamin A (retinol) causes vitamin A deficiency syndrome, leading finally to a lethal outcome that can be prevented by an ATRA replacement. A consistent pattern of ATRA effect on ALDH1 gene expression was seen in

embryos, where treatment with ATRA resulted in significant suppression of ALDH1 transcripts [6-8, 30]. A well-balanced ALDH/RA signaling pathway is essential for the correct developmental program in cells.

In addition to its roles during the embryonic period, ALDH is also a maker of stem cells in adulthood. The Aldefluor assay, which labels cells with high ALDH content, was initially designed to isolate hematopoietic stem cells from blood by staining cells with high ALDH enzymatic activity [31]. Stem cells identified and isolated by the Aldefluor assay have been expanded in regenerative medicine, such as for acceleration of tissue repair [32, 33]. It is proposed that the role of ALDH in normal stem cells is in the context of self-protection. This self-protective property is shared by CSCs that contain a high-level cytoplasmic ALDH expression. The accumulation of ALDH confers chemo-resistance and radio-resistance in CSCs. ALDH endows CSCs with chemo-resistance basically by acting as scavenger of cytotoxic reagents [3]. As a radio-resistance related gene in cervical cancer, the ALDH gene was screened out in 23,040 human cDNAs by cDNA microarray analysis [34]. In summary, ALDH exerts a potent role in ATRA generation and also has various functions in both TSCs and CSCs [3, 35].

In cervical embryonic cells, the vitamin A signaling pathway also maintains the differentiation progress [36]. In addition, ATRA participates in the inhibition of telomerase activity and in down-regulation of HPV oncoproteins [37, 38]. It is notable that patients suffering from cervical cancer show reduced serum ATRA concentrations, which makes them more vulnerable to cervical cancer development [39]. As such, the ALDH/RA signaling pathway is potentially a modulating factor in cervical cancer. Moreover, cervical $ALDH^{bright}$ cells are more resistant to cisplatin treatment than the $ALDH^{low}$ cells [40]. ALDH expression is also responsible for the abilities of tumori-genicity, migration, and self-renewal ability in cervical CSCs [40]. $ALDH^{bright}$ cells are identified with stronger CSC-properties compared to $ALDH^{low}$ cells in cervical cancer cell lines and primary tissues [40]. Thus, high ALDH activity may represent a functional marker for CSCs and consequently be a logical target for cervical CSC-targeting therapy. The studies on ALDH in cervical cancer are summarized in Table 1.

Table 1: Available studies on ALDH in cervical cancer

Study references	*General study purpose*	*Origin (cell lines or primary tissue)*	*CSCs referred*	*Methods for ALDH detection*
[41]	*Micro RNA and ALDH1A1 relationship*	*HeLa, SiHa, and other cell lines*	*Yes*	*PCR*
[42]	*Diagnostic value of ALDH in cervical cancer*	*Human serum*	*NO*	*Spectrofluoro-photometer*
[43]	*Identify and characterize CSCs population*	*CaSki*	*Yes*	*Western blot*
[44]	*Observation of a biomarker*	*CaSki*	*Yes*	*Aldefluor assay*
[45]	*Observation of protein expression*	*CaSki and SiHa*	*Yes*	*Aldefluor assay*
[44]	*Observation of drug effects*	*C33a and SiHa*	*Yes*	*Aldefluor assay*
[46]	*ALDH as a prognostic marker*	*Patients' tissue*	*No*	*IHC*
[47]	*Characterization of cervical CSCs*	*HeLa, SiHa, and other cell lines*	*Yes*	*Aldefluor assay*
[48]	*ALDH as a prognostic marker in cervical cancer*	*Patients' tissue*	*No*	*IHC*
[49]	*Immunotherapy of CSCs*	*CaSki*	*Yes*	*Aldefluor assay*
[50]	*Evaluation of a new liposomal formulation*	*HeLa and ME180*	*Yes*	*Aldefluor assay*
[23]	*ALDH as a marker of cervical CSCs*	*C33a, SiHa, other cell lines, and patient tissue*	*Yes*	*Aldefluor assay, IHC, Western blot*
[51]	*The expression of ALDH1 in cervical cancer*	*HeLa, SiHa, other cell lines, and patient tissue*	*Yes*	*Aldefluor assay, IHC, Western blot*
[52]	*Characterization of cervical CSCs*	*A431, SiHa, and other cell lines*	*Yes*	*Aldefluor assay*
[34]	*Radiation sensitivity of cervical cancer*	*Patient tissue*	*No*	*cDNA Microarray analysis*
[53]	*Chemo-sensitivity*	*HeLa*	*No*	*Western blot*

1.3 Cisplatin is getting increasingly important for cervical cancer treatment

Due to screening programs, developed countries such as the USA and European countries have had a sharp decrease in the incidence of, and mortality from, cervical cancer. However, cervical cancer is still the leading cause of cancer-related deaths in women in developing countries [1]. Worldwide, the treatment of cervical cancer is mainly dictated by its FIGO stage [54]. A general consensus has been established: for the early stages, either surgery or radiation combined with chemotherapy can be used; for later stages, radiation combined with chemotherapy is usually the primary treatment; chemotherapy is often an option for advanced and recurrent cervical cancer (summarized in Table 2). However, the final decision is not only stage-dependent but also dependent on available resources, especially in low-resource regions [1].

Table 2: Overview of staging and therapeutic options for cervical cancer

Staging		***Possible therapeutic options (single or combined depending on individual patient's extent of disease)***					
				Chemotherapy			
Staging (in brief)	*FIGO Staging*	*Radical surgery*	*Radical radiation*	*Con-current*	*NACT*	*Adjuvant*	*Palliative*
Early stages	*Ia*	√	√				
	Ib	√	√		√[1]		
	IIa	√	√		√[1]		
	IIb	√	√	√	√[1]		
Locally-advanced stages	*IIIa*		√	√			
	IIIb		√	√			
	IVa		√	√			
Advanced stage	*IVb*						√[2]
Recurrence	*Recurrence*						√[2]

√[1]: No consensus has been achieved, but NACT is commonly used in fertility-sparing cases to reduce the risk of cancer recurrence.√[2]: The palliative strategy is chemotherapy-based, individual-dependent, and comprehensive.

New developments have been expanding the application of cisplatin against cervical cancer in terms of neoadjuvant, concurrent, and adjuvant chemotherapy. Radiotherapy alone was

historically the standard treatment for locally-advanced cervical cancer. Since 1999, cisplatin-based concomitant chemo-radiation has taken the place of radiation alone, with an improvement of 12% in overall survival [55]. Additionally, it is supposed that neoadjuvant chemotherapy (NACT) might offer some advantages such as reduction of tumor size, elimination of micro-metastasis, and diminishing of tumor expansion [56]. Despite the controversy about a better prognosis, the use of NACT followed by radical surgery is a valid option for locally-advanced cervical cancer, especially in regions with limited access to radiation therapy [54, 57]. Moreover, NACT might be a valuable option for many young patients in need of fertility sparing therapy. Cervical cancer is most frequently diagnosed among women aged at 35-44, and almost half of cervical cancer patients are of the reproductive age in the USA and in Britain (Figure 2). Notably, the incidence of cervical cancer is increasing in young women, which might be as a consequence of the screening programs [58, 59]. Fertility preservation must be a consideration for the treatment plan in this population. It is estimated that more than 40% of patients who undergo a radical hysterectomy are eligible for fertility-sparing surgery [60]. With the goal of maintaining fertility options, but without sacrificing oncological outcomes, NACT might be an optional compensation to confine the recurrence risk in terms of a less radical procedure [61]. Accordingly, as the most effective reagent, cisplatin has been increasingly applied in cervical cancer therapy. Efforts have been made for the optimization of cisplatin usage in cervical cancer. However, there are still numerous problems requiring further investigation, such as the prognosis after NACT and the optimized dose of cisplatin [62]. To answer these questions, experimental work would be supplementary to clinical trials.

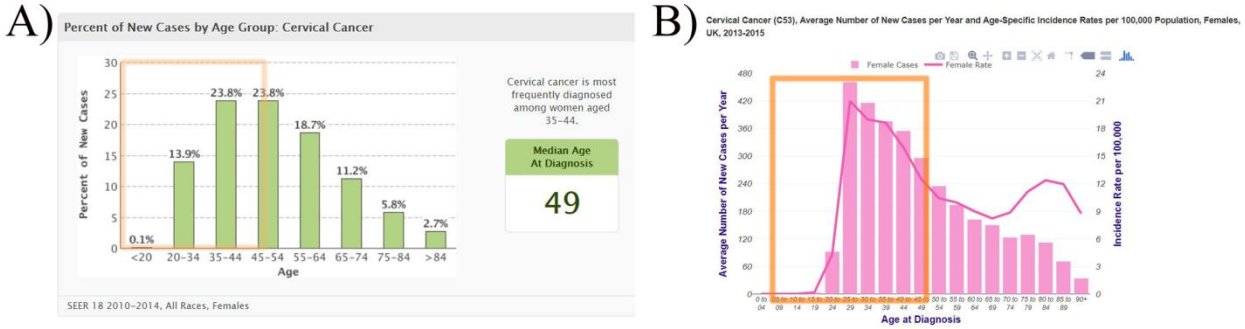

Figure 2: Potential request for fertility sparing therapy in cervical cancer patients. A) *Percentage of new cases by age group: cervical cancer, USA, (https://seer.cancer.gov).* ***B)***

Average number of new cases per 100,000 population, UK, (http://www.cancerresearchuk.org). The yellow boxes represent age ranges of women who are of reproductive age and may potentially request for fertility sparing therapy.

1.4 The implication of CSCs for cervical cancer therapy

1.4.1 CSCs raise a rethinking of chemotherapy strategies

The current treatment strategy offers satisfactory outcomes in early stage cervical cancer cases, but the prognosis of locally advanced cancer remains to be improved. The relapse rate of cervical cancer ranges between 11% and 22% in FIGO stages IB – IIA, and between 28% and 64% in FIGO stages IIB – IV [63, 64]. Recurrence of cervical cancer often shows strong resistance to current therapies and leads to a dismal prognosis. One of the greatest impediments for improving the survival rates is the insufficient understanding of the mechanisms by which residual tumor cells survive after treatment [65]. Therefore, more attempts are urgently needed to decipher the impact of cisplatin on cancer cells to provide a better insight into chemo-resistance.

Cancers are conventionally assumed to develop in a stochastic model, which describes cancer as consisting of biologically homogenous cells with an equal probability to initiate, maintain and promote tumor growth [66]. However, the most obvious limitation of this model is in explaining the cellular heterogeneity observed in the tumor bulk mass [9]. In the case of cervical cancer, the intra-tumor genetic heterogeneity has been seen in multi-facets such as chemo-radiation response, lymph node metastasis and pelvic recurrence [56, 67]. In contrast to the stochastic model, the heterogeneity can be explained well with a hierarchical model [68, 69]. It hypothesizes that not all cells, but only a subpopulation of cells, termed CSCs, have the ability to initiate and drive the growth and spread of a tumor. Chemo-resistance is believed to be an essential property of CSCs [70]. The residual CSCs, which escape from chemotherapy, cause the recurrence of disease (Figure 3 A). Consequently, this prompts a rethinking of the current anti-cancer regime, whereby CSCs should be concurrently included in the anti-cancer strategy.

1.4.2 Detrimental effects of cisplatin treatment should be overcome

Cisplatin is effective against various types of cancers, but it is generally accepted that cisplatin alone is not sufficient to eradicate cancer cells [71, 72]. This can now be explained and confirmed

by the identification and isolation of CSCs. A form of drug resistance is termed multiple drug resistance (MDR). MDR occurs when cancer cells become insensitive not only to the primary cytotoxic drug but also to other pharmaceutic drugs that have not been used during the previous course of therapy [3]. Despite a consistent rate of initial responses, cisplatin treatment frequently results in the development of MDR, leading to therapeutic failure. For example, one mainstay of treatment for ovarian cancer is platinum-based cytotoxic chemotherapy. However, conventional therapies and the tumor microenvironment generate a stem cell selective effect on tumor cells by killing the sensitive cells, resulting in the enrichment of more resistant CSCs. Recently accumulating evidence suggests that cisplatin may serve as an inductive pressure for the stem cell state, and consequently make alterations in the cellular phenotype [73, 74]. Consistent with the results in ovarian cancer, pretreatment of lung cancer cells *in vitro* with cisplatin at plasma concentrations resulted in an increase of colony formation, contributed to an enhanced expression of CSC-biomarkers, and led to resistance to chemotherapeutic agents, suggesting cisplatin pretreatment could enrich CSCs in lung cancer tissue [75].

Treatment with combinations of cytotoxic drugs is prevalent in the clinic. These efforts are intended to improve clinical outcome and to avoid severe side effects by synergistic medications instead of single high-dose reagents [76]. However, due to the inadequate understanding of CSC-biology, most of the current combinations are confined to cytotoxic drugs, which are not efficacious against CSCs. CSCs frequently evade these treatments due to specific characteristics including quiescence, decreased radical oxygen species (ROS), and high levels of chemo-resistance proteins (ALDH and ATP-binding cassette transporters) [5, 77]. Once treatment has ceased, the surviving CSCs can proliferate, producing highly resistant tumor cells, leading to disease recurrence and treatment refractory tumors (Figure 3 B). A number of therapies targeting CSCs are currently under investigation. ATRA, the product of the ALDH/RA signaling pathway, offers a new model for CSC-targeting therapy. Actually, ATRA is among the few drugs known to regulate the differentiation of embryonic stem cells [78]. The combination of ATRA with chemotherapeutic agents was efficacious in acute promyelocytic leukemia (APL) [79], for which it has become a standard of treatment, and is also promising in neuroblastoma [80]. Importantly, it is proposed that this kind of combination of cytotoxic drugs and CSC-targeting drugs is a

necessary condition for the successful outcome of cancer treatment [81].

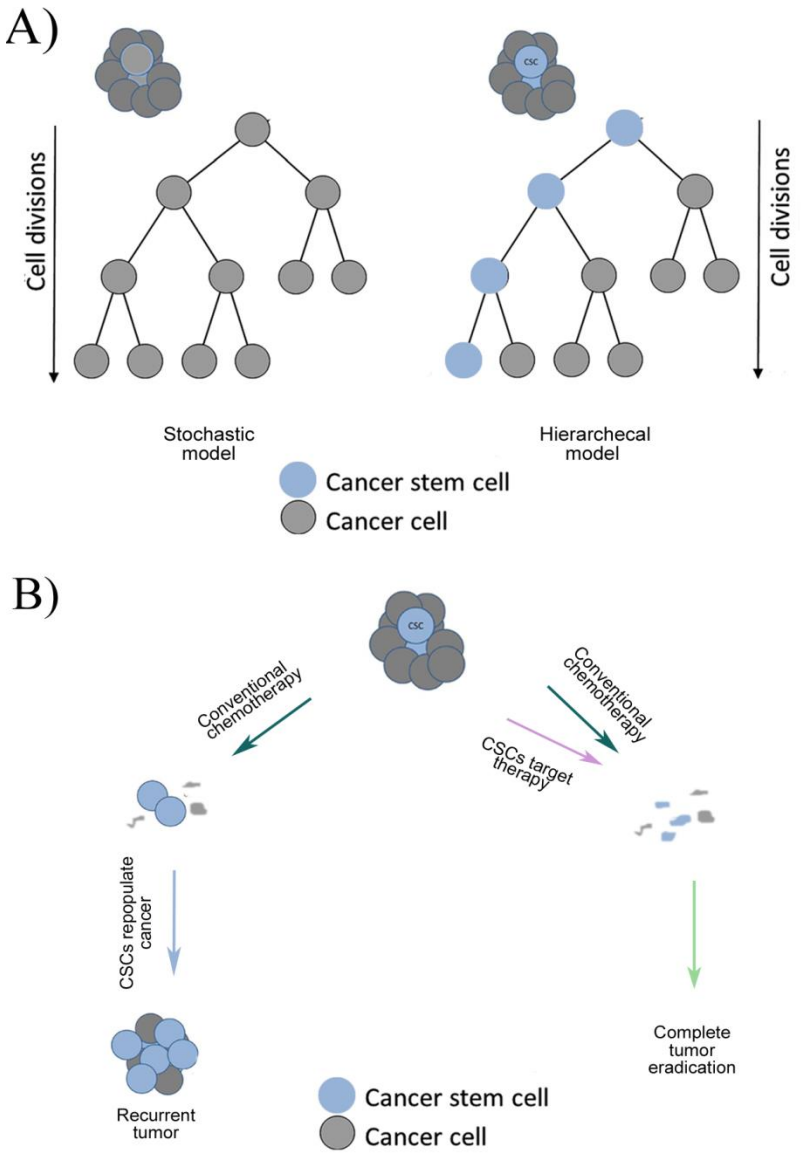

Figure 3: Schematic illustration of the two different models for sustainable-tumor growth and cancer therapeutic strategies. A) *In the stochastic model, all tumor cells have equal abilities to propagate and initiate tumors. The emerging CSC hypothesis dictates the hierarchical model, in which asymmetric division results in specific populations of CSCs and bulk cancer cells.* ***B)*** *Current cancer treatment strategies involve cytotoxic drugs that primarily target the bulk cancer cells. CSCs frequently evade these treatments due to specific resistance characteristics. Once treatment has ceased, the residual CSCs can proliferate, producing a more resistant tumor, leading to poor clinical outcome. New treatment strategies should combine standard cancer treatments with drugs designed specifically to target CSCs.*

1.4.3 Three-dimensional cell culture methods are more suitable for drug testing than conventional monolayer-adherent culture methods

One of the characteristics of CSCs is their ability to form floating spheroids under anchorage-independent conditions in serum-free medium, while normal cancer cells undergo anoikis [82]. Spheroids are a cluster of cells, which form a three-dimensional (3-D) structure, and represent an alternative model for conventional cell assays (a schematic illustration of spheroids is shown in Figure 4). Historically, two-dimensional (2-D) monolayer cells cultured on planar substrates were a practical option for cell-based screening, and a convenient means for drug testing. However, it is evident that these 2-D cultures suffer disadvantages associated with the loss of tissue-specific architecture, mechanical and biochemical cues, cell-cell interactions, and cell-matrix interactions, thus making them relatively poor models for drug efficacy and toxicity as well as cell biology [79, 83].

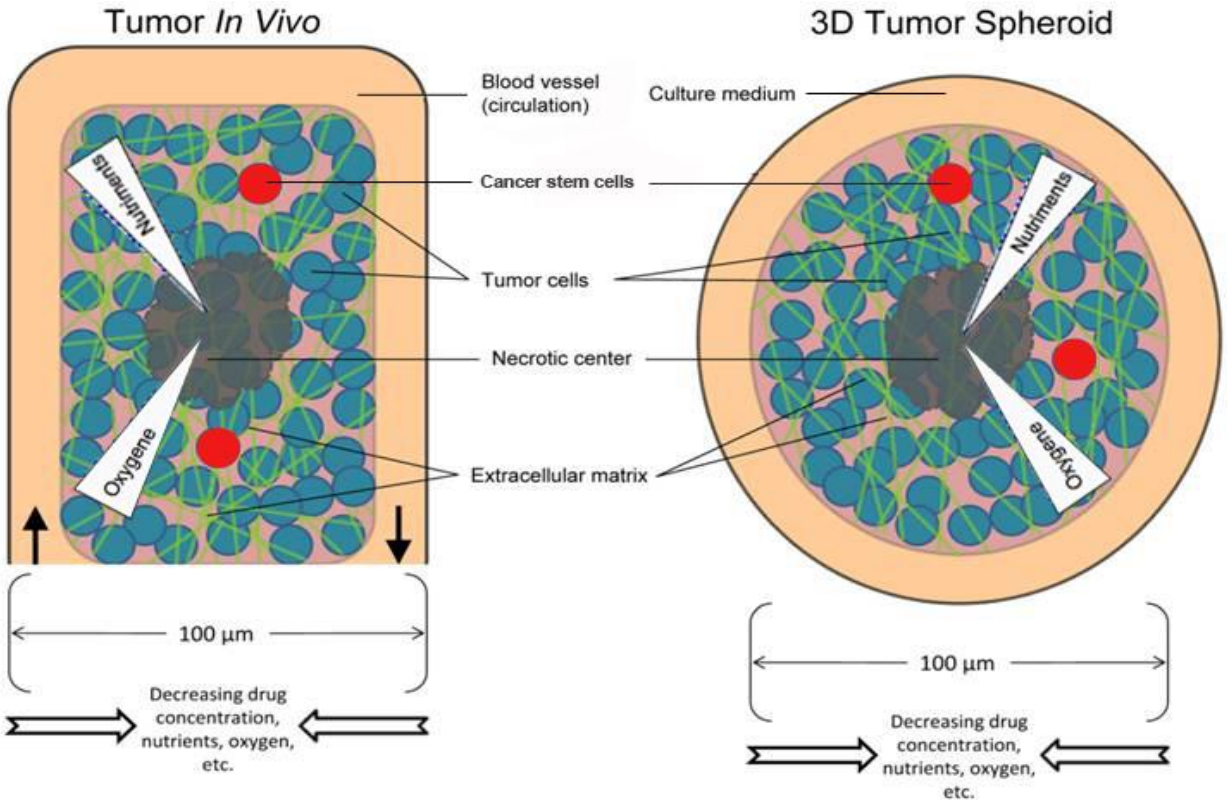

Figure 4: Schematic comparison of tumor in vivo and tumor spheroid in vitro. *Comparison of the components between a tumor and spheroid model. Spheroids can develop gradients of oxygen, nutrients, metabolites, and soluble signals, thus creating heterogeneous cell populations.*

Modified from Phung YT et al.[84].

Unlike 2-D environments, a spheroid-formation culture allows cells *in vitro* to grow in all directions, more similarly to how they would do *in vivo* (Figure 4) [84]. For example, spheroids can develop gradients of oxygen, nutrients, metabolites, and soluble signals, thus creating heterogeneous cell populations. In addition, spheroids have a well-defined geometry and optimal physiological cell-cell and cell-matrix interactions. The use of 3-D culture allows greater predictability of efficacy and toxicity in humans before drugs move into clinical trials [85]. As an example, compared with 2-D culture, colon cancer HCT-116 cells in 3-D culture are more resistant to specific anticancer drugs; such chemo-resistance has been observed *in vivo* as well [86]. Moreover, since the gene expression of the spheroids will more closely resemble gene expression *in vivo*, for the purposes of drug toxicology screening it is much more useful to test gene expression of *in vitro* cells grown in 3-D than in 2-D. Therefore, 3-D culture represents a modified condition for cancer simulation and it is more acceptable and adaptable as a drug testing assay [87, 88].

1.5 Perspective

Recent developments such as marker identification and culture technique make it possible to investigate the effects of cisplatin on CSCs more closely. The observation of cervical cancer cellular responses to cisplatin treatment could offer insights for improving the clinical outcome by optimizing the usage of cisplatin in cervical cancer treatment. Given the fact that ALDH is a universal CSC-marker as well as a functional key enzyme, ALDH inhibition is a reasonable approach for CSC-targeting. Furthermore, ATRA, an essential part of the ALDH/RA signaling pathway, will hopefully decrease expression of ALDH, which might be a complement to cisplatin treatment.

2. Hypothesis and aims of the study

Cisplatin might cause an up-regulation of ALDH activity in cervical cancer. As a component of the ALDH-ATRA signaling pathway, ATRA possibly represses ALDH activity. In order to test this hypothesis, the thesis had the following aims:

1) to evaluate the difference in CSC-related properties between $ALDH^{bright}$ cells and $ALDH^{low}$ cells in cervical cancer cell lines;

2) to compare the difference in CSC-related properties between spheroid-derived cells and monolayer-derived cells;

3) to characterize the proportion of $ALDH^{bright}$ cells after treatment by serial titrated concentration of cisplatin or/and ATRA;

4) to investigate the combination of ATRA and cisplatin on specific parameters including cell proliferation, apoptotic ratio, cellular motility, and mRNA expression of CSC-markers.

3. Materials

3.1. Laboratory equipment, kits, and other materials used

The information on laboratory equipment, commercial kits, chemical reagents, and other consumable materials is described in *Table 3, 4, 5*, and *6*, respectively.

Table 3: List of laboratory equipment

Terms	***Manufacturers***
Axiovert microscope	*Carl Zeiss, Jena, Germany*
Autoclave machine V150	*Systec, Linden, Germany*
FACS Calibur™ System	*BD Science, Franklin Lakes, USA*
FACS Jazz™ System	*BD Science, Franklin Lakes, USA*
Biological safety cabinet	*Nunctm, Wiesbaden, Germany*
BioRad, Chrome	*4-BioRad, Munich, Germany*
Freezer, -20 ℃	*Bosch, Stuttgart, Germany*
Freezer, -80 ℃	*Heraeus, Hanau, Germany*
Freezer, -150 ℃	*Sanyo, Osaka, Japan*
Incubator, HERA cell 150	*Heraeus, Hanau, Germany*
Lab water purification Systems Milli-Ro/Milli-Q Plus	*Millipore Corporation, Billerica, USA*
Lamin Air HB 2472 (Laminar flow work bench)	*Heraeus Instruments, Hanau, Germany*
Liquid suction system	*Ditabis, Pforzheim, Germany*
Multicentrifuge	*Heraeus, Hanau, Germany*
Microwave	*Bosch, Stuttgart, Germany*
Multipipettor (8×10 µl)	*Eppendorf, Hamburg, Germany*
Multipipettor (8×100 µl)	*Eppendorf, Hamburg, Germany*
Microplate photometer, Multifcan ™ FC	*Thermo Scientific, MA, USA*
Nanodrop	*Peqlab, Erlangen, Germany*
Pipettes (10 µl, 20 µl, 100 µl, 1000 µl)	*Eppendorf, Hamburg, Germany*

Refrigerator, 4 ℃	*Bosch, Stuttgart, Germany*
Steam sterilizer, varioklavtyp	*Heraeus Instruments, Hanau, Germany*
300/400/500 EP-Z	
Thermocycler	*Eppendorf, Hamburg, Germany*
Vortex mixer	*Scientific Industries, N.Y., USA*
Water bath, TW12	*Julabo, Seelbach, Germany*
Weight BP-3105	*Sartorius, Göttingen, Germany*

Table 4: List of commercial kits

Terms	***Manufacturers***
Aldefluor assay Kit	*Stem Cell Technologies, NC, USA*
Annexin-V/PI apoptosis Kit	*Rothe, Manheim, Germany*
Cell proliferation kit I (MTT)	*Sigma-Aldrich, MO, USA*
Corning Bio Coat™ matrigel	*Corning, N.Y., USA*
Invasion chambers	
DNase I kit	*Sigma-Aldrich, MO, USA*
Power SYBR Green PCR Master Mix	*Applied biosystems, MA, USA*
Revert Aid First Strand cDNA Synthesis Kit	*Thermo Scientific, MA, USA*

Table 5: List of chemical reagents

Terms	***Manufacturers***
Aqua (distilled water)	*Biochrom, Berlin, Germany*
Agarose	*Biozym, Oldendorf, Germany*
All-trans retinoic acid (ATRA)	*Sigma-Aldrich, MO, USA*
BD FACS Flow™	*BD Sciences, Franklin Lakes, USA*
Bovine serum albumin (BSA)	*Sigma, Steinheim, Germany*
Brefeldin A (BFA)	*BD Sciences, Franklin Lakes, USA*
Chloroform	*JT Baker, Deventer, Netherlands*
Cisplatin	*Sigma-Aldrich, MO, USA*

Countess cell counters	*Invitrogen, Carlsbad, CA, USA*
Dulbecco's modified Eagle's medium with Gluta MAXTM-I (DMEM)	*Invitrogen, Heidelberg, Germany*
Dimethyl sulphoxide (DMSO)	*Sigma, Steinheim, Germany*
Ethanol, 70%	*JT Baker, Deventer, Netherlands*
Ethanol, 96%	*Sigma, Deisenhofen, Germany*
Epidermal growth factor (EGF)	*Biochrom, Berlin, Germany*
Fetal bovine serum (FBS)	*Gibco BRL, Karlsruhe, Germany*
Fibroblast growth factor-basic (bFGF)	*Biochrom, Berlin, Germany*
Formalin solution 10% (v/v)	*JT Baker, Deventer, Netherlands*
Giemsa staining solution	*JT Baker, Deventer, Netherlands*
Isopropanol	*JT Baker, Deventer, Netherlands*
Methanol	*JT Baker, Deventer, Netherlands*
Penicillin/Streptomycin (P/S)	*Biochrom, Berlin, Germany*
Phosphate-buffered saline (PBS) without $Mg2^{+}$/$Ca2^{+}$	*Biochrom, Berlin, Germany*
Propidium iodide (PI)	*Sigma-Aldrich, MO, USA*
Quantum 263 medium	*PAA, Cölbe, Germany*
Taxol	*Sigma-Aldrich, MO, USA*
RNase away	*Sigma-Aldrich, MO, USA*
Trypan blue	*Biochrom, Berlin, Germany*
Trypsin/EDTA solution	*Biochrom, Berlin, Germany*
Trizol reagent	*Invitrogen, Carlsbad, CA, USA*

Table 6: List of consumable materials and others

Terms	***Manufacturers***
Cell culture dish (100×20 mm)	*BD Bioscience, Franklin Lakes, USA*
Cell culture flask (25 cm^2, 75 cm^2)	*BD Bioscience, Franklin Lakes, USA*

Cell culture plates (6-well, 24-well, 96-well)	*BD Bioscience, Franklin Lakes, USA*
Cell strainer (40 µm)	*BD Bioscience, Franklin Lakes, USA*
Optical 8-cap strips	*Applied systems, MA, USA*
Optical 8-tube strips	*Applied systems, MA, USA*
Pipette tips	*Sarstedt, Nümbrecht, Germany*
(0.5-10 µl, 10-100 µl, 100-1000 µl)	
Polypropylene conical tubes (15 ml, 50 ml)	*BD Science, Franklin Lakes, USA*
Polypropylene FACS tubes (1 ml, 5 ml)	*BD Science, Franklin Lakes, USA*
Reaction tubes (0.5 ml, 1 ml, 2 ml)	*Eppendorf, Hamburg, Germany*
BD Falcon™ polypropylene	*BD Science, Franklin Lakes, USA*

3.2 Cervical cancer cell lines

The information on cell lines is listed in *Table 7*.

Table 7: Information on cell lines

Cell lines	***HPV status***	***Culture medium***
HeLa	*HPV18⁺*	*DMEM + 10% FCS + 1% P/S or Quantum 263 + EGF* + bFGF# + 1%P/S*
MRIH186	*HPV16⁺*	*DMEM + 10% FCS + 1% P/S or Quantum 263 + EGF* + bFGF# + 1%P/S*
SiHa	*HPV16⁺*	*DMEM + 10% FCS + 1% P/S or Quantum 263 + EGF* + bFGF# + 1%P/S*

**: the final concentration of EGF is 10 ng/ml; #: the final concentration of bFGF is10 n*g/ml.

3.3 Primer sequences

The sequences of primers used for quantitative real-time PCR are listed in *Table 8*.

Table 8: Primer sequences used for quantitative real-time PCR (5'→ 3')

Transcripts	***Forward primer sequences***	***Reverse primer sequences***
*ABCG2**	*ACCTGAAGGCATTTACTGAA*	*TCTTTCCTTGCAGCTAAGAC*

*ALDH1A1**	*TGTTAGCTGATGCCGACTTG*	*TTCTTAGCCCGCTCAACACT*
*ALDH1A2**	*TGATCCTGCAAACACTGCTC*	*CTGGAGCTGGGTGGTAAGAG*
*ALDH1A3**	*TCTCGACAAAGCCCTGAAGT*	*TATTCGGCCAAAGCGTATTC*
*ALDH1B1**	*CTGGAGCTGGGTGGTAAGAG*	*CTTTCTCCACGGTTCTCTCG*
*ALDH1L1**	*ATCTTTGCTGACTGTGACCT*	*GCACCTCTTCTACCACTCTC*
*ALDH1L2**	*GCCTGGTCTCGTTACCAAAA*	*GCCACTTTCACCTCTTCAGC*
GAP-DH	*AGAAGGCTGGGGCTCATTTG*	*AGGGGCCATCCACAGTCTTC*
Nanog[#]	*AATACCTCAGCCTCCAGCAGATG*	*TGCGTCACACCATTGCTATTCTTC*
Oct3/4[#]	*GACAGGGGGAGGGGAGGAGCT AGG*	*CTTCCCTCCAACCAGTTGCCCCAA AC*
Sox2[#]	*CGAGTGGAAACTTTGTCGGA*	*TGTGCAGCGCTCGCAG*

*Primer sequences labelled with * were obtained from Nakahata et al. [89]; and with [#] were from Chen et al. [90].*

4. Methods

4.1 Monolayer-derived cells (MDCs) and cell line maintenance

Cell lines, i.e. HeLa ($HPV18^+$), MRIH186 ($HPV16^+$), and SiHa ($HPV16^+$), were initially maintained in Dulbecco's modified Eagle's medium (DMEM; Invitrogen, Heidelberg, Germany) supplemented with penicillin (100 U/ml), streptomycin (100 µg/ml) (Biochrom, Berlin, Germany) and 10% fetal calf serum (FCS; Gibco, Karlsruhe, Germany) (pre-inactivated at 56 ℃ for 30 min) at 37 ℃, 5% CO_2, and 95% humidified air atmosphere (culture condition). All experiments were conducted when cells were in an exponential growth phase (70%-80% confluence).

For the passaging of cells, the medium was removed. Cells were washed with 10 ml PBS (adding PBS, gently shaking, removing PBS). Subsequently, cells were washed and incubated twice with 2.5 ml Trypsin/EDTA (TE; Biochrom, Berlin, Germany) (adding TE, gently shaking, 30 sec incubation at room temperature, removing TE). Another 3 min incubation was carried out at 37 ℃ to detach the cells. When the cells were visibly round shaped under the microscope, the reaction was stopped by adding 8 ml of complete culture medium. The cell-containing medium was pipetted up and down 20 times to get a single cell suspension. After cell counting, the cells were split, for example 1:4, by 2 ml cell solution and 6 ml fresh medium into new dishes.

For long time storage, cells were frozen and kept at -150 ℃. After cells were detached and counted, the cell suspension was transferred into a falcon tube and centrifuged for 5 min at 1,400 rpm. The supernatant was removed and the cell pellet was resuspended in 3-5 ml of pre-cooled freezing medium (10% DMSO, 30% FCS, 60% DMEM). Cells were promptly transferred into well-labeled cryotubes at ~10^6 cells/tube on ice. These cryostocks were kept at -150 ℃ after a freezing interval at -80 ℃ overnight. For thawing out cells, a cryostock was immersed into 37 ℃ warm clean water, and gently shaken and tilted, to defrost cells quickly. These cells were transferred immediately to a culture dish with complete culture medium, which was at least 9-fold of the liquid volume in the cryotubes. After an overnight attachment step, a medium replacement was carried out to get rid of DMSO containing medium.

4.2 Spheroid formation and spheroid-derived cells (SDCs)

A glass bottle (100 ml) with a lid was sterilized by autoclaving at 121 ℃, 15 min. and 0.65 g

agarose (Biozym, Oldendorf, Germany) was weighed and transferred into the sterilized glass bottle under a clean hood. PBS (65 ml) was added into the bottle and the lid was loosely covered. The bottle was subsequently heated for 2 min at 600 w in a microwave. (do not screw the lid tightly, otherwise the bottle could explode due to the steam pressure during heating). The hot agarose liquid was immediately transferred into a culture container, carefully to avoid bubbles, at 6 ml/dish or 1 ml/well of a 6-well plate. To solidify the gel, the liquid containing dishes or plates were placed in the hood horizontally for 20 min at room temperature. Agarose coated dishes or plates can be stored in an incubator at 95% humidified air atmosphere for one week.

Parental monolayer cells were grown in culture dishes until there was 70%-80% confluence. After cells were detached as described above, the cell suspension was transferred to 15 ml tubes in which cells were subsequently washed twice with PBS. Cells were resuspended in Quantum 263 medium (PAA, Cölbe, Germany) supplemented with 10 ng/ml EGF and 10 ng/ml bFGF. To generate spheroids, single cells were plated in cell culture dishes coated with 10% agarose at a specific density of 2×10^3 cells/ml. Cells were kept in the incubator at culture condition. Every 3-4 days, half of the medium was replaced. The medium was aspirated slowly and filled into tubes with a conical bottom. Cell suspensions were left for 10 min to sediment, and the supernatant was carefully removed leaving the spheroids. The same volume of fresh medium was added and the spheroids were carefully resuspended. This suspension was placed back into the plates for further culturing.

To split the spheroids into the next generations, a sterile 40 µm mesh filter was used for collecting the spheroids. The spheroids were centrifuged at 1,500 rpm for 5 min, 2 ml of TE was added and the cell suspension was pipetted up and down. After a 5 min incubation at 37 ℃, the cells were washed with PBS, before resuspending them in fresh culture medium. The cell culture was continued in 10% agarose coated culture plates at a specific density of 2×10^3 cells/ml, and kept in the incubator at culture condition. For the experiments, 3rd or later generation spheroids were used.

4.3 Aldefluor assay staining and FACS sorting

The ALDH enzymatic activity of cells was determined by using the Aldefluor assay kit (Stem Cell Technologies, NC, USA). Spheroids were collected using a 40 µm mesh and disaggregated into single cells by TE digestion for 5 min followed by up- and down-pipetting 20 times using a 1,000

μl pipette tip. Then the single-cell suspension was washed once with Quantum263, and once with PBS. Cells were resuspended in 200 μl of Aldefluor assay buffer (1×10^3 cells/ μl) containing 1 μl ALDH substrate (BAAA), and incubated for 30 min at 37 ℃ in the dark. As a negative control, an aliquot was treated with 2 μl diethylaminobenzaldehyde (DEAB), a specific ALDH1 inhibitor (as shown in Figure 5 A). After additional staining and washing, all subsequent procedures were performed on ice to inhibit efflux of the ALDH substrate from cells.

To test the competitive inhibition of ATRA to BAAA, additional aliquots with different concentrations of ATRA (final concentrations: 3 μM, 30 μM, and 300 μM) were prepared before BAAA was added. The residual steps of Aldefluor assay staining were carried out as mentioned above.

To test the cellular recovery speed after ATRA competition, aliquots with 30 μM of ATRA were incubated for 30 min at 37 ℃ in the dark. Aldefluor assay staining was carried out immediately following ATRA removal, or after a 30 min incubation at room temperature following ATRA removal.

The BD FACS Calibur™ system was used for the data acquisition of the ALDH assay. The gating strategies were carried out as follows: 1) create a Forward Scatter (FSC) vs. Side Scatter (SSC) dot plot; 2) create a region R1 that encompasses the nucleated cells based on scatter; 3) create a Fluorescence Channel 1 (FL1) vs. SSC dot plot, gated on R1; 4) On the FL1 vs. SSC plot, adjust the FL1 photo-multiplier voltage to let the right edge of cells locate at the middle of screen; 5) for data acquisition, switch the analyzer from set-up mode to acquisition mode, collect 20,000 events or all the cells in the tube in R1 for each test, and control the sample using the same instrument settings (Figure 5 A). These assays were performed three times independently and analyzed by using the mean values of data. After data acquisition, Flowjo software (Treestar, OR, USA) was employed for subsequent data analysis.

The cell sorting was performed on a FACS Jazz™ System. ALDH-stained cells were resuspended in ALDH buffer at 5×10^6 cells/ml on ice. R1 was created on an FSC vs. SSC dot plot to encompass the nucleated cells based on scatter. With the detectors in linear mode, the voltage was adjusted so that the cellular debris and dead cells were seen in the lower left corner. Gated on R1, a FL1vs. SSC dot plot was created. The sorting gates were established by negative control cells, which were

treated with the ALDH inhibitor DEAB. The 10-20% most bright-side cells were sorted out as ALDH^{bright} cells, while the 10-20% lowest bright cells on the left side were collected as ALDH^{low} cells (Figure 5 B). During the sorting progress, cells were kept cold by the use of a cooling apparatus. The sorted cells were collected in Quantum 263 supplemented with EGF and bFGF for further experiments.

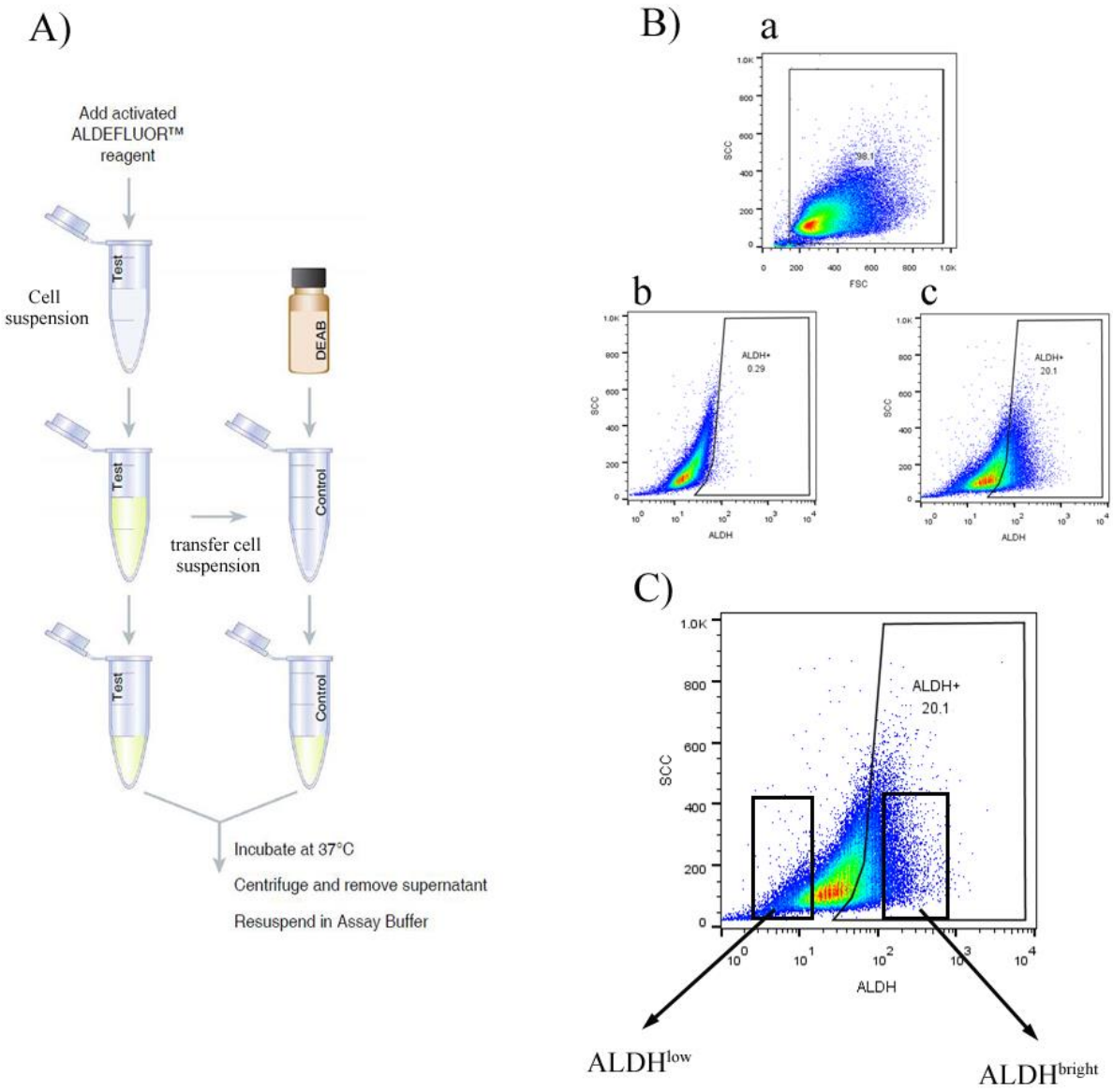

Figure 5: Aldefluor assay staining, gating strategy, and sorting strategy. A) *Illustration of Aldefluor assay staining.* ***B)*** *Gating strategy for Aldefluor assay staining: a) gating the nucleated cells; b) setting the threshold of negative control; c) gating out positive cells based on the negative control.* ***C)*** *The lowest and most bright cells are sorted out.*

4.4 MTT assay

4.4.1 IC_{50} of different drugs and drug resistance in MDCs

To observe drug resistance of cells in different conditions, and cell viability, and to calculate the IC_{50} of different drugs, MTT assay (Sigma-Aldrich, MO, USA) was used. Cells were seeded at 2×10^3 cells/well in a 96-well plate, and cultured for 24 h prior to the addition of drugs. Cisplatin was added into wells at 0.03 μM to 100 μM by 3-fold dilution in triplicates. Alternatively, paclitaxel was added into wells at 0.03 nM to 100 nM by 3-fold dilution in triplicates.

After a 72 h incubation at culture condition, 10 μl of the MTT labeling reagent (final concentration 0.5 mg/ml) was added to each well. The microplate was further incubated for 4 h. Subsequently, 100 μl of the solubilization solution was added into each well. The plate was allowed to stand overnight at 37 ℃. Absorbance was measured at 570 nm (reference at 590 nm). Cell viability was calculated by 100% × (absorbance of sample – absorbance of blank control) / (absorbance of untreated control – absorbance of blank control) for each cell line. For the drug resistance assay, a certain concentration of a drug (5 μM cisplatin or 5 nM paclitaxel) was used to treat cells.

4.4.2 IC_{50} of different drugs and drug resistance in SDCs

By placing 100 μL of 2×10^4 cells/ml in single-cell suspension, 2×10^3 SDCs were seeded into an ultra-low attachment 96-well plate with the respective medium. 50 μL of fresh medium was added on the 4^{th} day and 7^{th} day. Cisplatin was added into wells at 0.03 μM to 100 μM by 3-fold dilution in triplicates on the 10^{th} day. Alternatively, paclitaxel was added into wells at 0.03 nM to 100 nM by 3-fold dilution in triplicates. The next steps of IC_{50} determination were the same as described in the MDCs procedure.

4.4.3 Checkerboard titration experiments and drug-drug interaction calculation

96-well checkerboard titration experiments combined with MTT assay were used to evaluate cell proliferation, and to optimize the concentrations of two drugs in combination. The seeding protocol of cells was same as 4.4.1 and 4.4.2, in each well of 96-well plate. Cisplatin was 3-fold serially diluted along the ordinate, while the second drug, ATRA, was 3-fold serially diluted along the abscissa (Figure 6). The resulting checkerboard contains gradients of each combination of the two drugs. MTT assay was carried out after a 72 h incubation with drug administration at culture

condition. The drug-drug integration was further analyzed by calculating the combination index (CI) (Calcusyn software, Biosoft, USA; www.combosyn.com). A CI <0.9 represents synergistic effects, while 0.9 ≤CI ≤1.1means additive effects, and CI >1.1 antagonistic effects.

4.5 Annexin-*V*/Propidium iodide (PI) staining assay

After trypsinization, 1×10^5 cells were prepared and pelleted. 100 μL of working solution was prepared by adding 2 μL Annexin-*V* and 2 μL PI into 96 μL incubation buffer (Rothe, Manheim, Germany). The cells were resuspended and incubated for 15 min in the dark at room temperature. Subsequently, cells were resuspended in 100 μL of FACS buffer after washing with PBS. Based on single staining of an Annexin-*V* tube or PI tube, compensation was performed for every cell line to correct for the spectral overlap of different fluorochromes. The gating strategy was: 1) R1 was created on an FSC vs. SSC dot plot (Figure 7 A); based on R1, a quadruple gate was further employed on an FL1 vs. FL3 dot plot. The upper-right (Q2) and lower-right (Q3) population were regarded as apoptotic cells (Figure 7 B).

4.6 Colony formation assay

Cellular stemness was observed by colony formation assay. The initial cell density was 100 cells/ml in DMEM medium, supplemented with 10% FBS. The cell suspension was added into a 6-well plate at 2.5 ml/well. Cells were maintained in complete medium for 2 weeks. On the 14^{th} day, cells were fixed with cold methanol 100% for 20 min, then dried and stained with Giemsa (JT Baker, Deventer, Netherlands) solution for 20 min. After washing with distilled water and air drying, colonies were counted manually. Colonies that contained >50 cells or were >0.1 mm were counted with an ocular micrometer. The clone formation efficiency (CFE) was calculated according to the following formula: CFE =number of colonies/number of seeded cells ×100%.

4.7 Spheroid formation assay

Additionally, a spheroid formation assay was also used to assess the cellular stemness. A single cell suspension was adjusted to 200 per ml in Quantum 263 supplemented with 10 ng/ml EGF and 10 ng/ml bFGF. The cell suspension was added into a 6-well plate at 2.5 ml/well. Fresh medium was changed every 3-4 days. After 2 weeks culture, the spheroid formation efficiency (SFE) was calculated. The spheroid-containing medium was gently stirred by pipetting up and down using a

200 µL tip. After a 5 min settle-down, spheroids >0.1 mm were counted under an ocular micrometer. SFE was calculated according to the following formula: SFE =number of spheroids/number of seeded cells ×100%.

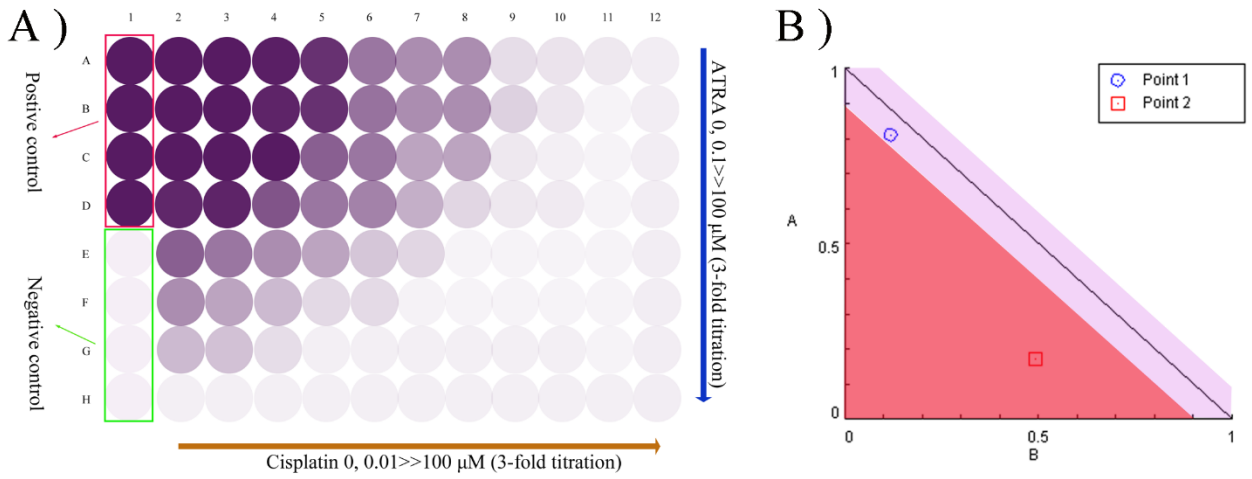

Figure 6: A) *Illustration of checkerboard test. 1A-1H: positive control compromises wells in which cells were treated with PBS; negative control represents wells in which cells were treated with the lethal concentrations of drugs. 2A-12H: different combinations of cisplatin and ATRA concentrations; cisplatin is 3-fold serially diluted horizontally, and ATRA is 3-fold serially diluted vertically.* ***B)*** *Example of CI readout. CI <0.9 stands for synergistic effects (point 2, with value of 0.32 as an example), while 0.9 ≤CI ≤1.1 stands for additive (for example point 1, with a value of 0.92), and CI >1.1 stands for antagonism.*

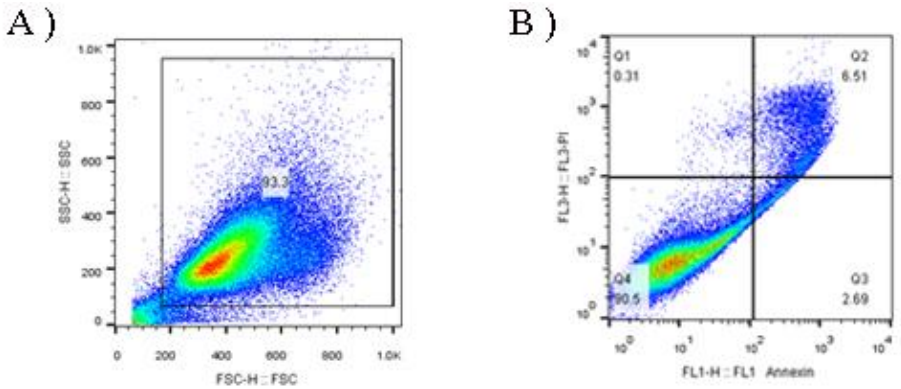

Figure 7: Gating strategy for Annexin-V/PI staining. A) *Gating the nucleated cells.* ***B)*** *For analysis, a quadruple plot is further employed on an FL1 vs. FL3 dot plot. The percentage of cells was determined in the four quadrants: live cells (Annexin-V$^-$/PI$^-$, lower-left quadrant), early*

apoptotic cells (Annexin-V^+/PI^-, lower-right quadrant), late apoptotic cells (Annexin-V^+/PI^+, upper-right quadrant), and necrotic cells (Annexin-V^-/PI^+, upper-left quadrant). Both early apoptotic cells and late apoptotic cells were regarded as cells undergoing apoptosis.

4.8 Wound healing assay

Cells were seeded at 1.5×10^5 cells/well into the prepared 24-well plate to create a confluent monolayer. The plate was incubated overnight at culture condition, allowing cells to adhere and spread on the substrate completely. A "wound" was created by scratching the cell monolayer in a straight line with a 200 μL tip. The debris was removed by washing the cells once with 1 ml of the growth medium, and then 1 ml of medium was replaced. To obtain the same field during the image acquisition, markings were created under the well to be used as reference points close to the scratch. The dish was placed under a phase-contrast microscope, and the reference mark was outside the capture image field, but within the eyepiece field of view. The image of the scratch was acquired every 12 h, until the scratching field was completely filled by migrated cells. The images acquired for each sample were further analyzed quantitatively using software (Adobe Photoshop version 5, CA, USA). For each image, the distance between one side of the scratch and the other side was measured at intervals (μm).

4.9 Invasion assay

Warm culture medium was added to the interior of the inserts and the bottom of Matrigel Invasion chambers (Corning, NY, USA), and allowed to rehydrate overnight. After rehydration, the medium was carefully removed without disturbing the layer of Matrigel on the membrane. A cell suspension was prepared in culture medium containing 5×10^4 cells/ml for 24-well chambers. 750 μL of DMEM, containing 10% FCS serving as chemo-attractant, was added to the wells of the plate. Sterile forceps were used to transfer the chambers into wells. Immediately, 0.5 ml of cell suspension was added to the 24-well chambers, which were subsequently incubated for 24 h. After incubation, the non-invading cells were removed from the upper surface of the membrane by gentle scrubbing, and the cells on the lower surface were stained with Giemsa (JT Baker, Deventer, Netherlands). Cell counting was facilitated using a photomicroscope at 100× magnification.

4.10 RNA isolation

For the monolayer: the medium was removed from the culture dish; 1 ml of Trizol (Invitrogen, Carlsbad, USA) reagent was added directly to the cells in the culture dish per 10 cm^2 of culture dish surface area; the cells were lysed directly in the culture dish by pipetting up and down several times. The lysate was transferred into a new 2 ml Eppendorf tube.

For the spheroids: the spheroids were harvested by filtration through a 40 μm mesh. Then the cells were centrifuged at 1,500 rpm for 5 min. Then the cells were washed with PBS twice. The supernatant was discarded and 1 ml of Trizol per 10^6 cells was added. The cells were lysed by pipetting up and down several times before being transferred into a new 2 ml Eppendorf tube.

Chloroform (0.2 ml per 1 ml of Trizol reagent) was added. The tube was capped securely and shaken vigorously by hand for 15 sec. After 15 min incubation, the tube was centrifuged at 13,000 rpm for 15 min at 4 ℃. The aqueous phase of the sample was carefully transferred into a new tube. Per 1 ml used for homogenization, 0.5 ml of 100% isopropanol was added, incubated on ice for 15 min, and then centrifuged at 13,000 rpm for 10 min at 4 ℃. The supernatant from the tube was discarded, leaving only the RNA pellet. The pellet was washed with 1 ml of 75% ethanol, vortexed briefly, and then centrifuged at 7500 rpm for 5 min at 4 ℃. After the supernatant was removed, the RNA pellet was air dried for 5-10 min. The concentration and quality of RNA was determined by a Nanodrop (Peqlab, Erlangen, Germany). Only RNA samples, which had an A280/A260 ratio between 1.8 and 2.0, were used for subsequent experiments.

To avoid genomic DNA contamination, the extracted RNA underwent a DNA removal procedure by a DNase kit (Sigma-Aldrich, MO, USA). The listed components were mixed in a PCR-grade tube in the indicated order: 8 μL RNA solution, 1 μL Reaction Buffer, and 1 μL DNase I (amplification grade, 1 unit/ml). Then the components were mixed gently by finger snipping and centrifuged briefly. After 20 min incubation at room temperature, 1 μL Stop Solution was added to bind calcium and magnesium ions, and to inactivate the DNase I. To denature both the DNase I and the RNA, the tube was heated at 70 ℃ for 10 min, chilled on ice, and the RNA solution was collected by a brief centrifugation. The DNase-treated RNA was used for cDNA synthesis or kept at -80 ℃ for long time storage.

4.11 Reverse transcription

Total RNA (1 μg) was converted to cDNA by RT-PCR using a High Capacity RNA-to-cDNA Kit (Thermo Scientific, MA, USA). The following components were combined in a tube on ice: 1 μg of DNAse-treated template RNA, 1 μl Oligo (dT) 18 primer, 10 μl nuclease free water, 4 μl of 5× Reaction Mix, 1 μl of RNase Inhibitor (20 U/μL), 2 μl dNTP solution, and 1 μl of Revert Aid RT (200 U/μL). The tube was capped and gently vortexed for mixing. Then the tube was centrifuged briefly to collect the contents. The reaction was incubated using a Thermal cycler (Eppendorf, Hamburg, Germany) at 42℃ for 60 min and the reaction terminated at 70℃ for 15 min. The obtained cDNA solution was held at 4℃ until use. For long-term storage, the cDNA solution was stored at -20℃.

4.12 Quantitative real-time PCR

Quantitative real-time PCR was performed using the Power SYBR Green mix (Applied biosystems, MA, USA) and run on a real time PCR machine (4-BioRad, Munich, Germany). The following components were combined in a tube on ice: 25 μl of Express SYBR Green ERTM qPCR Super Mix Universal, 0.4 μl of 10 μM specific forward primer, 0.4 μl of 10 μM specific reverse primer, 1 μl of cDNA solution, and 23.2 μl of PCR-grade water. PCR conditions were as follows: 95℃ for 10 min, 40 cycles of 95℃ for 15 sec, and 60℃ for 1 min. Reactions were carried out in triplicate with RT controls, GAP-DH was used as a reference gene, and data were analyzed using the delta – delta Ct method.

4.13 Statistical Analysis

Statistical paragraphs and analyses were performed using Graphpad Prism 5.01 software (La Jolla, CA, USA). The Student's t-test was used to determine the statistical significance of differences of 2 group comparisons. To examine differences among 3 groups, an ANOVA analysis was performed. The results are presented as the mean value and standard deviation (±SD). P values of <0.05 were regarded as statistically significant.

5. Results

5.1 ALDH^{bright} and ALDH^{low} cells possess different profiles to each other in chemo-resistance, colony formation ability, and RNA expression of CSC-markers

ALDH has been reported to label out CSCs in cervical cancer as a universal CSC-marker [40]. By Aldefluor assay, ALDH^{bright} cells and ALDH^{low} cells can be sorted. The differences in the CSC-related profile of these two sorted populations were investigated for chemo-resistance, colony formation ability, and RNA expression of CSC-markers (TFs and ALDH isotypes).

5.1.1 ALDH^{bright} cells are more chemo-resistant than ALDH^{low} cells

In order to investigate the chemo-resistance, cisplatin and paclitaxel, the two most commonly used chemotherapy reagents were tested. Sorted cells were cultured for 72 h with different cisplatin concentrations (0.03-100 μM, 3-fold dilution) or paclitaxel concentrations (0.03-100 nM, 3-fold dilution). Cell viability was determined by MTT, and IC_{50} was calculated by Graphpad 5.01 (Figure 8).

The IC_{50} of cisplatin was 1.46 ± 0.58 μM, 2.79 ± 0.92 μM, and 7.05 ± 1.80 μM in ALDH^{low} cells of HeLa, MRIH186, and SiHa, respectively (Figure 8 B). In each cell line, ALDH^{bright} cells were more resistant to cisplatin than ALDH^{low} cells. The IC_{50} of HeLa ALDH^{bright} cells was 7.29 ± 1.20 μM, about 3.99-fold higher than that in ALDH^{low} cells. The IC_{50} was 9.92 ± 0.88 μM in MRIH186 ALDH^{bright} cells and 15.16 ± 1.73 μM in SiHa ALDH^{bright} cells (Figure 8 B). Additionally, cell viability was measured after 72 h treatment with 5 μM cisplatin. The cell viability was at 77.98 ± 5.01%, 81.45 ± 2.90%, and 86.03 ± 5.54% in HeLa, MRIH186, and SiHa ALDH^{bright} cells, respectively; however, the viable proportion was reduced to 16.47 ± 3.56%, 25.80 ± 4.42%, and 52.76 ± 6.93% in the corresponding ALDH^{low} cells, which was significantly lower than in ALDH^{bright} cells ($p < 0.05$; Figure 8 C). Similarly, in their response to cisplatin treatment, ALDH^{bright} cells also exhibited increased paclitaxel resistance compared to ALDH^{low} cells in these cell lines (Figure 8 D). The IC_{50} of HeLa, MRIH186, and SiHa ALDH^{low} cells was 1.45 ± 0.41 nM, 3.19 ± 1.90 nM, and 2.76 ± 1.51 nM, respectively. The ALDH^{bright} cells had an IC_{50} of 3.20 ± 1.08 nM, 10.12 ± 2.43 nM and 7.92 ± 0.32 nM, which represents an increment about 1.20-fold, 2.17-fold, and 1.87-fold, respectively (Figure 8 E). The cellular viability of ALDH^{bright} cells were

about 2.15-fold, 2.49-fold and 1.28-fold higher than that of ALDH^{low} cells after 5 nM paclitaxel treatment in HeLa, MRIH186, and SiHa cells, respectively (Figure 8 F).

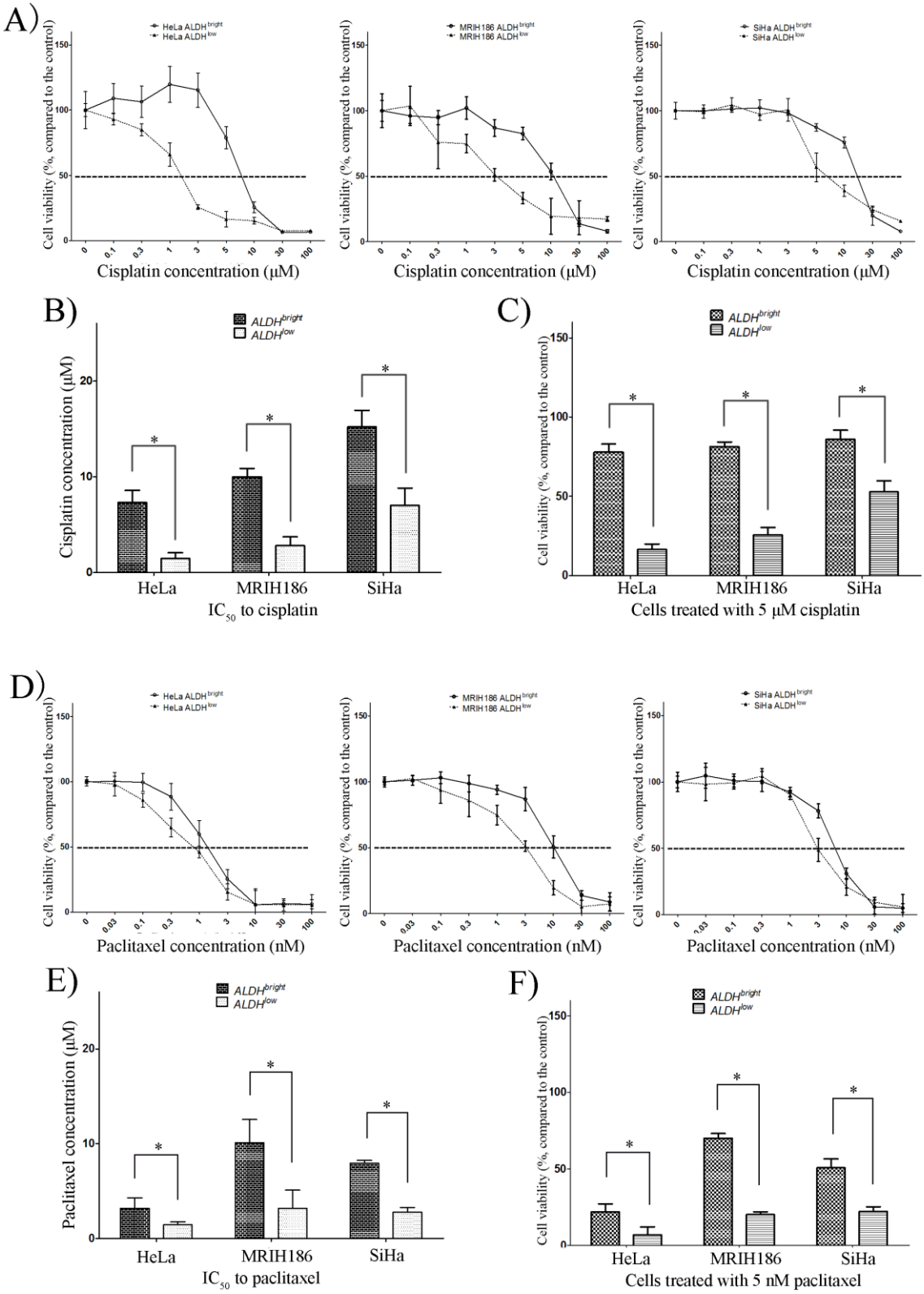

Figure 8: Chemo-resistance in ALDH^{bright} cells and ALDH^{low} cells sorted from cervical cancer

cell lines. A) *The response of ALDH^{bright} and ALDH^{low} cells to cisplatin (0.03-100 µM, 3-fold dilution) determined by a MTT assay. Dashed lines indicate the 50% viability of cells.* ***B)*** *The IC_{50} to cisplatin is calculated from the data of a MTT assay.* ***C)*** *Quantification of cellular viability after 5 µM cisplatin treatment in ALDH^{bright} and ALDH^{low} cells.* ***D)*** *The response of ALDH^{bright} and ALDH^{low} cells to paclitaxel (0.03-100 nM, 3-fold dilution) determined by MTT assay. Dashed lines describe the 50% viability of cells.* ***E)*** *The IC_{50} to paclitaxel is calculated from the data of a MTT assay.* ***F)*** *Quantification of cellular viability after 5 nM paclitaxel treatment in ALDH^{bright} and ALDH^{low} cells. Error Bars: mean values ± SD of three replicates. *: p <0.05.*

5.1.2 ALDH^{bright} cells are more clonogenic than ALDH^{low} cells

Colony formation assay represents a measure of stemness. In HeLa cells, the clone numbers formed by ALDH^{bright} cells were 5.48 times higher than those formed by ALDH^{low} cells ($p < 0.05$). This colony formation efficiency of ALDH^{bright} cells was also 5.53-fold higher than the ALDH^{bright} cells of MRIH186 ($p < 0.05$). The ALDH^{bright} cells of SiHa had a 3.29-fold ($p < 0.05$) greater capacity to form clones than ALDH^{low} cells (Figure 9). Of note, the size of the colonies was different with a consistently larger diameter in ALDH^{bright} cells in all three cell lines.

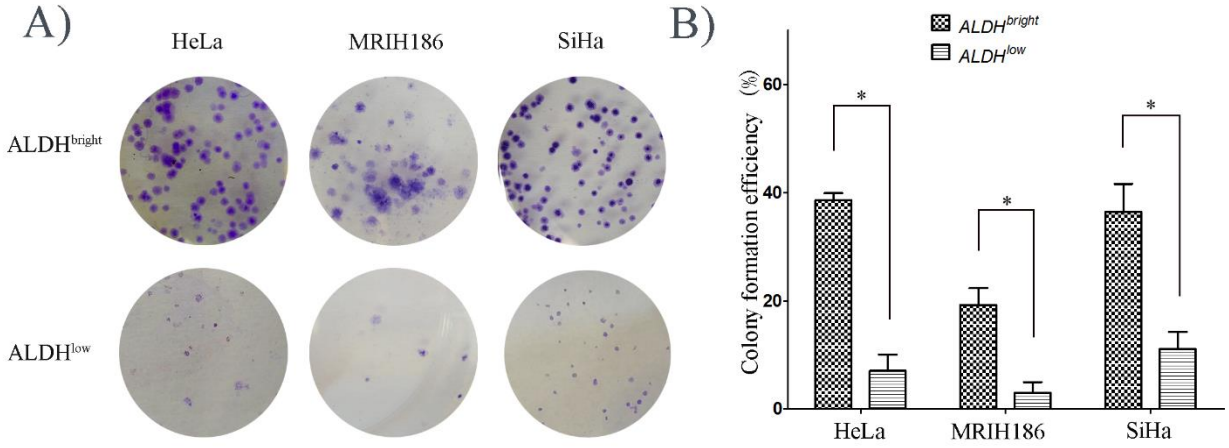

Figure 9: Colony formation ability of ALDH^{bright} cells and ALDH^{low} cells sorted from cervical cancer cell lines. A) *Representative photos of the colony formation assay. Dark blue dots represent the colonies.* ***B)*** *Quantification of colony formation efficiency in ALDH^{bright} cells compared to ALDH^{low} cells. Error bars: mean values ± SD of three replicates. *: p <0.05.*

5.1.3 Characterization of mRNA expression of ALDH isotypes and other CSC-markers in

ALDH^{bright} cells and ALDH^{low} cells

Considering the various isotypes of the ALDH supergene family, it is intriguing to know which isotype is expressed in a given cell line and responsible for Aldefluor assay results. This question can be further answered by mRNA expression measurement. mRNA of important CSC-markers, such as ABCG2 and TFs, was also included in the analysis.

As shown in Figure 10, the ALDH1A3 mRNA showed the biggest difference in expression between ALDH^{bright} and ALDH^{low} cells, being 6.27-fold higher in the ALDH^{bright} cell population than the ALDH^{low} cell population in HeLa, 2.82-fold higher in MRIH186, and 3.55-fold higher in SiHa. Slight differences were found in other isotypes. Expression of ABCG2 mRNA showed a difference between ALDH^{bright} and ALDH^{low} cell populations with 2.31- and 2.47-fold in HeLa and SiHa. The mRNA levels of TFs were generally increased in the ALDH^{bright} when compared to ALDH^{low}. However, the increase was variable and cell line dependent. For example, Oct3/4 mRNA was 0.97-, 4.25-, and 2.56-fold in HeLa, MRIH186, and SiHa, respectively. mRNA of Sox2 had a 1.23-, 2.07-, and 3.21-fold increase, while Nanog had an 1.14-, 0.82-, and 2.14-fold change between ALDH^{low} and ALDH^{bright} cells in HeLa, MRIH186, and SiHa, respectively.

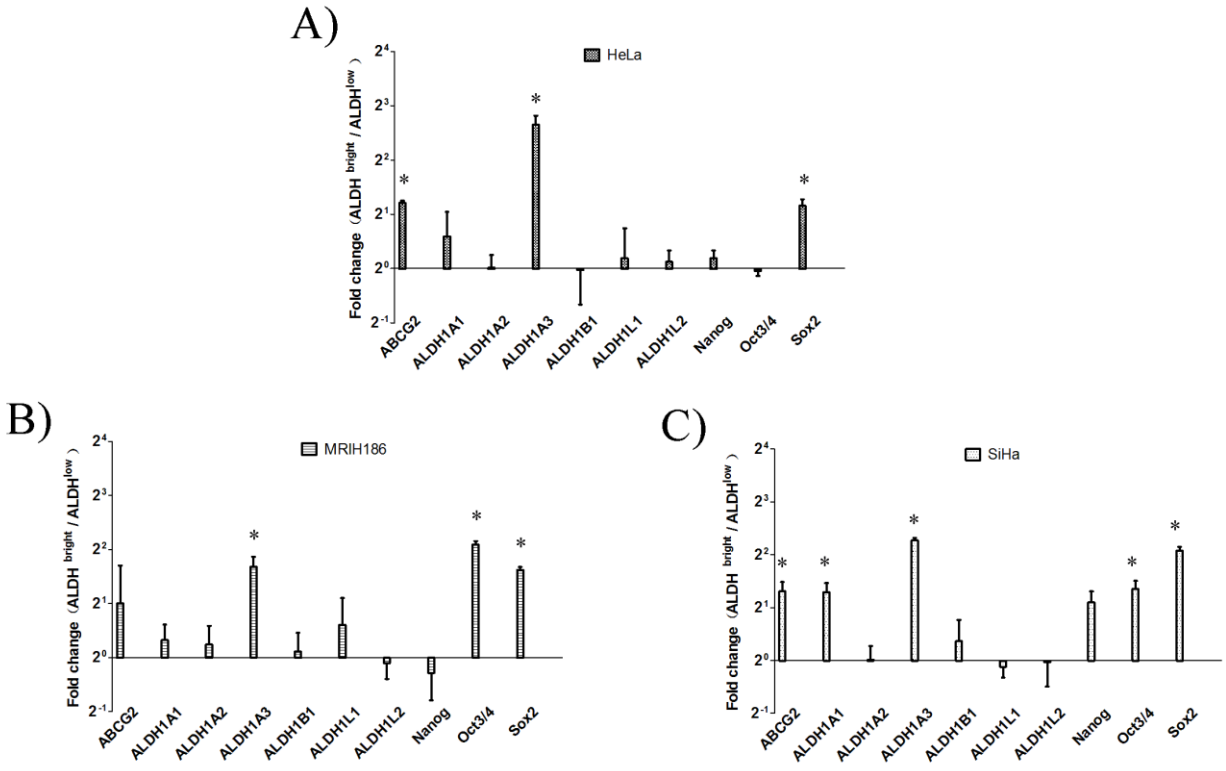

Figure 10: Quantitative real-time PCR analysis of mRNA expression of CSC-markers. *The fold*

change (ALDH^{bright} cells sorted from cervical cancer cell lines/the corresponding ALDH^{low} cells) is given (delta – delta Ct method). The CSC-markers are generally up-regulated in ALDH^{bright} cells in the cervical cancer cell lines. ***A)*** *HeLa;* ***B)*** *MRIH186;* ***C)*** *SiHa. Error bars: mean values ± SD of three replicates. *: p <0.05.*

5.2 SDCs display different biological properties compared to MDCs

In the first part of the study, it was confirmed that ALDH works as a CSC-marker in cervical cancer cell lines. According to the literature and our previous results [47, 87, 88], spheroid culture is not only a way to obtain more ALDH^{bright} cells, but also a more suitable method to mimic the condition *in vivo* than monolayer culture. Therefore, spheroid culture represents a more suitable and advanced way for drug administration research. The following experiments were done in order to show the difference between SDCs and MDCs in CSC-properties such as colony formation ability, chemo-resistance, and mRNA expression of CSC-markers.

5.2.1 Cervical cancer cell lines are able to form spheroids

The three cell lines HeLa, MRIH186, and SiHa were grown in suspension at a specific density of 2×10^4 cells/ml in Quantum 263 medium with 10 ng/ml EGF and 10 ng/ml bFGF for 7-14 days. All three cell lines exhibited an ability for spheroid formation. This typically started at 3-5 days after plating suspension cultures and the spheroid size became progressively larger. After 7-10 days, the number of the spheroids continued to increase and the cell clusters became more compact (Figure 11).

When the spheroids were transferred back to regular tissue culture flasks for 2-D monolayer cell culture, the spheroids adhered to the flask and cells migrated out from the spheroid and formed a confluent monolayer. Spheroids maintained in long-term culture up to the 10th generation of 3-D spheroid passage still showed this self-renewing ability, which generated adhesively growing cervical cancer cells. The older generation of spheroids were tighter than early generations. Additionally, the spheroid formation capacity of ALDH^{bright} was also greater than ALDH^{low} cells. This capacity was enhanced up to 7.24-fold in HeLa, 10.83-fold in MRIH186, and 3.61-fold in SiHa (all, $p < 0.05$; Figure 12).

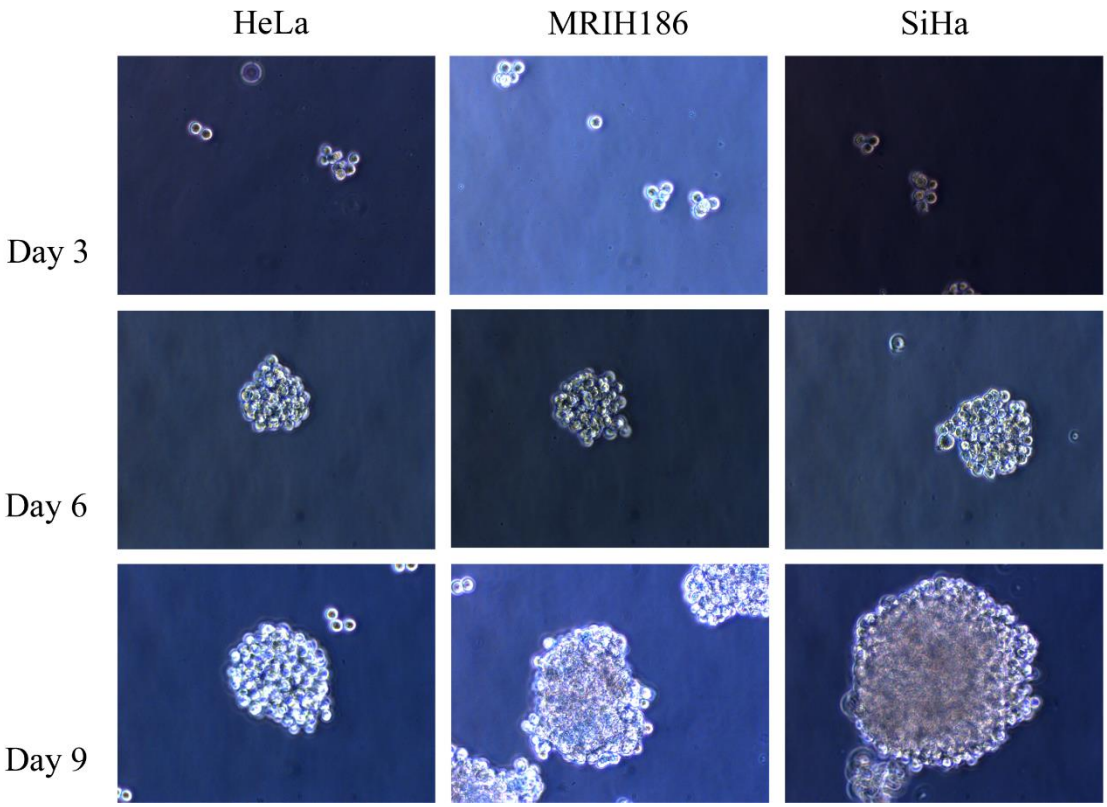

Figure 11: Time course of spheroid formation in cell lines HeLa, MRIH186, and SiHa. *The magnification is 200×.*

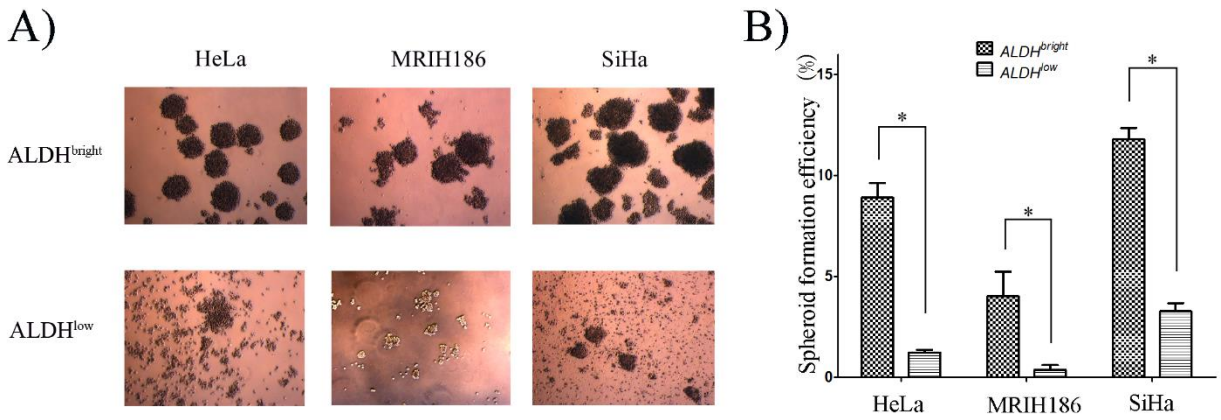

Figure 12: Spheroid formation abilities of ALDH^{bright} cells and ALDH^{low} cells sorted from cervical cancer cell lines. A) *Representative photos of the spheroid formation assay. The magnification is 50×.* ***B)*** *Quantification of spheroid formation efficiency in ALDH^{bright} cells compared to ALDH^{low} cells. Error bars: mean values ± SD of three replicates. *: p <0.05.*

5.2.2 Higher stemness is found in SDCs than in MDCs

Colony formation efficiency (CFE) and spheroid formation efficiency (SFE) were employed to

characterize the stemness (renewal ability) of cervical cancer cells. In HeLa cells, the clone numbers formed by SDCs were about 1.29-fold of MDCs; however, this slight differences was not statistically significant. The CFE was 1.35-fold higher in SDCs than MDCs derived from MRIH186 ($p < 0.05$). In SiHa, the CFE of SDCs was also significantly stronger than by MDCs with a 2.13-fold increase ($p < 0.05$). The ability of spheroid formation was also observed in the MDCs and SDCs of each cell lines (Figure 14). When the same number of cells were seeded on an agarose-coated plate, the SDCs formed more, and tighter spheroids than MDCs. In SDCs of MRIH186, this ability was 2.43-fold more than MDCs; SDCs displayed a 1.35-fold higher SFE than MDCs in SiHa (both, $p < 0.05$).

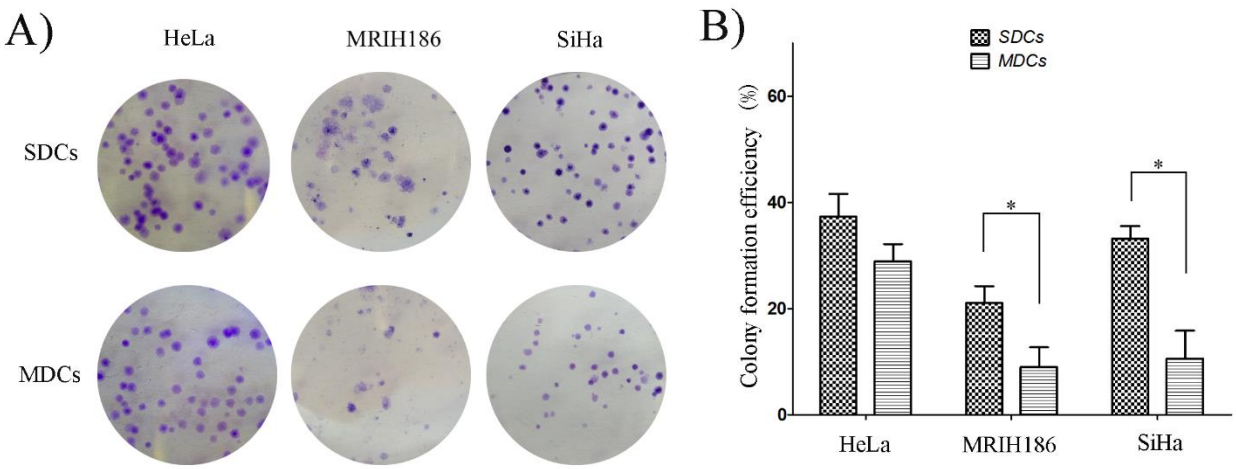

Figure 13: Colony formation ability of SDCs and MDCs in different cervical cancer cell lines. ***A)*** *Representative photos of the colony formation assay. Dark blue dots represent the colonies formed by cells.* ***B)*** *Quantification of colony formation efficiency in SDCs compared to the corresponding MDCs. Error bars: mean values ± SD of three replicates. *: $p < 0.05$.*

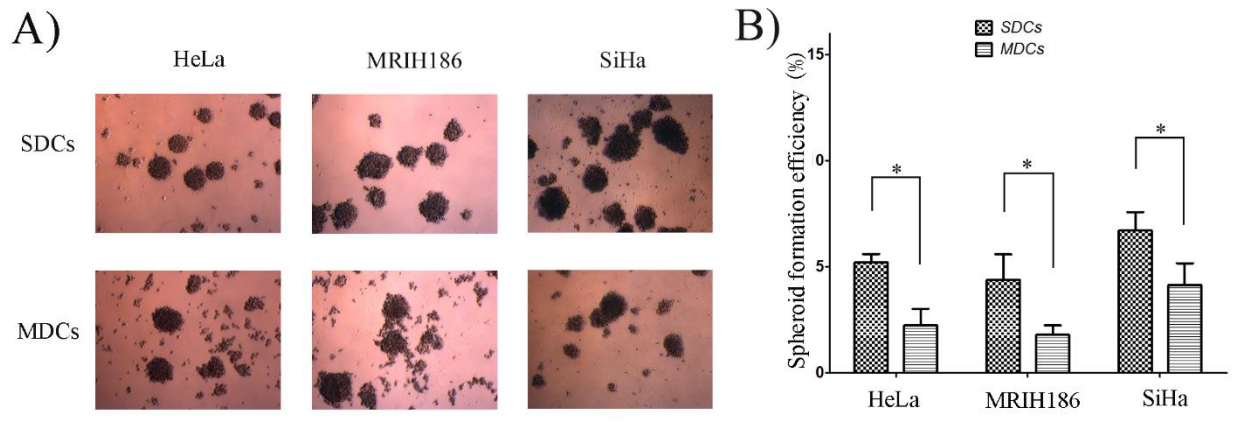

Figure 14: Spheroid formation ability of SDCs and MDCs in different cervical cancer cell lines.

A) *Representative photos of the spheroid formation assay. The magnification is 50×.* ***B)*** *Quantification of spheroid formation efficiency in SDCs compared to the corresponding MDCs. Error bars: mean values ± SD of three replicates. *: p <0.05.*

5.2.3 A higher ALDH^{bright} cell proportion is found in SDCs than in MDCs

The enzymatic activity of ALDH was measured in the SDCs of cervical cancer cell lines and their matched MDCs by Aldefluor assay. As a control, cells incubated with Aldefluor substrate (BAAA) together with the specific ALDH inhibitor (DEAB) were used to establish the background fluorescence, and to define the cut-off between the ALDH^{bright} and ALDH^{low} population. All cervical cancer cell line-derived SDCs showed an increase in the proportion of ALDH^{bright} cells compared to their parental MDCs. In SDCs of HeLa, MRIH186, and SiHa, the ALDH^{bright} cells were 11.70 ± 2.41%, 42.70 ±1.24%, and 28.52 ± 3.21%, which were about 5.12-fold, 1.89-fold, and 1.85-fold of their corresponding parental MDCs, respectively (all, p <0.05; Figure 15).

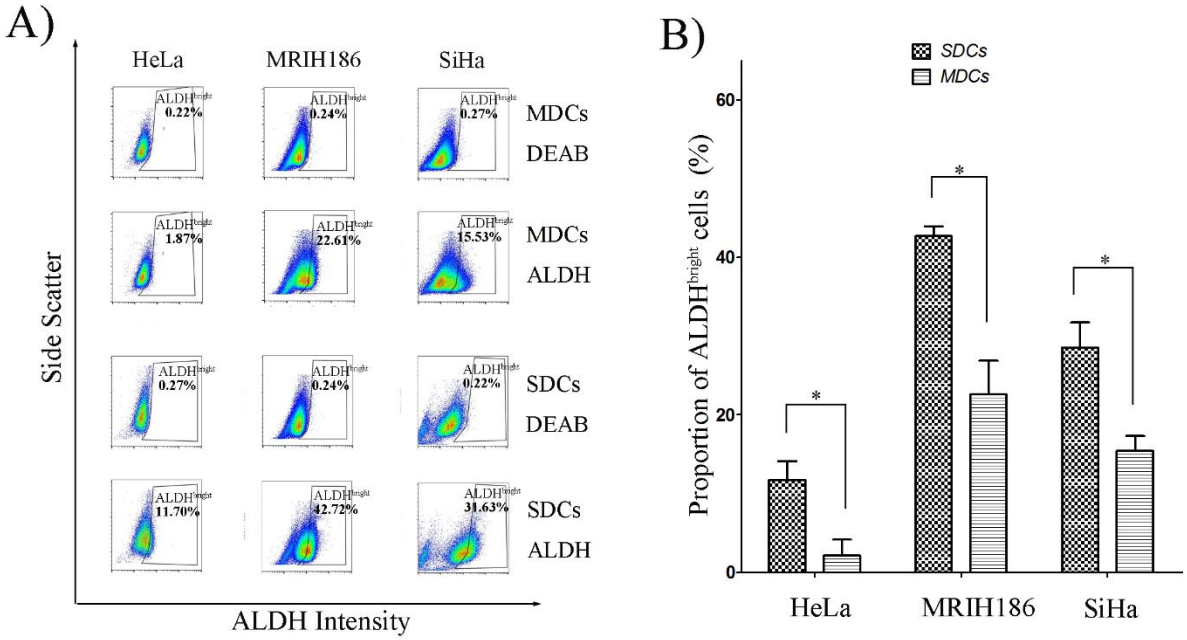

Figure 15: The proportion of ALDH^{bright} cells in SDCs vs. parental MDCs. A) *Aldefluor assay staining in MDCs and SDCs from each cell line. DEAB is used to define the cut-off between the ALDH^{bright} and ALDH^{low} populations. Subsequently, the proportion of ALDH^{bright} cells can be read out in the polygonal gate.* ***B)*** *The proportion of ALDH^{bright} cell is significantly higher in SDCs than in the parental MDCs. Error bars: mean values ± SD of three replicates; *: p <0.05.*

5.2.4 SDCs are more resistant to cisplatin than MDCs

As a critical hallmark for CSCs, chemo-resistance was also tested. SDCs and their parental MDCs were cultured for 72 h with serially diluted cisplatin concentration (Figure 16 A). The IC_{50} of cisplatin was 2.42 ± 1.23 µM, 3.95 ± 1.52 µM, and 8.10 ± 2.16 µM in MDCs of HeLa, MRIH186, and SiHa, respectively (Figure 16 B). In all cell lines, the SDCs were more resistant to cisplatin than the corresponding MDCs. The IC_{50} of HeLa SDCs was 4.87 ± 0.53 µM, about 2.21-fold of corresponding MDCs. The IC_{50} in MRIH186 and SiHa SDCs was 9.85 ± 1.04 µM and 14.54 ± 0.97 µM. In addition to IC_{50} determination, cell viability was also measured after 72 h of treatment with 5 µM cisplatin. There were still 45.99 ± 2.42%, 65.98 ± 3.93% and 87.19 ± 3.42% of cells viable in HeLa, MRIH186, and SiHa SDCs respectively. However, the viable population was reduced to 16.27 ± 1.57%, 43.88 ± 1.96%, and 71.22 ± 2.57% (Figure 16 C) in corresponding MDCs, respectively, which was significantly lower than in corresponding SDCs (all, $p < 0.05$).

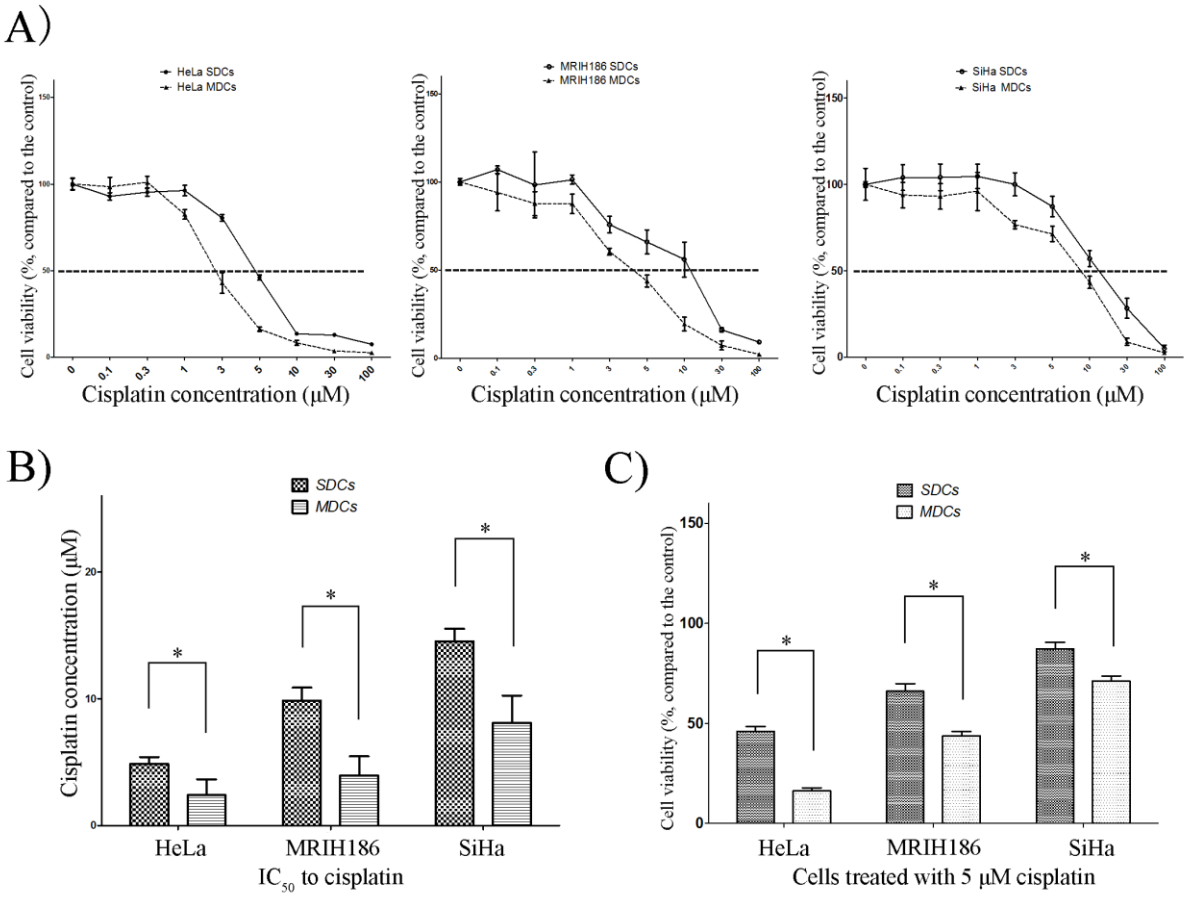

Figure 16: Chemo-resistance to cisplatin in SDCs derived from cervical cancer cell lines vs. in the corresponding MDCs. A) *Cell viability measured by MTT assay after cisplatin treatment (0.1-*

100 µM, 3-fold dilution) in cervical SDCs and MDCs. Dashed lines indicate the 50% viability of cells. ***B)*** *The IC_{50}, calculated from MTT assay data, is higher in SDCs than in MDCs.* ***C)*** *The cellular viability measured by MTT assay after treatment with 5 µM cisplatin in SDCs and in MDCs. Error bars: mean values ± SD of three replicates. *: p <0.05.*

Similar to the response to cisplatin treatment, SDCs also exhibited increased resistance to paclitaxel than the corresponding MDCs of MRIH186 and SiHa. (Figure 17). The IC_{50} of MRIH186 and SiHa MDCs was 3.42 ± 0.90 nM and 3.96 ± 0.33 nM, respectively. The IC_{50} of MRIH186 and SiHa SDCs was 7.58 ± 1.26 nM and 7.43 ± 1.83 nM, with an increase of about 2.21-fold and 1.87-fold, respectively (Figure 17 B).

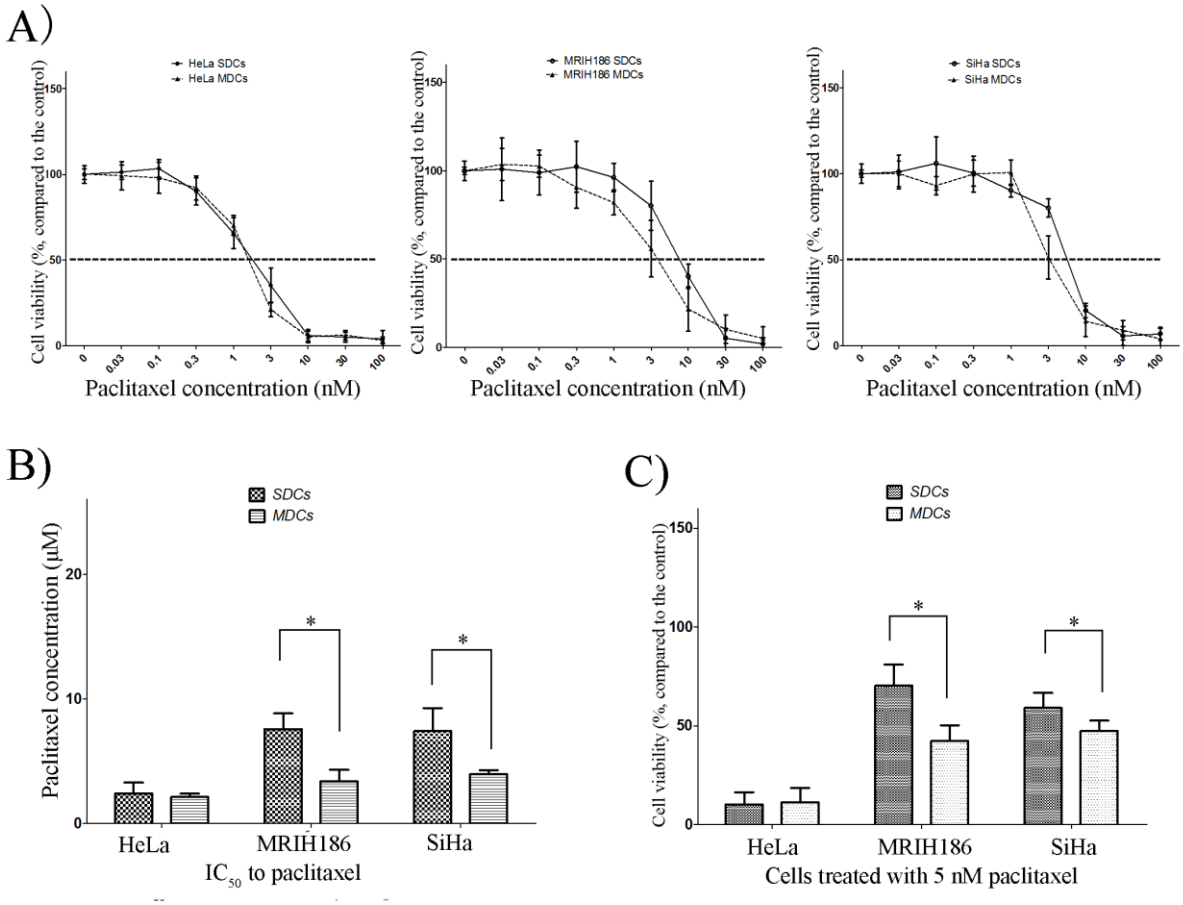

Figure 17: Chemo-resistance to paclitaxel in SDCs derived from cervical cancer cell lines vs. in the corresponding MDCs. *A) Cell viability measured by MTT assay after paclitaxel treatment (0.03-100 nM, 3-fold dilution) in cervical SDCs and MDCs. Dashed lines describe the 50% viability of cells.* ***B)*** *The IC_{50}, calculated from MTT assay data, is lower in MDCs than in SDCs.*

C) *The cellular viability measured by MTT assay after treatment with 5 nM paclitaxel in SDCs and in MDCs. Error bars: mean values ± SD of three replicates. *: p <0.05.*

However, the IC_{50} was 2.14 ± 0.26 nM in HeLa SDCs, which was slightly lower than in HeLa MDCs which had 2.43 ± 0.87 nM, but not significantly different. The cellular viability of SDCs was 10.24 ± 6.12%, 70.21 ± 10.77%, and 59.03 ± 7.66% after 5 nM paclitaxel treatment, while this data was 11.34 ± 7.23%, 42.34 ± 7.89%, and 47.27 ± 5.32% in parental MDCs derived from HeLa, MRIH186, and SiHa cells, respectively (Figure 17 C).

5.2.5 Characterization of CSC-related mRNA expression in MDCs and in SDCs

As described previously for ALDH sorted cells (see 5.1.3), the isolated mRNA from SDCs and MDCs was also tested by real time PCR for the same markers. There were various differences in the mRNA expression between MDCs and corresponding SDCs. Overall, most of the CSC-markers showed an increased expression in SDCs versus MDCs. However, only a few of them showed a meaningful or statistically significant difference. The overall data of mRNA expression is shown in Figure 18.

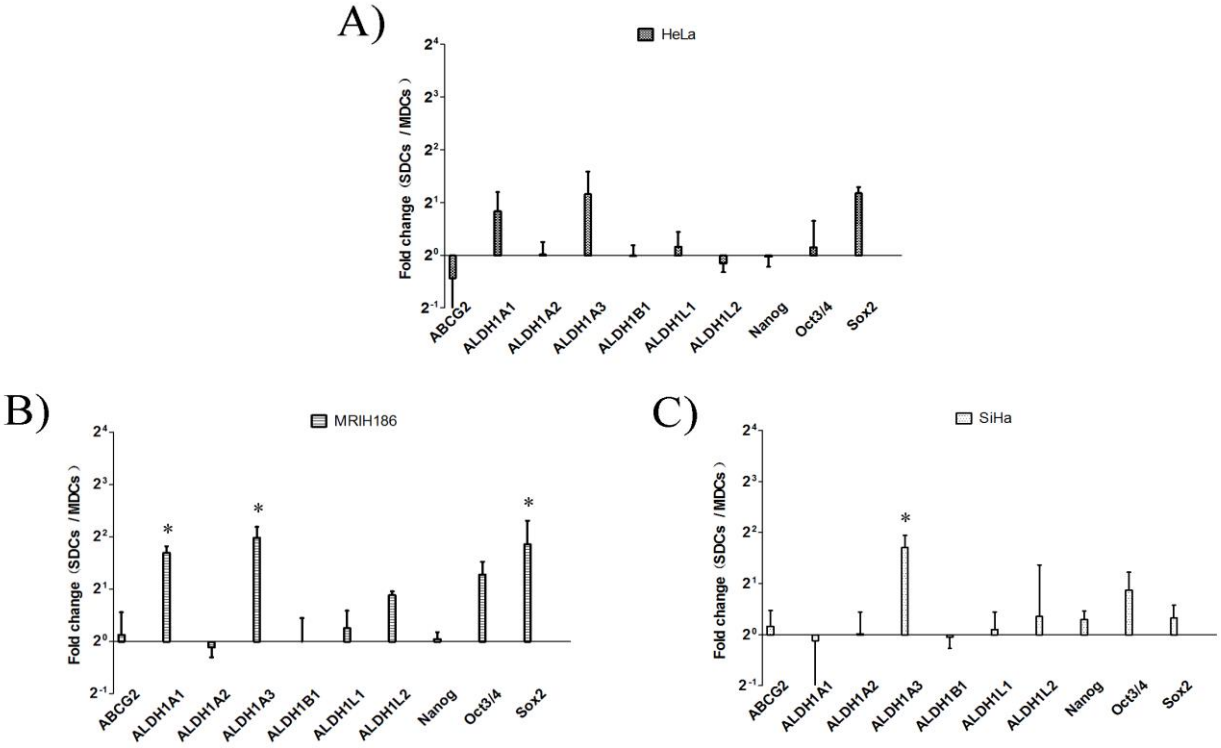

Figure 18: Quantitative Real-time PCR analysis on mRNA expression in SDCs derived from cervical cancer cell lines vs. in the corresponding MDCs. *mRNA isolated from SDCs and MDCs*

was quantified for expression of the CSC-markers. The ratio of mRNA expression (SDCs/MDCs) is shown (delta – delta Ct method). ***A)*** *HeLa;* ***B)*** *MRIH186;* ***C)*** *SiHa. Error bars: mean values ± SD of three replicates. *: p <0.05.*

In HeLa, Sox2 mRNA expression was 2.06-fold higher in SDCs than in MDCs (Figure 18 A). In MRIH186, ALDH1A1, ALDH1A3, Oct3/4 and Sox2 mRNA expression was 3.13-fold, 3.94-fold, 2.42-fold, and 3.62-fold higher in SDCs than in MDCs, respectively (Figure 18 B). In SiHa, the mRNA of ALDH1A3 expression was a 2.58-fold increase in SDCs compared to MDCs (Figure 18 C). To summerize, SDCs contain a higher $ALDH^{bright}$ population and display higher CSC-related properties than MDCs. Considering the differences between SDCs and MDCs, the following experiments were based on SDCs.

5.3 Different responses of ALDH activity to cisplatin treatment and ATRA treatment

Cisplatin induces multiple drug resistance (MDR) in many cancers despite its initial therapeutic effects. Its poor effect on CSCs might be an explanation for this dilemma. ALDH is helpful to reveal the response of CSCs as a CSC-marker in cervical cancer cell lines. Additionally, the effects of ATRA, a potential ALDH inhibitor which might target CSCs, were also observed.

5.3.1 The proportion of $ALDH^{bright}$ cells changes in a bi-phasic manner by cisplatin treatment

In HeLa, MRIH186, and the SiHa cell line, the proportion of $ALDH^{bright}$ cells in SDCs consistently responded in a bi-phasic manner to serial cisplatin concentrations (Figure 19). When the cells were treated with low-dose cisplatin (the threshold was lower than 1 μM in HeLa and SiHa, and was lower than 3 μM in MRIH186), the proportion of $ALDH^{bright}$ cells gradually increased. For example, the $ALDH^{bright}$ cell frequency reached its climax at 55.21% by treatment with 1 μM cisplatin. This is an increase of 1.83-fold compared to the untreated SDCs from SiHa cells. Conversely, concentrations higher than 1 μM led to a reduced $ALDH^{bright}$ cell frequency in a dose-dependent manner (Figure 19 A).

Similar results were also found in HeLa and MRIH186 (Figure 19 B). In HeLa, the proportion of $ALDH^{bright}$ cells reached 30.32% (2.04-fold more than the untreated cells) at the concentration of 1 μM cisplatin. In MRIH186, 3 μM cisplatin increased the proportion of $ALDH^{bright}$ cells to 62.44% (1.67-fold of the untreated cells). In addition to the altered proportion of $ALDH^{bright}$ cells, the mean

fluorescence intensity (MFI) of ALDH was also changed by cisplatin treatment in a bi-phasic way. Overlay-histogram analysis showed that 1 µM cisplatin increased ALDH intensity (the right shift of MFI) in SDCs, while 10 µM reduced the ALDH intensity (the left shift of MFI) in SDCs of HeLa, MRIH186, and SiHa cell lines (Figure 19 C and Table 9).

Based on the bi-phasic response of the proportion of $ALDH^{bright}$ cells, the EC_{50} of up-regulation and down-regulation were determined in each of the cell lines. The EC_{50} of up-regulation was 0.28 ±0.11 µM, 0.82 ±0.30 µM, and 0.27 ±0.15 µM for HeLa SDCs, MRIH186 SDCs, and SiHa SDCs, respectively. The EC_{50} of down-regulation was 12.57 ± 4.21 µM, 15.12 ± 3.17 µM, and 12.19 ± 4.28 µM for HeLa SDCs, MRIH186 SDCs, and SiHa SDCs, respectively. These values of EC_{50} were calculated for use in the following studies.

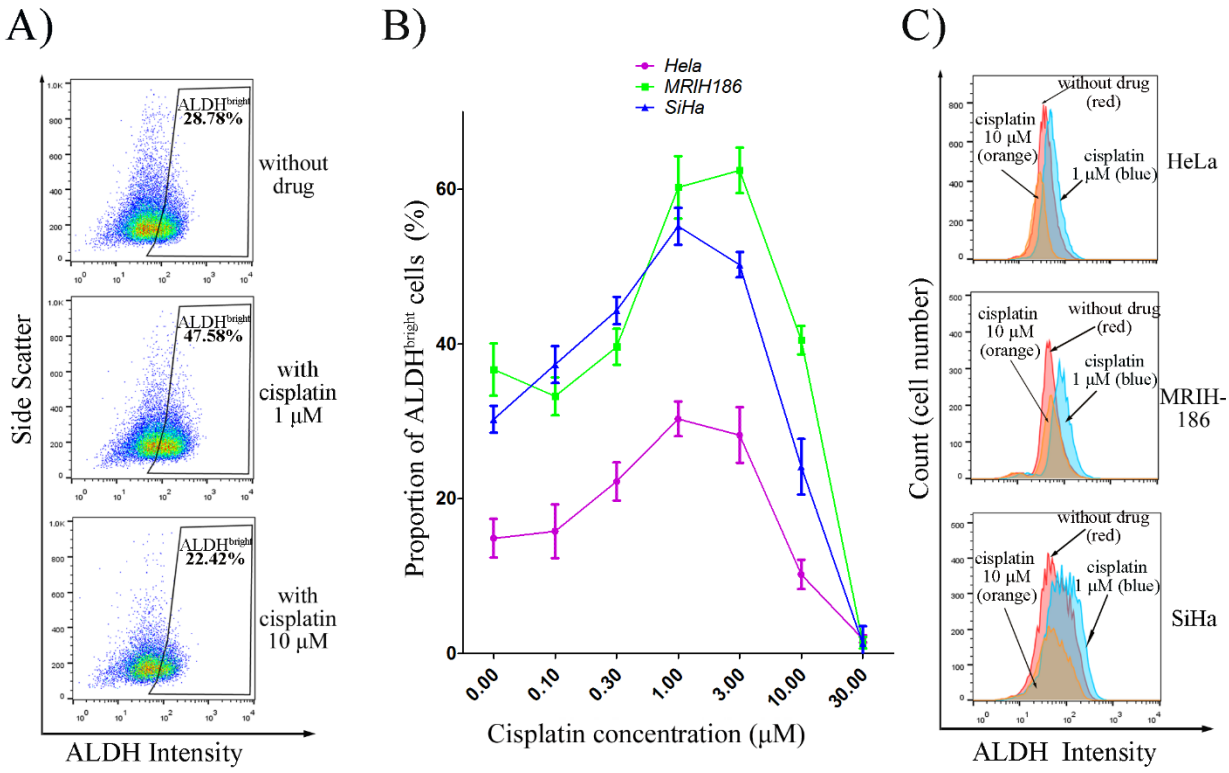

Figure 19: Response of $ALDH^{bright}$ cell frequency by Aldefluor assay staining after titrated cisplatin treatment in SDCs derived from cervical cancer cell lines. A) *Example of bi-phasic alteration in $ALDH^{bright}$ cell frequency in SiHa SDCs. Cells were treated with different concentrations of cisplatin (top plot: 0 µM; middle plot: 1 µM; bottom plot: 10 µM); gating strategy is shown in detail in section 4.3.* ***B)*** *Bi-phasic response of $ALDH^{bright}$ cell frequency is observed after treatment with serial cisplatin concentrations (0.1-30 µM, 3-fold dilution) in the*

SDCs of each cell line investigated. The proportion of ALDH^{bright} cells is read out by Aldefluor assay. Error bars: mean values ± SD of three replicates. ***C)*** *Example of bi-phasic alteration in ALDH MFI (mean fluorescence intensity) in SDCs. Treatment with 1 μM cisplatin results in a right-shift of the MFI, while 10 μM cisplatin results in a left shift of the MFI in cervical SDCs. Data was obtained by Aldefluor assay using the overlay-histogram model.*

5.3.2 ATRA reduces the proportion of ALDH^{bright} cells in SDCs in a dose-dependent manner

Differently to the cisplatin treatment, the proportion of ALDH^{bright} cells in SDCs was inhibited consistently by ATRA treatment in a dose-dependent manner (Figure 20). For instance, in the SDCs of SiHa, the ALDH^{bright} cell proportion was reduced from 30.88 ± 3.82 % to 22.29 ± 3.23% by a treatment with 10 μM ATRA, with a significant left shift of MFI simultaneously (Figure 20 A and B). 1 μM of ATRA did not up-regulate the ALDH^{bright} cells proportion; a slight reduction of ALDH^{bright} cell proportion was found instead. ATRA treatment led to a 4.20% reduction in ALDH^{bright} cell proportion at 1 μM and 15.55% reduction at 10 μM in MRIH186. The MFI of ALDH intensity was dose-dependent in terms of left shift as well. This dose-dependent inhibition of ALDH activity was also found in SDCs derived from SiHa (Figure 20 A). Treatment with 1 μM ATRA led to a 4.56% reduction in ALDH^{bright} cell proportion and 8.59% reduction at 10 μM in SiHa. The MFI of ALDH intensity was also dose-dependent in terms of left shift (Table 9 and Figure 20 C). Taking in account the consistent inhibition of ALDH^{bright} cells proportion, the EC_{50} of ALDH inhibition by ATRA was determined for each cell line. The EC_{50} was 15.05 ± 5.13 μM, 18.22 ± 4.89 μM, and 18.94 ± 3.02 μM for SDCs derived from HeLa, MRIH186, and SiHa, respectively.

Table 9: The changes in MFI after cisplatin treatment or ATRA treatment by Aldefluor assay

	Mean fluorescence intensity (MFI)				
	control	*1 μM cisplatin*	*10 μM cisplatin*	*1 μM ATRA*	*10 μM ATRA*
HeLa	*46.38 ± 1.05*	*56.23 ± 1.37*	*44.13 ± 3.43*	*40.46 ± 1.29*	*34.69 ± 0.87*
MRIH186	*65.43 ± 1.75*	*82.47 ± 11.90*	*66.92 ± 2.86*	*61.23 ± 2.54*	*55.60 ± 14.03*
SiHa	*79.08 ± 1.92*	*113.34 ± 7.14*	*52.17 ± 11.05*	*77.02 ± 2.62*	*72.81 ± 5.94*

Error bars: mean values ± SD of three replicates

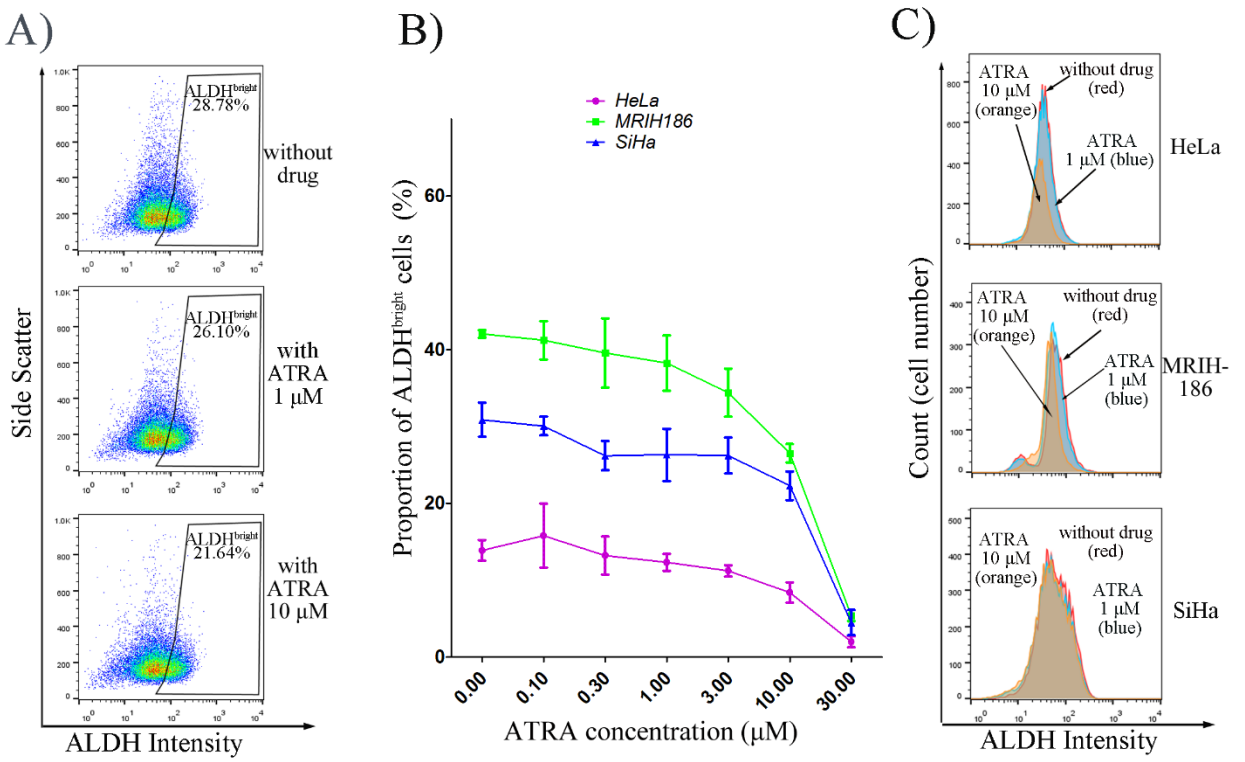

Figure 20: Response of ALDH^{bright} cells by Aldefluor assay staining after titrated ATRA treatment in SDCs derived from cervical cancer cell lines. A) *Example of the proportion of ALDH^{bright} cell reduction in SiHa SDCs. Cells were treated with different concentrations of ATRA (top plot: 0 µM; middle plot: 1 µM; bottom plot: 10 µM); gating strategy is shown in detail in section 4.3.* ***B)*** *The proportion of ALDH^{bright} cells is reduced in a dose-dependent way after treatment with serial ATRA concentrations (0.1-30 µM, 3-fold dilution) in SDCs of each cell line. The proportion of ALDH^{bright} cells is read out via Aldefluor assay. Error bars: mean values ± SD of three replicates.* ***C)*** *Example of consistent reduction (left shift) in ALDH MFI (mean fluorescence intensity) in SDCs. Data was obtained via Aldefluor assay in the overlay-histogram model.*

5.3.3 ATRA inhibits ALDH function competitively, but this competitive effect reverses promptly after ATRA washout

The classical model that explains the kinetic behavior of enzyme reactions is the Michaelis-Menton model [91, 92]. This model is based on the assumption that the substrate binds to the enzyme to form an intermediate complex. The complex subsequently dissociates to the enzyme in its original form and the final product. Reaction rates are measured under the condition that the

product is continuously removed. In reality, this is not always the case. In the present study, ATRA, the investigated reagent, but also a product of the ALDH enzyme, could not be removed before the cells were collected. Therefore, ATRA is able to bind ALDH enzyme as a competitor to BAAA in the Aldefluor assay. To clarify the competitive relationship, different concentrations of ATRA (3 μM, 30 μM, and 300 μM) were added to the reaction buffer before BAAA was added. ATRA decreased the proportion of $ALDH^{bright}$ cells gradually in a dose-dependent way (Figure 21). 3 μM ATRA displayed a slight inhibitory effect to the proportion of $ALDH^{bright}$ cells. 30 μM ATRA decreased $ALDH^{bright}$ population from 9.89% to 2.67% in HeLa, from 38.90% to 7.12% in MRIH186, and from 30.22% to 12.9% in SiHa. 300 μM ATRA reduced the proportion of $ALDH^{bright}$ cells to lower than 1%.

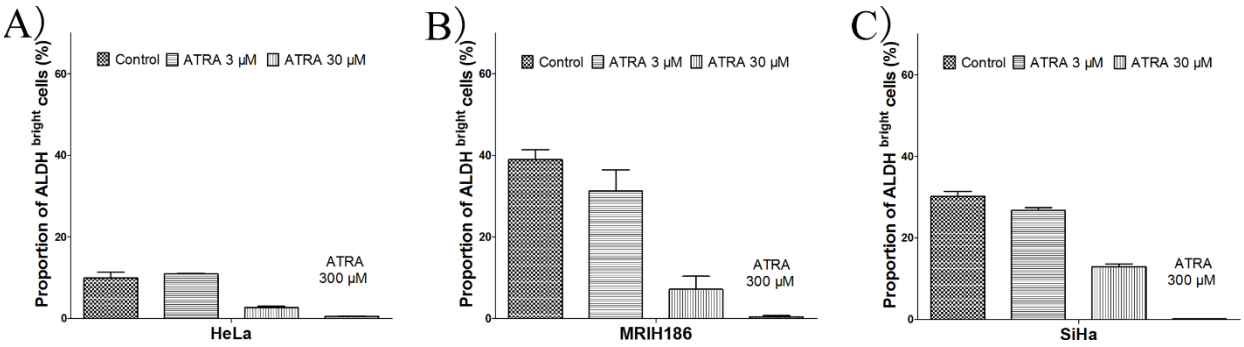

Figure 21: The competitive effect of ATRA to BAAA in the Aldefluor assay. *3 μM, 30 μM, or 300 μM of ATRA were added into tubes before BAAA was added.* ***A)*** *HeLa;* ***B)*** *MRIH186;* ***C)*** *SiHa. Error bars: mean values ± SD of three replicates.*

The binding of ATRA and ALDH might be weak due to the irreversible process of ATRA generation. Considering the fact that Aldefluor assay staining is carried out after cell collection, this procedure (including medium washout and the time consumed for cell collection) might influence the final read-out of the Aldefluor assay. The proportion of $ALDH^{bright}$ cells recovered to the control level immediately after ATRA washout in the SDCs of MRIH186 (Figure 22 B). In the SDCs of HeLa and SiHa, the $ALDH^{bright}$ population after ATRA washout were lower than control, but the proportion restored completely after 30 min incubation at room temperature, which is a simulation of the time necessary for the cell collection (Figure 22 A and C). These experiments indicate that ATRA has a competitive ability to BAAA in the Aldefluor assay. However, this competitive ability is reversible. ATRA removal recovers the function of ALDH promptly. The

washing out and cell collection procedure before Aldefluor assay staining is sufficient to remove the competitive effect of ATRA to BAAA.

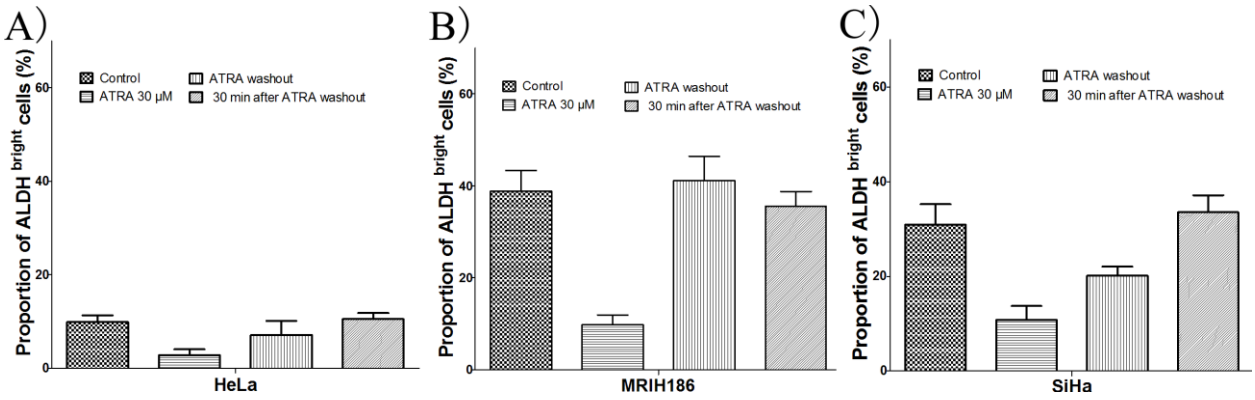

Figure 22: Recovery of the ALDH^{bright} population after ATRA washout in Aldefluor assay. *Cells were incubated with 30 µM ATRA for 30 min at 37 °to let ATRA bind to ALDH. Aldefluor assay staining was carried out immediately following ATRA washout, or after 30 min incubation at room temperature following ATRA washout.* ***A)*** *HeLa;* ***B)*** *MRIH186;* ***C)*** *SiHa. Error bars: mean values ± SD of three replicates.*

5.3.4 The proportion of ALDH^{bright} cells increased by low-dose treatment with cisplatin can be overcome by ATRA co-treatment

In order to counteract the up-regulation of ALDH^{bright} population resulting from low-dose cisplatin, the combined treatment of ATRA and cisplatin was carried out. According to the EC_{50} in ALDH down-regulation, 12 µM, 18 µM, and 18 µM ATRA was used for the combination of ATRA and cisplatin in HeLa, MRIH86, and SiHa, respectively. After the combination with ATRA, the up-regulation of the ALDH^{bright} cells proportion was gradually overcome (Figure 23 C). In SDCs derived from HeLa, the peak of up-regulation was entirely overcome by administration of ATRA. The up-regulation peak was considerably reduced by co-treatment with ATRA in SDCs derived from MRIH186 and from SiHa. ATRA antagonized the increase of ALDH^{bright} cell proportion from 30.32 ± 3.89 % to 8.26 ± 2.99 % at 1 µM cisplatin, and decreased the proportion from 10.21 ± 3.27 % to 5.51 ± 3.29 % at 10 µM cisplatin in HeLa. In MRIH186, ATRA antagonized the increase of the ALDH^{bright} population from 60.26 ± 6.29 % to 24.21 ± 6.14% induced by 1 µM cisplatin treatment, and decreased the proportion from 40.51 ± 3.17 % to 16.12 ± 2.23 % with 10 µM cisplatin. In SiHa, ATRA antagonized the ALDH^{bright} proportion from 55.21 ± 4.14 % to 25.37

± 5.61 % with 1 µM cisplatin, and decreased the portion from 24.12 ± 6.23 % to 17.89 ± 4.89 % with 10 µM cisplatin (Figure 23 A and C). The intensified MFI was also released by ATRA treatment (Figure 23 B).

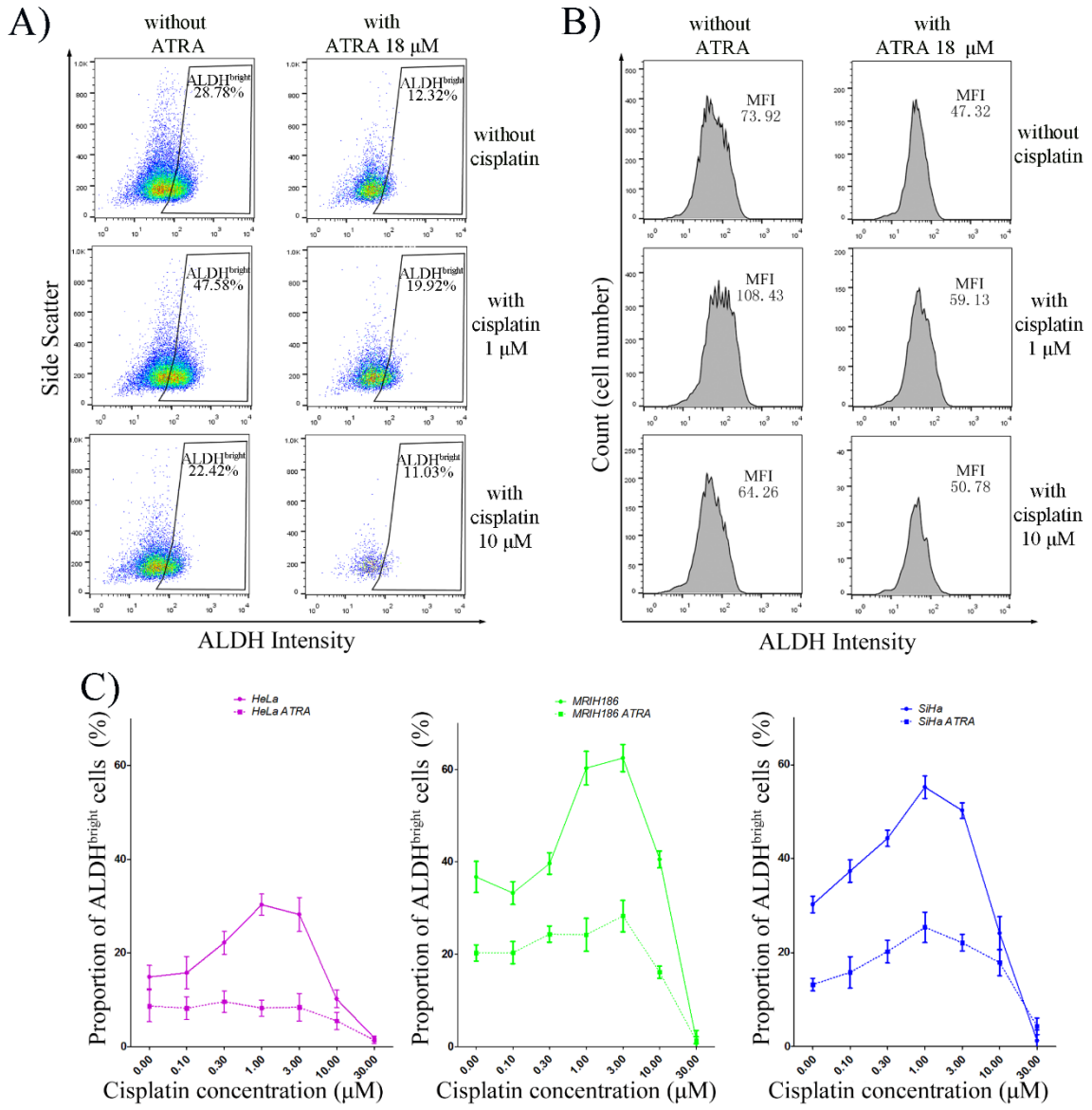

Figure 23: ATRA overcomes the increased ALDH^{bright} population caused by low-dose cisplatin in SDCs derived from cervical cancer cell lines. A) *Example of increased proportion of ALDH^{bright} cells reduced by ATRA in SiHa SDCs. Data obtained by Aldefluor assay.* ***B)*** *Example where ATRA treatment reverses the increased ALDH intensity after low-dose cisplatin treatment in SiHa SDCs. Data obtained by Aldefluor assay presented as histogram.* ***C)*** *ATRA counteracts the increased ALDH^{bright} population resulting from low-dose cisplatin in SDCs; ALDH^{bright} cell proportion is*

read out by Aldefluor assay. Error bars: mean values ± SD of three replicates.

5.4 ATRA partially overcomes the detrimental effects caused by cisplatin treatment

ATRA has the ability to overcome the increased proportion of $ALDH^{bright}$ cells caused by low-dose treatment with cisplatin. The co-effects of ATRA and cisplatin were further investigated in the following aspects including: cell proliferation, apoptosis, stemness (CFE and SFE), invasiveness, and motility. The mRNA expression of the CSC markers was also measured.

According to the values calculated in section 5.3, treatment by drug concentrations of EC_{50} values of up-regulation or down-regulation in $ALDH^{bright}$ cells proportion were used in the following experiments. In brief, the EC_{50} value of the up-regulation by cisplatin was assigned as "cisplatin-low"; the EC_{50} value of the down-regulation by cisplatin was assigned as "cisplatin-high"; and the EC_{50} value of the down-regulation by ATRA was assigned as "ATRA".

5.4.1 ATRA enhances the inhibition of cervical cancer proliferation by cisplatin

Calculation of combination index (CI) is a method to evaluate the cooperative-effects of drugs by MTT assays. Addition of ATRA enhanced the inhibition of cell proliferation with both cisplatin-low and cisplatin-high treatments (Table 10). When ATRA was combined with cisplatin-low, the CI was 0.93, 0.92, and 1.06, which suggested an additive effect of both drugs in SDCs. The CI value was 0.98 in MRIH186 for the combination treatment of ATRA and cisplatin-high. ATRA and cisplatin-high synergistically inhibited cell growth in HeLa cells with a CI value of 0.66 and in SiHa of 0.78.

Table 10: Combination index for the co-administration of ATRA and cisplatin

	HeLa	*MRIH186*	*SiHa*
	ATRA	*ATRA*	*ATRA*
Cisplatin-low	*0.93*	*0.92*	*1.06*
Cisplatin-high	*0.66*	*0.98*	*0.78*

CI values less than 0.9 suggest synergism; 0.9 ≤CI values ≤1.1 suggest additive effects; CI values more than 1.1 suggest antagonism.

5.4.2 ATRA promotes apoptosis induction by cisplatin

As an anticancer agent, cisplatin functions by the induction of apoptosis. The proportion of

apoptotic cells was accessed by Annexin-*V*/PI staining assay by flow cytometer. In the control group, SDCs from all cell lines had less than 10% apoptotic cells. As shown in Figure 24, the apoptotic proportion in SiHa SDCs was 11.19 ± 1.69% after cisplatin-low treatment, and 50.23 ± 5.62% after cisplatin-high treatment. In MRIH186 SDCs, the apoptotic proportion was 15.84 ± 3.71% and 40.11 ± 5.09% with cisplatin-low and cisplatin-high treatment, respectively. The ratio of the apoptotic cells in HeLa SDCs was 13.12 ± 3.15% and 42.51 ± 3.94% for cisplatin-low and cisplatin-high treatment, respectively. Moreover, ATRA alone also led to cellular apoptosis. The apoptotic proportion after ATRA treatment was 22.29 ± 0.92%, 21.32% ± 3.21%, and 22.23 ± 2.09% in SDCs of HeLa, MRIH186, and SiHa, respectively. The apoptotic ratio in HeLa SDCs was increased to 27.17 ± 2.01% or 55.89 ± 5.23% by the combination treatment of ATRA with cisplatin-low or with cisplatin-high. Similarly, the corresponding data in MRIH186 SDCs was 25.11 ± 1.80% or 45.02± 3.55%, and in SiHa SDCs was 25.28 ± 1.98% or 57.21 ± 4.23%. The apoptotic proportion in the three cell lines after treatment with the combination of ATRA, and cisplatin-low was significantly higher than with cisplatin-low alone ($p < 0.05$; Figure 24 B).

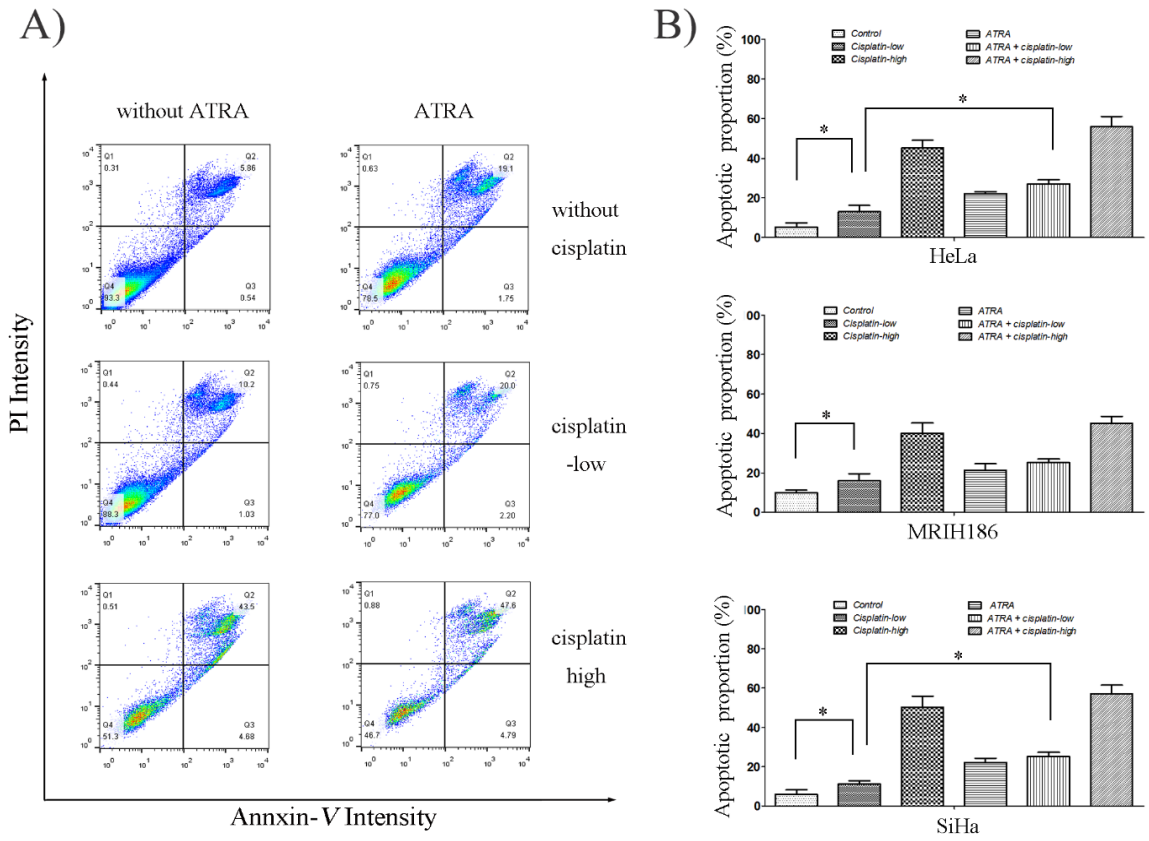

Figure 24: Flow cytometric apoptosis assay by Annexin-V/PI staining in SDCs derived from

cervical cancer cell lines. A) *The populations of SiHa SDCs were determined in the four quadrants: live cells (Annexin-V^-/PI^-, lower-left quadrant), early apoptotic cells (Annexin-V^+/PI^-, lower-right quadrant), late apoptotic cells (Annexin-V^+/PI^+, upper-right quadrant), and necrotic cells (Annexin-V^-/PI^+, upper-left quadrant). Both lower-right and upper-right quadrant were counted as apoptotic proportion.* ***B)*** *Quantification of apoptotic proportion in cervical SDCs after treatment with cisplatin-low, cisplatin-high, ATRA and their combination. Error bars: mean values ± SD of three replicates. *: $p < 0.05$.*

5.4.3 ATRA decreases the stemness enhanced by cisplatin-low treatment

Cisplatin-high treatment diminished the CFE of SDCs-derived cells. ATRA also inhibited the CFE. Conversely, cisplatin-low incited this stemness-related ability in cervical SDCs. In SiHa, the CFE was 42.70 ± 3.04% after cisplatin-low treatment, which is a 12.37% increase over the control. The combination of ATRA and cisplatin-low reversed this efficiency to 25.04 ± 2.94%. Similar results were also found in SDCs of HeLa and MRIH186 (Figure 25).

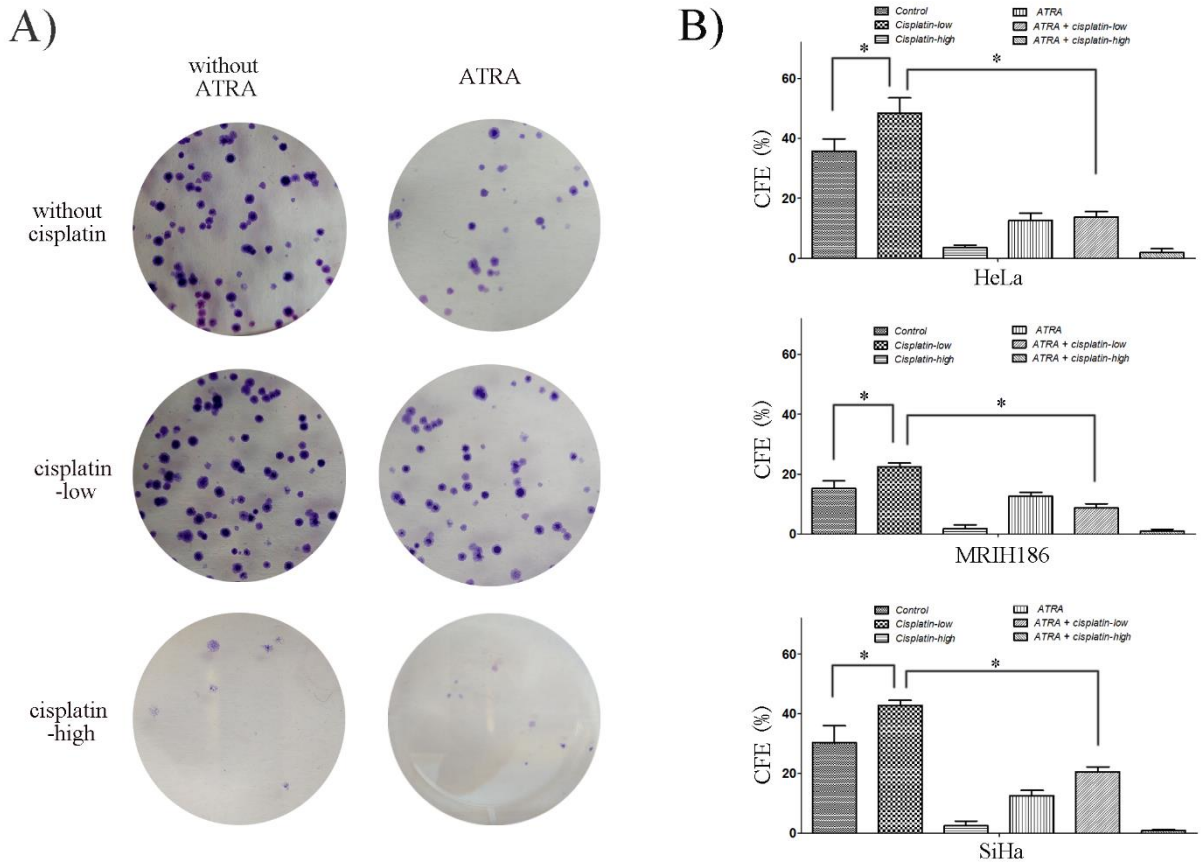

Figure 25: Colony formation ability in SDCs derived from cervical cancer cell lines after

cisplatin-low, cisplatin-high, ATRA treatment, and their combinations. A) *Representative clones formed by SiHa SDCs; dark blue dots represent the colonies.* ***B)*** *Quantitation of colony formation efficiency (CFE). Three replicates were counted. Mean values ±SD were plotted. *: p <0.05.*

SFE was also inhibited significantly by treatment with a cisplatin-high dose or ATRA alone. Cisplatin-low incited and enhanced this ability in cervical SDCs. For example, the SFE was 8.70 ±2.73% in SiHa, and cisplatin-low enhanced this efficiency to 17.33 ±3.52%. When ATRA was combined with cisplatin-low, SFE was reduced to 8.25 ±2.12% (Figure 26 A and B). Comparable effects were also observed in HeLa and MRIH186 (Figure 26 B).

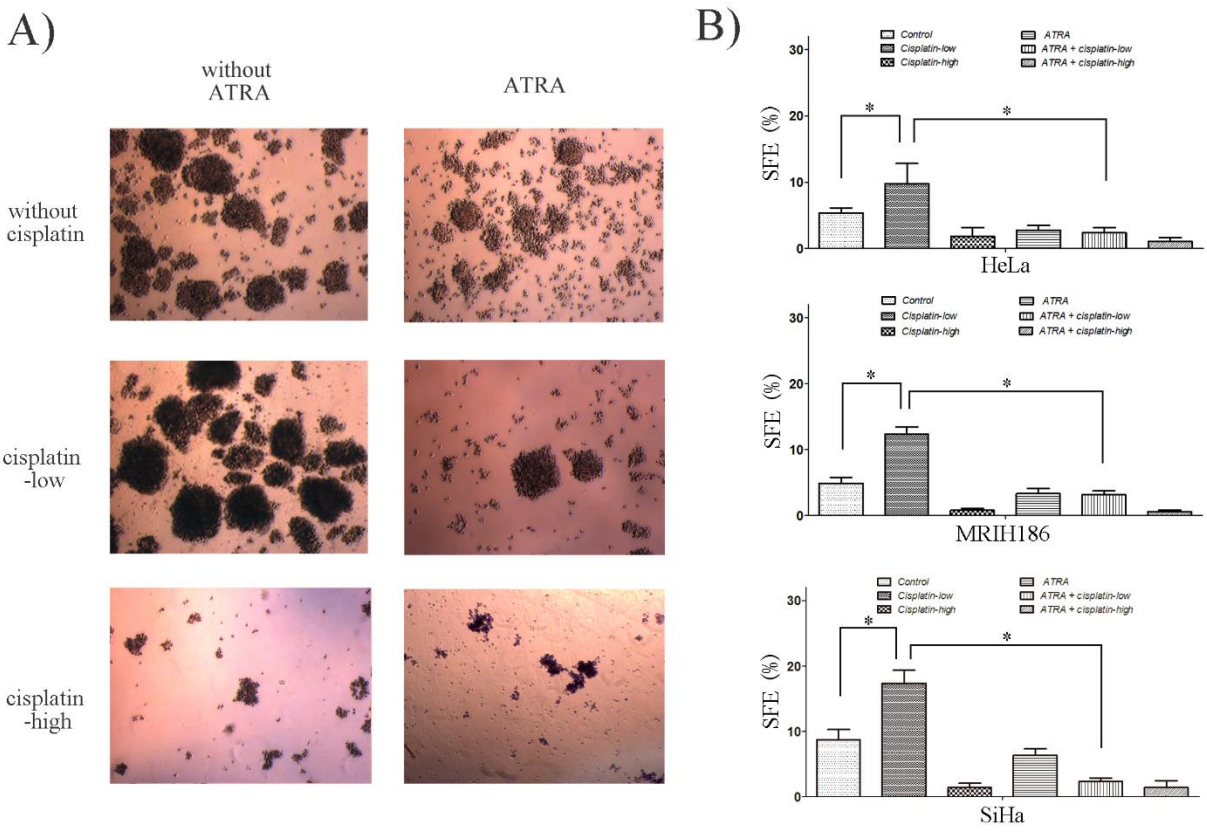

Figure 26: Spheroid formation ability in SDCs derived from cervical cancer cell lines after cisplatin-low, cisplatin-high, ATRA treatment, and their combinations. A) *Representative spheroids formed by SiHa SDCs; the magnification is 50×.* ***B)*** *Quantitation of spheroid formation efficiency (SFE). Three replicates were counted. Mean values ±SD were plotted. *: p <0.05.*

5.4.4 ATRA restricts cell invasiveness

As shown in Figure 27 A and B, the trans-well migrated cell number was 99.67 ±11.59 cells/field

in the control group of SiHa SDCs. A comparable number of cells was found in the cisplatin-low group with 95.33 ± 24.13 cells/field. However, treatment with cisplatin-high or ATRA alone reduced this number to 13.33 ± 24.13 cells/field or 32.00 ± 7.55 cells/field, respectively. Combination of ATRA and cisplatin-low reduced the trans-well migrated cell number to 21.33 ± 12.34 cells/field, while co-administration of ATRA and cisplatin-high decreased the number to 2.33 ± 2.25 cells/field. These results suggested that both cisplatin-high and ATRA treatment impaired the cellular invasiveness. The combination of cisplatin and ATRA enhanced this inhibition. A similar tendency was also found in SDCs of HeLa and MRIH186, and the detailed data is shown in Figure 27 B.

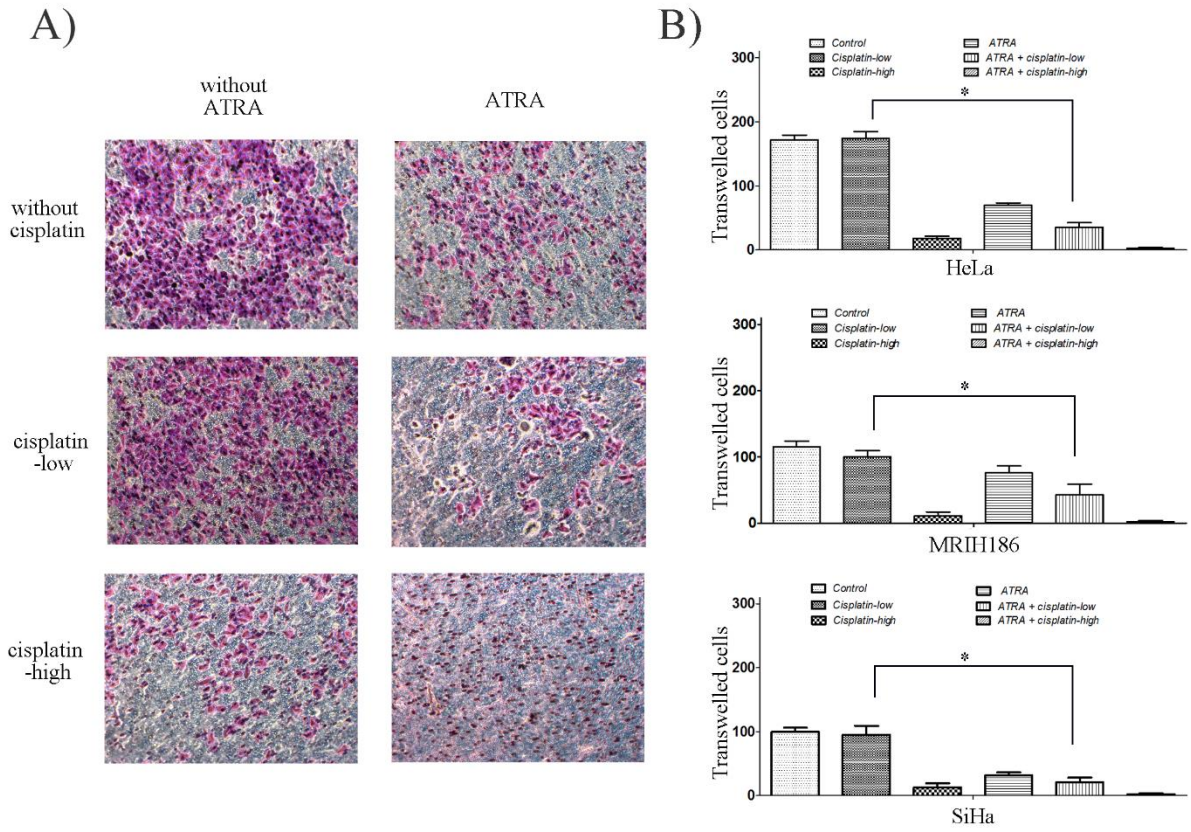

Figure 27: Invasiveness of SDCs derived from cervical cancer cell lines after cisplatin-low, cisplatin-high, ATRA treatment, and their combinations. A) *Representative photos of cell invasion assay in SiHa SDCs. The magnification is 100×.* ***B)*** *Quantitation of cell invasiveness. Three replicates were measured. Mean values ±SD were plotted. *: p <0.05.*

5.4.5 The enhanced motility caused by cisplatin-low is reduced by ATRA treatment

The scratching assay was employed to observe the cellular motility. From Figure 28 A and B, it

was shown that the cellular moving motility in the control group of SiHa SDCs was 15.12 ± 0.95 µm/h, while the cell motility was increased to 32.60 ± 2.71µm/h after cisplatin-low treatment and it was reduced to 15.75 ± 2.58 µm/h or 12.78 ± 3.40 µm/h after cisplatin-high or ATRA treatment. Interestingly, the combination treatment of cisplatin-low and ATRA reduced the motility to 15.56 ± 1.19 µm/h and the combination treatment of cisplatin-high and ATRA lowered the motility to 3.90 ± 1.03 µm/h.

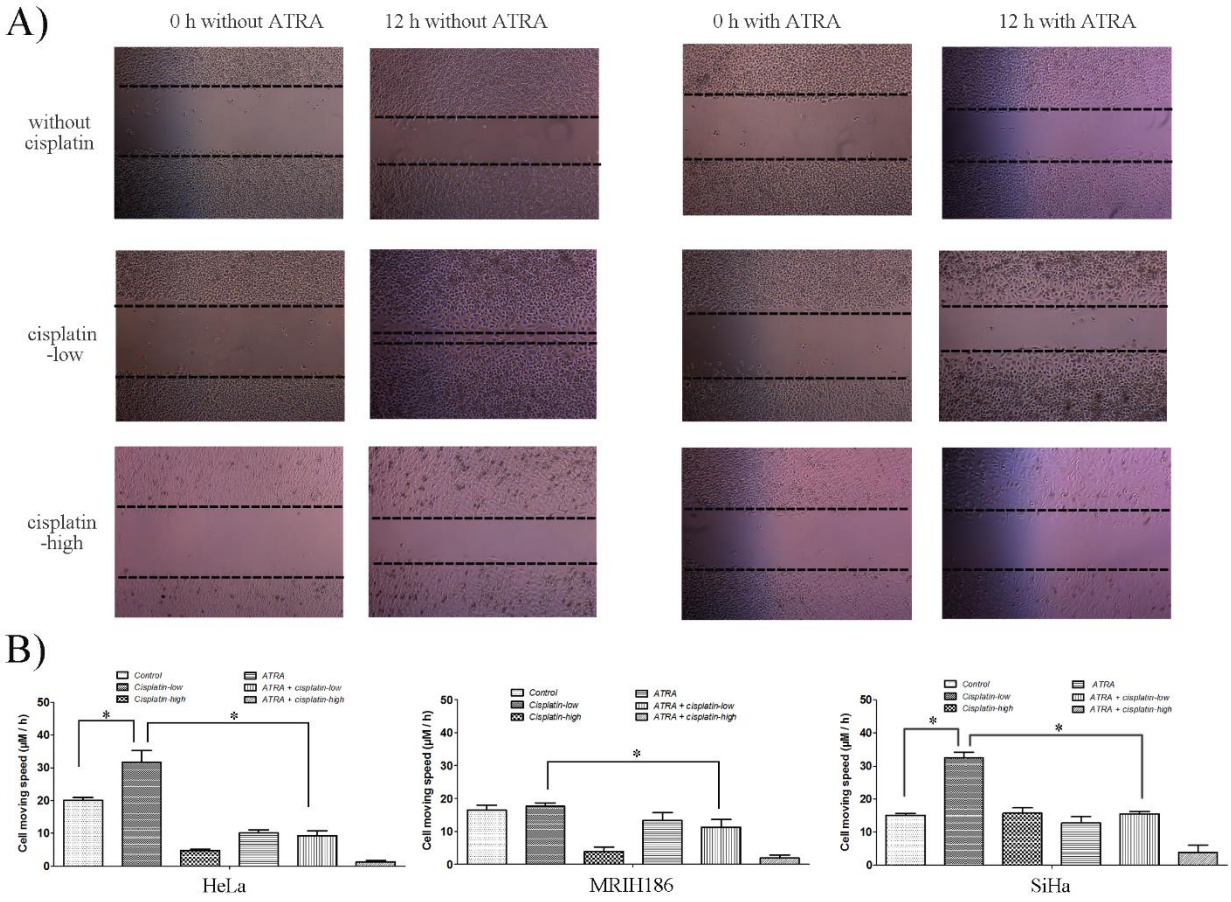

Figure 28: Cellular motility of SDCs derived from cervical cancer cell lines after cisplatin-low, cisplatin-high, ATRA treatment, and their combinations. A): *Representative photos of scratching assay in SiHa SDCs; the magnification is 50×.* ***B)*** *Quantitation of cell motility. Three replicates were measured. Mean values ± SD were plotted. *: p <0.05.*

In HeLa SDCs, the cell motility was 20.04 ± 1.63 µm/h, and it was increased to 31.64 ± 7.06 µm/h or 4.28 ± 0.78 µm/h after cisplatin-low or cisplatin-high treatment, while ATRA reduced the cell motility to 10.11 ± 1.65 µm/h. When the ATRA was combined with cisplatin-low, the cell motility

was reduced to 9.28 ± 2.64 μm/h. After the treatment with ATRA and cisplatin-high, the cell motility was reduced to 1.25 ± 0.87 μm/h. In MRIH186 SDCs, the moving motility of the cells in the control group was 16.42 ± 1.21 μm/h. The motility was 17.6 ± 1.77 μm/h, 5.61 ± 4.58 μm/h, and 13.29 ± 4.29 μm/h under the treatment with cisplatin-low, cisplatin-high, and ATRA, respectively. However, the combination of ATRA with cisplatin-low or cisplatin-high reduced the cell motility to 11.24 ± 4.11 μm/h or 3.61 ± 1.23 μm/h, respectively. The details and statistical significance are shown in Figure 28.

5.4.6 Characterization of CSC-related mRNA expression after cisplatin or/and ATRA treatment

The mRNA expression of the CSC-markers was variably changed by the different combination of drugs in the three cell lines. The ALDH1A3 and ALDH1A1 were generally up-regulated by cisplatin treatment and down-regulated by ATRA treatment. The ALDH1A1 was increased (1.81 to 5.39-fold) by cisplatin, and decreased (1.21 to 3.33-fold) by ATRA. The ALDH1A3 was increased (1.42 to 6.38-fold) by cisplatin, and decreased (1.05 to 3.05-fold) by ATRA. ALDH1A2, ALDH1B1, ALDH1L1, and ALDH1L2 were stably expressed after the different treatments in all cell lines, and only negligible variation was detected.

The mRNA of ABCG2 was able to be induced by cisplatin treatment (2.56 to 10.25-fold increase). ATRA treatment also up-regulated the ABCG2 mRNA expression (1.56 to 1.90-fold). The combination of ATRA could not reverse the cisplatin-induced increase of ABCG2 expression. Either cisplatin-low or cisplatin-high led to the up-regulation of Sox2 expression (1.92 to 6.21-fold). The highest effects were found in SiHa, being 6.21-fold higher than control after cisplatin-high treatment. ATRA treatment was able to restrict this up-regulation. The expression of Oct3/4 was increased in MRIH186 after cisplatin treatment (2.16-fold); however, no significant change was observed in Hela and SiHa. The response of Nanog expression to the different treatments varied in less than 2-fold and not significantly in the different cell lines. ATRA alone had slight effects on mRNA expression. The addition of ATRA had little effect on the up-regulation of Sox2 that was increased by cisplatin treatment. The overall data of mRNA expression is listed in Figure 29.

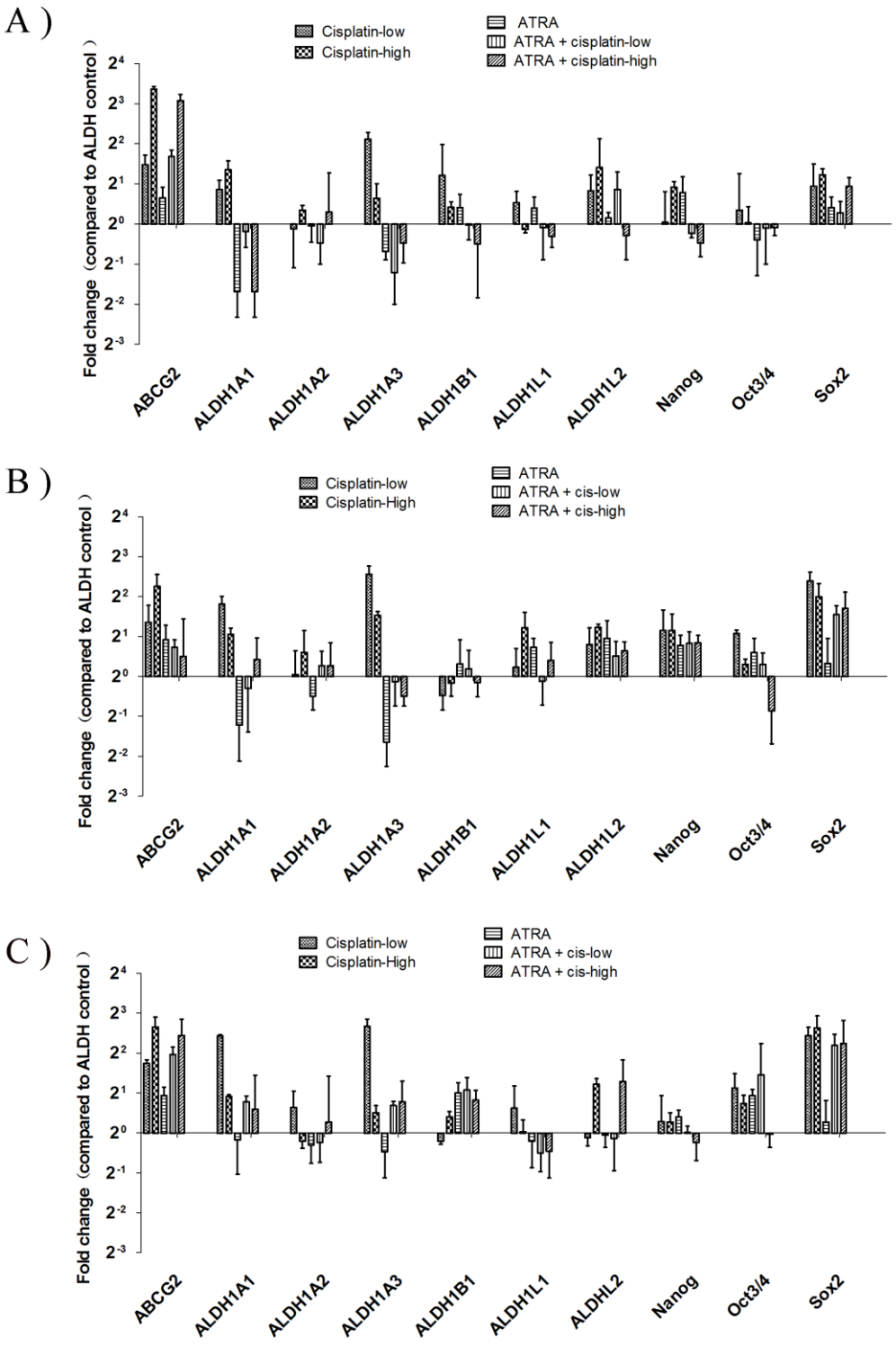

Figure 29: Real-time PCR analysis on mRNA expression in cervical SDCs after cisplatin or/and ATRA treatment. *mRNA isolated from drug-treated cells was quantified for expression of the CSC-markers. The ratio of mRNA expression (each treatment group/control group) is shown (delta – delta Ct method).* ***A)*** *HeLa;* ***B)*** *MRIH186;* ***C)*** *SiHa. Error bars: mean values ±SD of duplicates.*

6. Discussion and conclusions

This study focused on the response of the proportion of $ALDH^{bright}$ cells in SDCs after cisplatin or/and ATRA treatment. Technically, the current study adopted spheroid culture, a sort of 3-D culture method, and carried out the further experiments using spheroid-derived cells. The data in the first part confirms that the high ALDH activity is a marker to distinguish cells with CSC-properties from non-CSCs. The subsequent investigation discovered that cisplatin treatment led to a biphasic response of the $ALDH^{bright}$ population. Low-dose cisplatin treatment, which is in a serum-available range, resulted in several detrimental effects, although applied concentration of cisplatin also led to apoptosis of cervical cancer cells. This result might be an explanation for the findings in clinical trials that some patients cannot benefit from NACT. ATRA reduces the proportion of $ALDH^{bright}$ cells in a dose-dependent manner and releases partial cisplatin-related detrimental effects. These findings highlight the importance of cisplatin treatment optimization and suggest that ALDH-targeting might be meaningful for cervical cancer treatment.

6.1 High ALDH activity is associated with CSC-properties

In the presence of nicotinamide adenine dinucleotide phosphate (NADP) or nicotinamide adenine dinucleotide (NAD), ALDH plays its basic roles in the oxidation of intracellular aldehydes to carboxylic acids [93] (Figure 30 A). Earlier methods used to determine ALDH expression were based on detecting enzyme activity or immunoblotting of enzymes in cell lysates [7]. The Aldefluor assay uses the catalytic process from colorless BAAA to fluorescent BAA^- [94] (Figure 30 B). Given that the functional assay can be carried out on the vital cells, this kit makes it possible for the selection of labeled cells for the subsequent experiments. In light of this valuable progress, a lot of research focusing on $ALDH^{bright}$ cells has since revealed the crucial significance of this sub-population of cells, which possess CSC-properties such as protection from toxic drugs, self-renewal ability, and stemness-like characteristics [95, 96].

The deadly property of CSCs is chemo-resistance, which has garnered the most attention clinically [97]. The presented results confirm that $ALDH^{bright}$ cells that have enhanced CSC-properties are more resistant to both cisplatin and paclitaxel than $ALDH^{low}$ cells, regarded as tumor bulk cells. The IC_{50} to cisplatin is significantly higher in $ALDH^{bright}$ cells than in $ALDH^{low}$ cells. In other

words, the viability of ALDH^{bright} cells is greater than of ALDH^{low} cells after drug treatment with equal concentrations (Figure 8). This matches previous studies in cervical cancer and other malignancies. In addition to cisplatin and paclitaxel, there is an extended list of chemo-reagents that includes: cyclophosphamide, temozolomide, irinotecan, epirubicin, and doxorubicin [35, 97]. Given the reported functions of ALDH enzymes, it is not surprising that ALDHs are regarded as detoxification enzymes that protect cells against various endogenous and exogenous hazards [3]. Interestingly, ALDH might neutralize toxic drugs by only binding to them. Dead enzymes are gene products (proteins) that lack key residues required for catalytic activity. It has been reported that isotypes of ALDH, such as ALDH1A1, work as a dead enzyme in certain conditions [98]. Moreover, ALDH performs multi-functions including ester hydrolysis, serving as ultraviolet light absorption, and hydroxyl radical scavenging [99]. On the basis of these disruptions, ALDH plays the roles of a guardian in protecting cells.

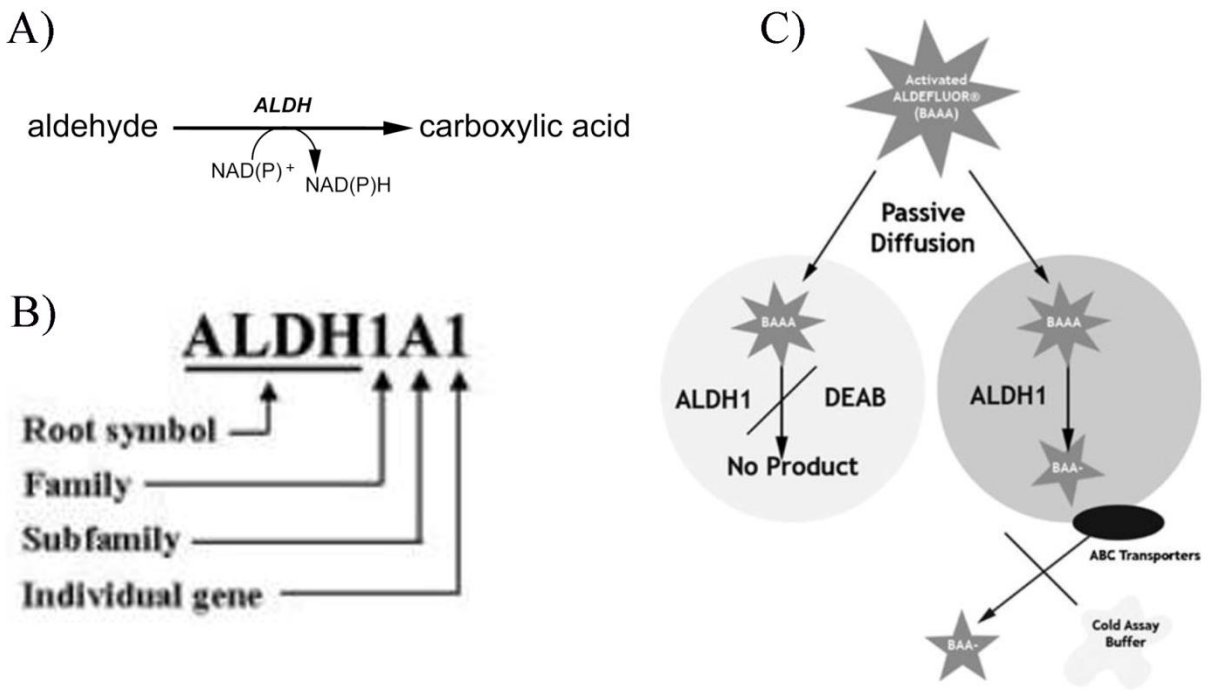

Figure 30: Illustration of the nomenclature system for ALDH genes and schematic principle of Aldefluor assay. A) *ALDH oxidizes aldehydes to the corresponding carboxylic acid.* ***B)*** *For naming each gene, the root symbol ALDH is followed by the Arabic numeral representing the family, and when needed, a letter which designates the subfamily. The Arabic numeral which follows the letter denotes the individual gene within the subfamily.* ***C)*** *Cells uptake BAAA by*

passive diffusion and then convert it into negatively-charged BAA$^-$. BAA$^-$ is retained inside cells, causing the subset of ALDH^{bright} cells to become highly fluorescent. As a negative control, DEAB, a specific ALDH1 inhibitor, is used to define the threshold of ALDH^{bright} cells. The figure is adapted from an information sheet on the Aldefluor assay (www.stemcell.com).

ALDH^{bright} cells form significantly more tumor clones in an adherent condition and more tumor spheroids in a floating condition than ALDH^{low} cells [40, 43, 95]. The greater CFE and SFE suggest that ALDH is a marker for higher self-renewal ability in addition to drug resistance (Figure 9 and 12). By using the same kit, Liu et al. reported the ALDH^{bright} cells could form a tumor xenograft but ALDH^{low} cells could not [40]. They concluded that these ALDH^{bright} cervical cancer cells possessed the ability to self-renew and had enhanced tumorigenicity. Our data are in line with this hypothesis. Importantly, numerous studies have suggested that high cellular ALDH activity is indicative of the presence of CSCs [95]. The mRNA profile of stemness-related TFs also supports this concept. In SiHa cells, the investigated TFs, Oct3/4, Sox2, and Nanog, are generally increased in ALDH^{birght} cells compared to ALDH^{low} cells. These markers are found in an increased status in MRIH186, consistently. However, only Sox2 is found increased in HeLa. This might be ascribed to the loss of Oct3/4 and Nanog in the HeLa cell line, which has been repeatedly reported in other studies [43, 100]. Sox2 is associated with early events of carcinogenesis in cervical epithelial cells [20]. Both *in vitro* and *in vivo* studies have shown that cervical cancer cells with over-expressed Sox2 exhibited increased radio-resistance, and tumorigenicity [23, 24]. ABCG2, another guardian of CSCs in many cell lines, is also increased in ALDH^{bright} compared to ALDH^{low} cells. High expression levels of ABCG2 and ALDH enzymes in CSCs suggests that these molecules might cooperate in the development of drug resistance in cancers [3]. By confirming that the ALDH^{bright} cells harbor important CSC-properties such as chemo-resistance, enhanced self-renewal ability, and increased stemness-related markers, our data reinforce the hypothesis that ALDH is a CSC-marker in cervical cancer.

Aldefluor assay offers a great advantage for closely observing ALDH^{bright} subset cells; however, it is still a matter for deeper investigation owing to the numerous members of the ALDH supergene family. More than 160 ALDH cDNAs or genes have been isolated, and 19 isotypes of ALDH have

been termed, based primarily on evolutionary differences and amino acid homology [94, 101]. A standardized gene nomenclature system was established in 1998 (www.aldh.org; Figure 30 B). Some reports identified ALDH1A1 as the main enzyme supporting the discovered function, especially in stemness-related properties [102]. Additionally, other studies have found enzymatic participation of ALDH1A3, and ALDH1L2 in different types of tumor [93]. These multiple ALDH isoforms may contribute not only to the readout of Aldefluor assay but also to cellular functions in a tissue-specific role. Thus, it is controversial which isotype supports the readout of Aldefluor assay. To determine the ALDH isotypes measured by this assay, characterization of mRNA pattern is a reasonable method for identification. Considering numerous reports that DEAB of the enzyme inhibitor of the ALDH1 family, and the importance of ALDH1-signaling pathway, the expression of isotypes belonging to the ALDH1 family was investigated [89]. The initial result highlights ALDH1A1 and ALDH1A3 for their differential expression between $ALDH^{bright}$ and $ALDH^{low}$ cells. The variation in these two subtypes matches the alternation reflected by Aldefluor assay. Other isotypes are stably expressed between different ALDH statuses. Furthermore, the expression of ALDH1A1 and ALDH1A3 are also changed in the same way with ALDH activity after cisplatin and ATRA treatment. The expression of other isotypes was negligibly altered by cisplatin treatment. These data indicate that ALDH1A1 and ALDH1A3, two RA-producing ALDH isotypes, are possibly the predominant ALDH1 isotypes detected by Aldefluor assay in cervical cancer cells. The Table 11 is an overview of ALDH1 isotypes. ALDH1A2 is the first ALDH isotype expressed during embryogenesis. ALDH1A1 and ALDH1A3 have a more limited role during development. In these isotypes, ALDH1A3 is the most catalytically efficient enzyme, and ALDH1A1 is the least potent of the three enzymes. Among RA-producing ALDH isotypes, ALDH1A1 and ALDH1A3 (but not ALDH1A2) are the most common isotypes related to a poor prognosis in a diverse range of malignant tumors [96]. This might be attributed to its aforementioned CSC-properties. In addition to the accumulation of ALDH1A1 or ALDH1A3 in cancer with poor clinical outcome, there have been a few reports about the increase of other isotypes such as ALDH1B1/L2,which are also found in some cancers [103, 104]. This might be attributable to the fact that the dominant isotype is cell- or tissue-dependent [99, 105, 106]. Therefore, the isotype of ALDH should be clarified more clearly and be the focus of further study.

Table 11. Overview of ALDH1 family

Family	*isotypes*	*NAD or NADP$^+$ dependent [93]*	*Sub-cellular distribution*	*Preferential Substrate*	*Tissue Distribution*	*Chromosomal Localization [102]*
ALDH1	*ALDH1 A1*	*NAD dependent*	*Cytosol*	*Retinal*	*Brain, breast, lens, liver, lung, kidney, ovary, pancreas, prostate, red blood cells, skeletal muscle, stomach, testis,*	*9q21,13*
	ALDH1 A2	*NAD dependent*	*Cytosol*	*Retinal*	*Kidney, liver, testis,*	*15q21.3*
	ALDH1 A3	*NAD / NADP$^+$ dependent*	*Cytosol*	*Retinal*	*Breast, kidney, lung, salivary glands, skeletal muscle, stomach*	*15q21.3*
	ALDH1 B1	*NAD dependent*	*Mitochondria*	*Acetaldehyde, lipid peroxidation-derived aldehydes*	*Brain, heart, liver, kidney, lung, placenta, prostate, skeletal muscle, testis*	*9q11.1*
	ALDH1 L1	*NADP$^+$ dependent*	*Cytosol*	*10-Formyltetra-hydro folate*	*Liver, skeletal muscle, kidney*	*3q21.3*
	ALDH1 L2	*NADP$^+$ dependent*	*Mitochondria*	*10-Formyltetra-hydro folate*	*Pancreas, heart, and brain[107]*	*12q23.3*

ALDH8A1 is another RA-producing ALDH isotype. It is responsible for the production of 9-cis retinoic acid which is negligible in vivo. This Table is adapted from the data reviewed by Ma et al. in [94].

However, it is interesting that ALDH1A2 is rarely reported as a tumor promoter, but rather as a tumor suppressor instead. Since retinoids are ubiquitous molecules that influence nearly every cell type, a delicate homeostasis of the ALDH/RA signaling pathway is of importance in controlling the right developmental program in cells [27]. An aberrant ALDH/RA signaling pathway was observed was in two different ways: down-regulation of the normal isotype (ALDH1A2) and up-regulation of the abnormal type (ALDH1A1/A3) [108-110]. Considering the function of ATRA and the overlap of enzymatic activity, there might be an interesting assumption to explain this phenomenon. A disordered ALDH/RA axis might be a compensation for the vital ATRA signal, by an aberrant isotype (ALDH1A1/A3) signaling replacing the impaired right isotype (ALDH1A2) signaling.

6.2 Low-dose cisplatin leads to detrimental effects in cervical cancer

Apoptosis induction by cisplatin is the principal mechanism for its cellular toxicity [111]. The DNA adduction is formed during the proliferation process and subsequently causes the DNA strand breaks in proliferating cells [111, 112]. In the present study, cisplatin treatment leads to a dose-dependent effect of apoptosis. Moreover, MTT assay data also indicate cisplatin inhibits the proliferation of cancer cells significantly (Figure 8). These results fit the common sense view that cisplatin is an efficacious anti-cancer drug under the current criteria. However, several problems have also been raised in this study. Besides the inhibition of proliferation and induction of apoptosis in cancer cells, the $ALDH^{bright}$ subpopulation of cells was another indicator for read-out during drug administration. Inconsistent to the dose-dependent effect in apoptosis, the ALDH response shows dual-phase to serial concentrations of cisplatin. The low-dose of cisplatin (the threshold is lower than 1 μM in HeLa and SiHa, and lower than 3 μM in MRIH186; Figure 19 B) causes an increase of the $ALDH^{bright}$ cells, and a higher concentration reverses this up-regulation gradually. A high-dose cisplatin treatment kills cells drastically and reduces the colony formation ability vigorously.

It has been reported that a short-term treatment by chemotherapy in ovarian cancer cells would lead to an enrichment of CSCs [113]. As the most commonly used drug, unfortunately, cisplatin is among the most effective reagents to induce MDR and enrichment of CSCs. It is speculated that a low-dose of cisplatin causes selection pressure on cells, and creates a preferential

microenvironment for CSCs [74]. This might happen in cervical cancer as well. Besides the inhibition of proliferation and induction of apoptosis, low-dose cisplatin leads to a series of unfavorable activities in the present study. Stemness markers such as Sox2 are increased after treatment with both low- and high-dose cisplatin. The increased RNA expression of ALDH and ABCG2 supports this assumption. As a marker of CSCs, the frequency of ALDH^{bright} cells is increased after cisplatin treatment. One explanation is the enrichment of CSCs by the killing of drug-sensitive cells. The potential change of the different cellular populations is schematically illustrated in Figure 31. It is worth to noticing the emergence of ALDH$^{extra\text{-}bright}$ cells (the cells locate beyond the right side of original ALDH^{bright} cells, which means these cells have stronger ALDH activity than original ALDH^{bright} cells) which is negligible or even non-detectable before treatment. Some reports indicated that cisplatin might induce CSC formation by the alteration in cellular profile (i.e. on genetic level), in addition to enriching the CSC population by killing of non-CSC [74, 114]. More attention and effort should be put into elaborate these relationships.

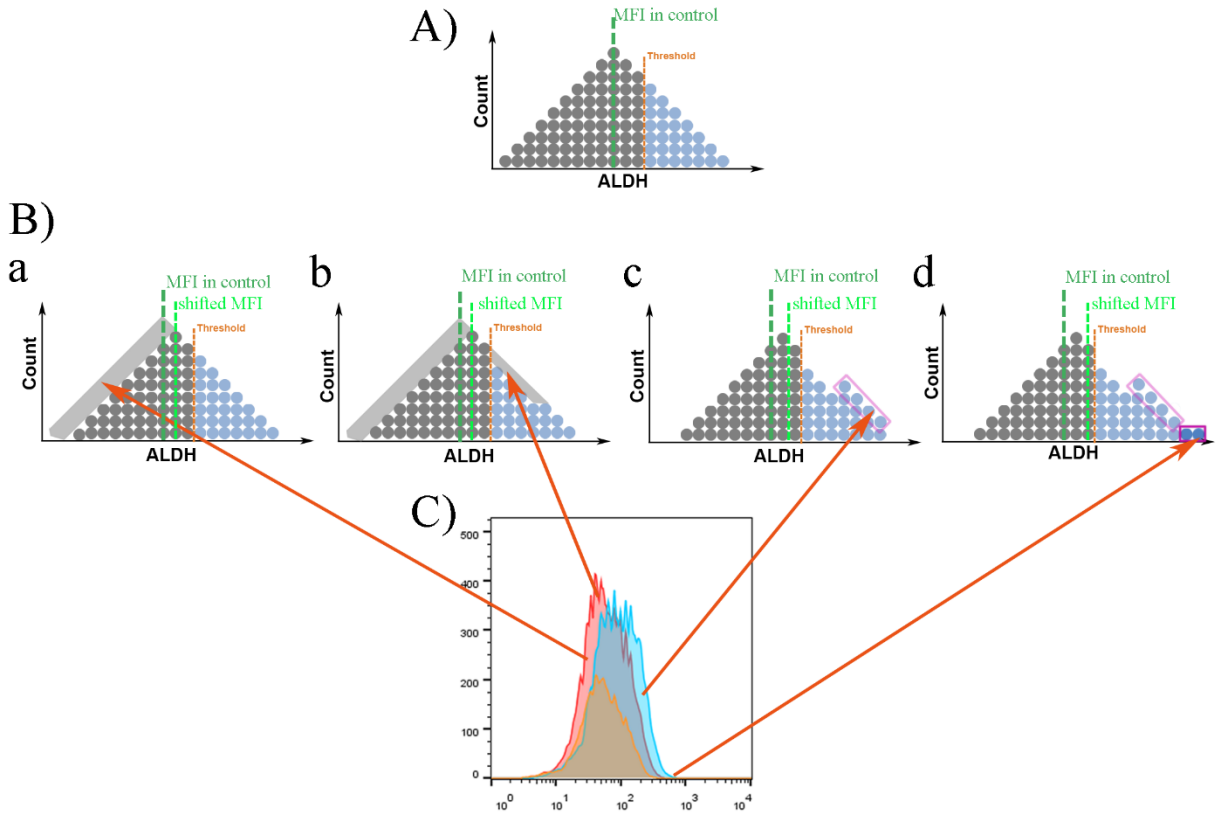

Figure 31: Possible explanation for the increased proportion of ALDH^{bright} cells in the Aldefluor assay. A) *Control;* ***B)*** *The possible cases for alternation in proportion of ALDH^{bright} cells after treatment with low-dose cisplatin. a: ALDH^{low} cells are killed more efficiently by cisplatin, but*

ALDH^{bright} cells are killed less due to resistance; b: more ALDH^{low} cells are killed by cisplatin than ALDH^{bright} cells; c: emergence of new ALDH^{bright} cells after cisplatin treatment; d: emergence of ALDH$^{extra\text{-}bright}$ cells after cisplatin treatment. ***C)*** *The increased ALDH^{bright} population might be the result of multiple models shown in (B).*

Further investigation revealed that the low-dose cisplatin has an increased colony formation ability, which is in contrast to the expected cisplatin effects. In the scratching assay, the low-dose treated cells move faster having spreading activity. The increased mRNA expression of ALDH family genes and ABCG2 imply that a slight cisplatin treatment might initiate the self-protection system of cancer cells, such as the increased expression of detoxification protein and pump-proteins. The up-regulation in mRNA of ALDH and ABCG2 also suggests that the residual cells might exhibit augmented drug resistance to anticancer reagents. These results are helpful for optimizing the use of cisplatin as a medication by avoiding low-dose cisplatin application for curative purposes. The serum concentration of cisplatin during clinical treatment is variable. The maximum peak ranked between 1.63 to 3.60 μg/ml (about 5.38 to 11.98 μM); however, free platinum, which is the active form of cisplatin, varied from 0.06 to 1.23 μg/ml (about 0.20 to 4.10 μM) according to the different schedules and routes of drug delivery [115]. These serum-available concentrations are in the range for not only apoptosis induction, but also the emergence of adverse effects. This broad deviation in the serum concentration might be an explanation for the dilemma that NACT before definitive radio therapy was not beneficial or even detrimental [62]. Therefore, insufficient cisplatin, which might result in a detrimental effect, is not recommended in spite of the apoptosis induced. Currently, the effects of chemotherapeutics are evaluated concerning how a drug induces tumor remission or to decrease tumor size. While this judgment of success is intuitive, and numerous reagents judged by these criteria are adopted in effective chemotherapeutic regimens, the dilemma is becoming increasingly evident that eliminating the bulk of cancer may efficiently lead a selection for resistant cells [114, 116]. As a consequence, alteration of the evaluation criteria is a reasonable consequence of a concept update coinciding with the understanding of CSCs. A more efficient way to eradicate cancer might be the combination of different mechanisms including cytotoxic drugs and CSC-targeting drugs [81].

The first case of CSCs was found in leukemia [117], and subsequently, the existence of CSCs in

various cancer was proved, including glioblastoma, lung cancer, gastric cancer, ovarian cancer, and cervical cancer [118]. The use of ATRA in APL has achieved promising results [119], and the application of ATRA in other kinds of leukemia such as acute myeloid leukemia also got a positive response [120]. The abnormality in the retinoic signaling pathway plays a causative role in the carcinogenesis, therefore it becomes the primary target of cancer therapy in APL. By the combination of ATRA (targeting CSCs) and cytotoxic drugs (killing normal cancer cells), this strategy saves over 90% patients with a curative effect in APL. There are many causative factors and reasons for cancer development. A high expression of ALDH is the hallmark of CSCs, and plays critical roles in the maintenance and protection of CSCs. Consequently, ALDH is a logical target of cancer therapy. The usage of ATRA is supposed to be based on the effects of targeting stem cells, which can be labeled out by ALDH staining [121-125]. Therefore, the use of ATRA targeting CSCs might be a critical complimentary part for a curative outcome. The importance of the combination of differently roled drugs has been noted for a successful treatment. By summarizing the behavior of CSCs and normal cancer cells, a statistical model indicates that the combination of these two strategies can substantially reduce the population sizes and densities of all types of cancer cells [81]. Otherwise, the benefit of these agents can easily be missed. These findings emphasize the feasibility and importance of combing the treatment of ATRA and cytotoxic drugs.

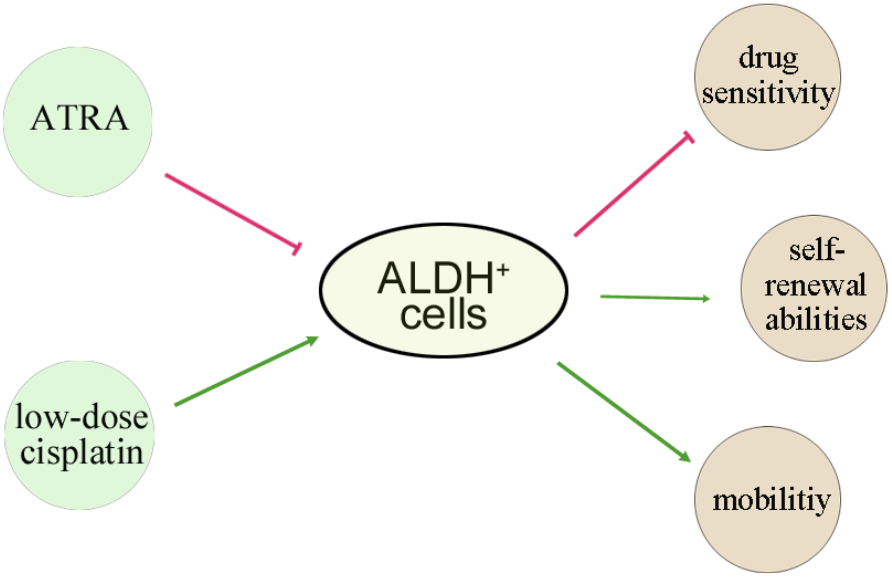

Figure 32: Schematic illustration for treatment effects after low-dose cisplatin or ATRA on

ALDH*^{bright} *cells. Low-dose cisplatin increases the proportion of ALDH*^{bright} *cells, which is associated with enhanced drug resistance, enhanced renewal ability (stemness), and motility. ATRA decreases the ALDH*^{bright} *population and counteracts the adverse effects associated with ALDH*^{bright} *cells.

6.3 ATRA reduces the proportion of ALDH^{bright} cells and partly overcomes refractory effects caused by low-dose cisplatin

In section 5.3.2, ATRA has the effect of reducing the ALDH^{bright} population without the dual-phase at low-concentration. Both the frequency and intensity of ALDH^{bright} cells are reduced by ATRA, consistent to the increased concentration of ATRA (Figure 20). Given the fact that ATRA is the product of ALDH, ATRA might work as an enzymatic inhibitor of ALDH in a competitive inhibition manner. However, the enzymatic activity of ALDH recover promptly after ATRA wash-out which is an standard procedure of Aldefluor assay staining. These results (Section 5.3.3) indicate enzymatically competitive inhibition is not the main mechanism for the reduction of the ALDH^{bright} population. Considering the decreased mRNA expression of ALDH isotypes after ATRA treatment, ATRA might suppress the ALDH expression at gene level. According to retrieved literature, very little extra data concerns the effects ATRA has on ALDH expression. By detection of ALDH activity in cell lysis, Moreb et al. discovered that ATRA treatment inhibited the ALDH function in lung cancer cells [7]. The consequent result by western blotting indicated the functional repression might be due to a reduced expression of the total ALDH protein. Additionally, they found a reduced expression of ALDH protein can increase the toxicity of cyclophosphamide after ATRA treatment. An innate loop of ALDH-RA signaling offers a potential molecular mechanism for the ALDH inhibition by ATRA [6, 8] (Figure 33 and 34). When there are low intracellular RA concentrations, retinoic acid receptors (RARs) and CCAAT/enhancer-binding protein b (C/EBPb) activate the ALDH1 promoter, thereby increasing the ALDH1 activity to increase retinoic acid concentration. As RA levels increase, C/EBPb mRNA increases, which also increases GADD (growth arrest- and DNA damage-inducible gene 153) mRNA. A complex of GADD and C/EBPb then forms to decrease the DNA binding activity of C/EBPb to the CCAAT box of the ALDH1 promoter, thereby inhibiting ALDH1 expression. In addition to the transcriptional mechanism, Moreb et al. also emphasized the roles of

posttranslational regulation in lung cancer [7]. However, some inconsistent reports were also found. For example, 1 μM ATRA was reported to up-regulate the mRNA of ALDH1A3, but not ALDH1A1 and ALDH1A2 in primary keratinocytes [126]. These variations might be caused by the differences between the cell lines used in these studies. On the other hand, this diversity emphasizes the importance of determining the right isotype dominating the ALDH function in different tissue.

The proliferation and apoptosis response to ATRA were additionally observed in cervical cancer. Cervical cancer cells are not sensitive to ATRA when the concentration is lower than 10 μM. ATRA inhibits cellular growth in concentrations above 10 μM in a dose-dependent manner. With the increase of growth inhibition, the proportion of apoptotic cells is increased. Previous studies also reported that the ATRA-induced apoptosis effects cervical cells. However, the concentration of ATRA was lower than that applied in the current study. This can be potentially explained by the difference in culture conditions as their data were acquired in MDCs where cells are more sensitive to drugs than in SDCs. Anna et al. further explored the mechanism inducing apoptosis; they found that CD95 was presumably the vital element mediating the apoptosis [127]. Another report suggested that the inhibition of telomerase activity and arrest of cells at G0/G1 phase might be the key steps through which ATRA inhibits the proliferation of cervical cancer cells [37].

The combination of ATRA and cisplatin can work in an additive or synergistic fashion (Table 10). ATRA also induces the apoptosis in cervical SDCs. Importantly, ATRA is able to reverse the increased population of $ALDH^{bright}$ cells caused by low-dose cisplatin treatment. Other detrimental effects such as the enhanced stemness and motility can be overcome by the combination with ATRA treatment (shown in Results 5.4.1 - 4). The mRNA expression of CSC-markers can be partially reduced by ATRA. Despite that cisplatin-induced Sox2 is not reversed, ATRA treatment reduces mRNA expression of the CSC-markers. However, ATRA increases mRNA expression of ABCG2 in all three cell lines. This suggests that ATRA is not sufficient to inhibit the ABC family function. Additional drugs for corresponding signaling pathway might be helpful to fulfill this aim. Indeed, an addition of demethylases significantly increased the anti-cancer effects of ATRA [128]. Hence, the multi-combination of different functional drugs might be a promising way for better outcomes. A new treatment protocol of 9 repurposed drugs (i.e. CUSP9) for recurrent glioblastoma

appears to be safe with good tolerability. The preliminary results are an important milestone in brain tumor research [129, 130]. As such, a cocktail strategy like "CUSP9" in neuroblastoma [131], possibly is possibly a reasonable way to solve the dilemma caused by cisplatin.

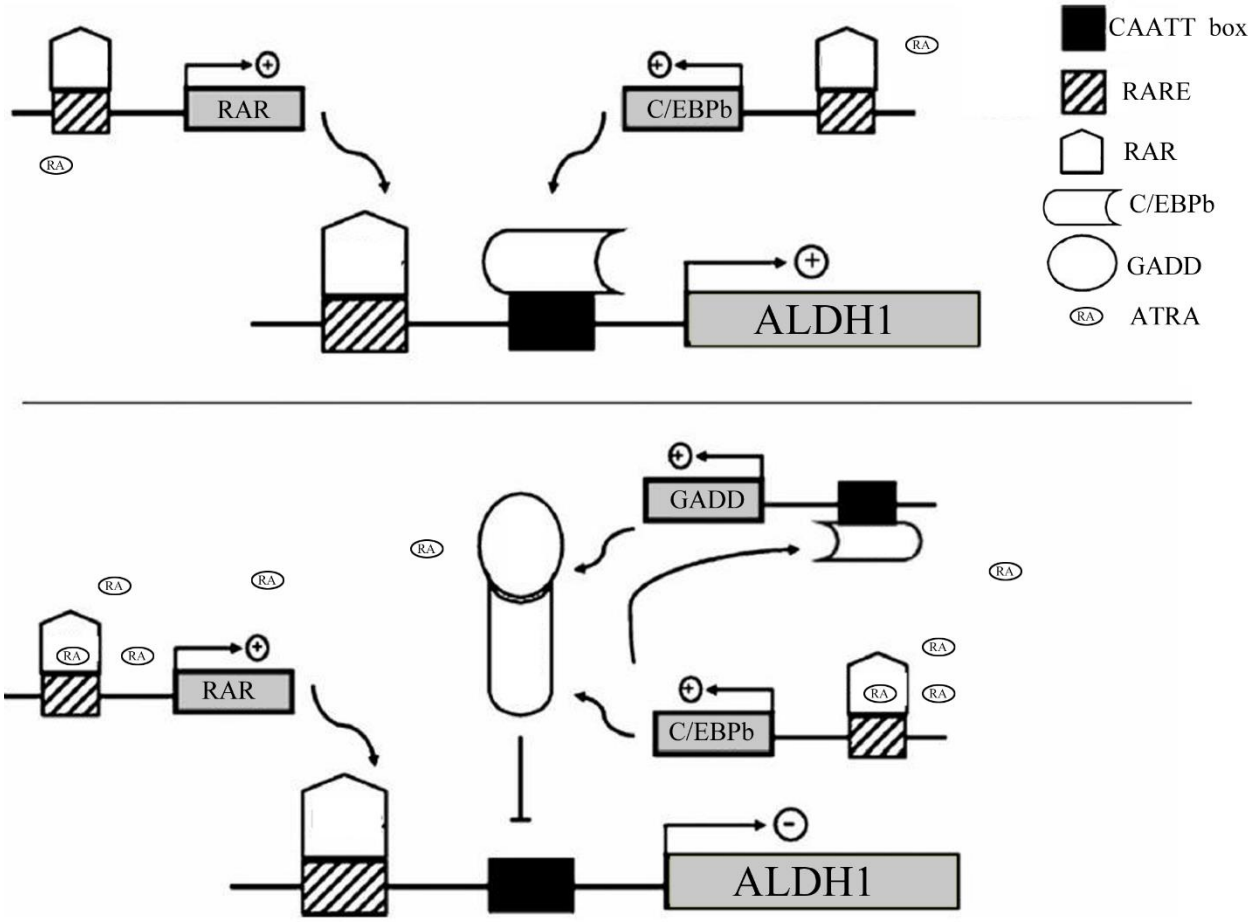

Figure 33: Potential mechanism of feedback-regulation on the aldh gene. *Upper panel: at low ATRA (endogenous) concentrations, RARs and C/EBPb transactivate the aldh promoter. Lower panel: when the ATRA concentration increases (for example extrinsic resources), RAR activates the C/EBPb promoter increasing the C/EBPb abundance, resulting in an increase of the GADD amount and the formation of GADD-C/EBPb heterodimers which block the transcription of the aldh gene. Modified from Guillermo Elizondo et al. [8].*

6.4 3-D spheroid culture is an improved cellular assay for drug testing compared to 2-D monolayer culture

The present study confirms that the $ALDH^{bright}$ population is increased in SDCs vs. MDCs. Plenty of studies have acknowledged that spheroid culture is a way to enrich CSCs, by the hypothesis that

bulk cancer cells will undergo anoikis in the floating condition [82]. In addition to the increase of the $ALDH^{bright}$ population, the renewal ability is also enhanced in SDCs vs. MDCs. The higher SEF in SDCs than in MDCs might be owing to the selection effects of suitable cells in 3-D condition. It is noticeable that SDCs are a more natural mimic of the real situation *in vivo* than MDCs [84]. In colony formation assay, the enhanced CFE is not as strong as in SFE, and this might be due to the culture condition.

In accordance with the up-regulated $ALDH^{bright}$ population in SDCs, cisplatin and paclitaxel, the two most commonly used drugs, were employed to test the pharmaceutical sensitivity of SDCs and MDCs. On average, SDCs showed doubled resistance to cisplatin compared to MDCs in cervical cancer cell lines. Consistently with the cisplatin data, SDCs displayed reduced sensitivity to paclitaxel compared to MDCs. These effects can be further supported by the evidence from other cancers. A number of studies have indicated that cells cultured in 3-D models were more resistant to anticancer drugs than 2-D models. For instance, ovarian cancer cell survival and proliferation after paclitaxel treatment was reduced by about 50% in 3-D spheroids, while the same treatment led to an 80% reduced cell viability in the 2-D monolayer [132, 133]. These differences might be attributed to the enrichment of the $ALDH^{bright}$ cells, which are more resistant than $ALDH^{low}$ cells. However, other diversities between SDCs and MDCs may also be important factors, such as the organization and morphology in the shape of cells, different nutritional distribution, spatial interaction between cells, and cellular protein or receptor expression.

These heterogeneities contribute not only to the formation of drug gradients, but also other facets which are indispensable for the effects of drugs. For instance, a mathematical model suggested that cancer bulk was governed by a "quorum sensing" control mechanism, in which CSCs proliferated or differentiated according to the feedback they received from neighboring cell populations [81]. Thus, cellular interaction plays very important roles in a cancer growth model and the response to drugs. Besides the alternation of the $ALDH^{bright}$ population, which stands for a change of cytoplamatic protein, various cancer cell lines grown in 2-D and 3-D culture often differ in membrane receptors. For example, the expression levels of the epidermal growth factor receptor (EGFR) and the downstream kinases *in vivo* were more similar to cells grown in 3-D, and distinct from 2-D [134, 135]. This altered EGFR expression is critical for the effects of anti-EGFR

therapy, which represents a promising new approach for treating cancers [136].

Historically, chemo-sensitivity testing was expected to guide the selection of cytotoxic drugs in the clinic. Unfortunately, the data achieved from traditional 2-D cell culture models failed to predict the effects of chemo-reagents *in vivo*. The innate difference of 2-D culture and the *in vivo* environment might be the reason for the failure. SDCs show different biological properties compared to MDCs and compensate critical disadvantages of MDCs. Notably, cellular responses to drug treatments have been shown to be more similar in 3-D cultures to what occurs *in vivo* compared to 2-D cultures. Considering the drawbacks of 2-D, the advantages of 3-D (summarized in Table 12), and the fact that MDCs show a difference with SDCs, SDCs were used for the drug-test assay instead of conventional MDCs in the current study.

6.5 Limitations of the study and future perspectives

The presented data reveal that low-dose cisplatin could increase the proportion of $ALDH^{bright}$ cells which can be reversed by ATRA treatment, highlighting the importance of cisplatin treatment optimization, and suggesting that ALDH-targeting might be meaningful for cervical cancer treatment. However, several problems are not well elucidated and require further investigation. The study indicates that the ALDH1A1 and ALDH1A3 might be the predominating isotypes detected by Aldefluor assay. This result calls for further confirmation at the protein level. The cross-talking of different isotypes is commonly reported in the ALDH supergene family. Therefore, a systematic characterization of ALDH isotype expression and their function is necessary to be elaborated. Additionally, ATRA can counteract the increase of proportion of $ALDH^{bright}$ cells and some of concomitant detrimental effects caused by low-dose cisplatin treatment. However, the mechanism for the reduction of $ALDH^{bright}$ population by ATRA is still not well elaborated (a potential mechanism is proposed in Figure 34). It would be helpful to understand the function of ATRA by elucidating the mechanism by which it reduces $ALDH^{bright}$ population. In the light of effects concomitant with inhibition of ALDH after ATRA treatment, a stronger ALDH inhibitor might work better to overcome the unfavorable effects of cisplatin. A combination strategy, i.e. combination of CSC-targeting drugs and anti-non CSC drugs, could be tried to solve the detrimental effects occurred during chemotherapy.

Table 12. Overview of the different properties between 3-D derived cells and 2-D derived cells

Cellular properties	***3-D***	***2-D***	***Reference***
Morphology	***Spheroid/aggregate structures***	***Sheet-like flat and stretched cells in monolayer***	*[137]*
Cell cycle	*Spheroids contain proliferating, quiescent, hypoxic and necrotic cells*	*More cells are likely to be at the same stage of cell cycle due to being equally exposed to medium*	*[133]*
Proliferation	*May proliferate at a slower rate compared to 2-D cultured cells depending on cell type and/or type of 3-D model system*	***Often proliferate at a faster rate***	*[138]*
Gene expression	*Cells often exhibit gene/protein expression profiles more similar to those of in vivo tissue origins*	*Often display differential gene and protein expression levels compared to in vivo models*	*[94]*
Exposure to medium/drugs	*Nutrients and growth factors or drugs may not be able to fully penetrate the spheroid, reaching cells near the core*	***Cells often succumb to treatment and drugs appear to be very effective***	*[139]*
Cellular Matrix	*Complex*	*Simple*	*[133]*
Drug sensitivity	*Cells are often more resistant to treatment compared to those in a 2-D culture system, often being better predictors of in vivo drug responses*	*Cells often succumb to treatment and drugs appear to be very effective*	*[140]*
Time consuming	***High (more than one week)***	***Low (Less than one week)***	*[90]*
Financial consuming	***Relative high***	***Relatively low***	*[133]*
Requirement for nutrition	***Specific stimulation***	***Standard manufactured***	*[90]*

The bold text represents issues which have also been observed in the current study.

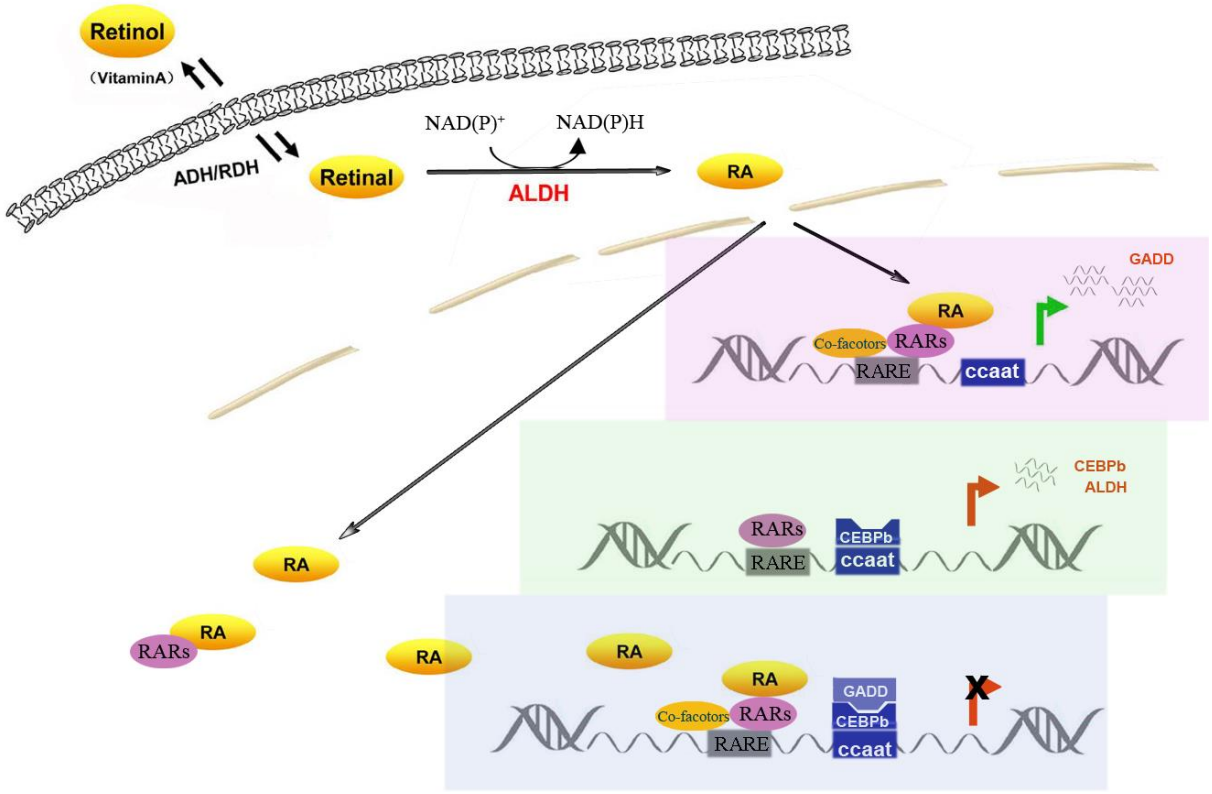

Figure 34: Schematic illustration of the ALDH-RA signaling pathway. *Mammals obtain retinol (vitamin A) from food. Once inside the cell, vitamin A can be metabolized by several different enzymes; however, only ALDH irreversibly converts retinal to retinoic acid in the help of NAD(P) in cytoplasm. When RA (i.e. ATRA) enters nucleus, RA starts its signaling cascade by binding to RARs which further bind to RARE locating on DNA. At low RA concentrations, RARs and C/EBPb trans-activate the aldh gene promoter. When RA levels increase (for example extrinsic resources), RARs activate the C/EBPb promoter increasing the C/EBPb abundance resulting in an increase of the GADD amount. The formation of GADD-C/EBPb heterodimers blocks the transcription of the aldh gene. Therefore, increased retinoic acid may give a negative feedback to ALDH expression. Abbreviations (from the top-left to bottom-right): ADH: alcohol dehydrogenase; RDH: retinol dehydrogenase; NAD(P): nicotinamide adenine dinucleotide (phosphate); RA: Retinoic acid; RARs: Retinoic acid receptors; RARE: Retinoic acid receptor elements; CEBPb: CCAAT/enhancer-binding protein b; GADD: Growth arrest and DNA damage-inducible gene).*

6.6 Conclusions

Low-dose cisplatin increases the proportion of $ALDH^{bright}$ cells in cervical cancer cell lines and enhances the CSC-properties in cervical cancer SDCs. According to this finding, low-dose cisplatin treatment should be avoided. ATRA, by its role in the reduction of ALDH activity, might be a candidate to target CSCs. More importantly, this study indicates that ALDH-targeting therapy might be a potential way to complement current cisplatin-based cytotoxic chemotherapy.

7. References

1. Small W, Jr., Bacon MA, Bajaj A, Chuang LT, Fisher BJ, Harkenrider MM, Jhingran A, Kitchener HC, Mileshkin LR, Viswanathan AN and Gaffney DK. Cervical cancer: A global health crisis. Cancer. 2017; 123(13):2404-2412.
2. Chhabra R. Cervical cancer stem cells: opportunities and challenges. Journal of cancer research and clinical oncology. 2015; 141(11):1889-1897.
3. Januchowski R, Wojtowicz K and Zabel M. The role of aldehyde dehydrogenase (ALDH) in cancer drug resistance. Biomedicine & pharmacotherapy = Biomedecine & pharmacotherapie. 2013; 67(7):669-680.
4. Vassalli G. Aldehyde Dehydrogenases: Not Just Markers, but Functional Regulators of Stem Cells. Stem Cells Int. 2019; 2019:3904645.
5. Clark DW and Palle K. Aldehyde dehydrogenases in cancer stem cells: potential as therapeutic targets. Annals of translational medicine. 2016; 4(24):518.
6. Elizondo G, Corchero J, Sterneck E and Gonzalez FJ. Feedback inhibition of the retinaldehyde dehydrogenase gene ALDH1 by retinoic acid through retinoic acid receptor A and CCAAT/enhancer-binding protein beta. J Biol Chem. 2000; 275(50):39747-39753.
7. Moreb JS, Gabr A, Vartikar GR, Gowda S, Zucali JR and Mohuczy D. Retinoic acid down-regulates aldehyde dehydrogenase and increases cytotoxicity of 4-hydroperoxycyclophosphamide and acetaldehyde. The Journal of pharmacology and experimental therapeutics. 2005; 312(1):339-345.
8. Elizondo G, Medina-Diaz IM, Cruz R, Gonzalez FJ and Vega L. Retinoic acid modulates retinaldehyde dehydrogenase 1 gene expression through the induction of GADD153-C/EBPbeta interaction. Biochemical pharmacology. 2009; 77(2):248-257.
9. Albers AE, Chen C, Koberle B, Qian X, Klussmann JP, Wollenberg B and Kaufmann AM. Stem cells in squamous head and neck cancer. Critical reviews in oncology/hematology. 2012; 81(3):224-240.
10. Aponte PM and Caicedo A. Stemness in Cancer: Stem Cells, Cancer Stem Cells, and Their Microenvironment. Stem Cells Int. 2017; 2017:5619472.
11. Durst M, Gissmann L, Ikenberg H and zur Hausen H. A papillomavirus DNA from a cervical carcinoma and its prevalence in cancer biopsy samples from different geographic regions. Proceedings of the National Academy of Sciences of the United States of America. 1983; 80(12):3812-3815.
12. Zhu Y, Wang Y, Hirschhorn J, Welsh KJ, Zhao Z, Davis MR and Feldman S. Human Papillomavirus and Its Testing Assays, Cervical Cancer Screening, and Vaccination. Advances in clinical chemistry. 2017; 81:135-192.
13. Herfs M, Yamamoto Y, Laury A, Wang X, Nucci MR, McLaughlin-Drubin ME, Munger K, Feldman S, McKeon FD, Xian W and Crum CP. A discrete population of squamocolumnar junction cells implicated in the pathogenesis of cervical cancer. Proceedings of the National Academy of Sciences of the United States of America. 2012; 109(26):10516-10521.
14. Forman D, de Martel C, Lacey CJ, Soerjomataram I, Lortet-Tieulent J, Bruni L, Vignat J, Ferlay J, Bray F, Plummer M and Franceschi S. Global burden of human papillomavirus and related diseases. Vaccine. 2012; 30 Suppl 5:F12-23.
15. Herfs M, Soong TR, Delvenne P and Crum CP. Deciphering the Multifactorial Susceptibility of Mucosal Junction Cells to HPV Infection and Related Carcinogenesis. Viruses. 2017; 9(4).
16. Mirkovic J, Howitt BE, Roncarati P, Demoulin S, Suarez-Carmona M, Hubert P, McKeon FD, Xian W, Li A, Delvenne P, Crum CP and Herfs M. Carcinogenic HPV infection in the cervical squamo-columnar junction. The Journal of pathology. 2015; 236(3):265-271.
17. Organista-Nava J, Gomez-Gomez Y and Gariglio P. Embryonic stem cell-specific signature in cervical cancer.

Tumour biology : the journal of the International Society for Oncodevelopmental Biology and Medicine. 2014; 35(3):1727-1738.

18. Kashyap V, Rezende NC, Scotland KB, Shaffer SM, Persson JL, Gudas LJ and Mongan NP. Regulation of stem cell pluripotency and differentiation involves a mutual regulatory circuit of the NANOG, OCT4, and SOX2 pluripotency transcription factors with polycomb repressive complexes and stem cell microRNAs. Stem cells and development. 2009; 18(7):1093-1108.

19. Fong H, Hohenstein KA and Donovan PJ. Regulation of self-renewal and pluripotency by Sox2 in human embryonic stem cells. Stem cells. 2008; 26(8):1931-1938.

20. Martinez-Ramirez I, Del-Castillo-Falconi V, Mitre-Aguilar IB, Amador-Molina A, Carrillo-Garcia A, Langley E, Zentella-Dehesa A, Soto-Reyes E, Garcia-Carranca A, Herrera LA and Lizano M. SOX2 as a New Regulator of HPV16 Transcription. Viruses. 2017; 9(7).

21. Gut A, Moch H and Choschzick M. SOX2 Gene Amplification and Overexpression is Linked to HPV-positive Vulvar Carcinomas. International journal of gynecological pathology : official journal of the International Society of Gynecological Pathologists. 2017.

22. Canham M, Charsou C, Stewart J, Moncur S, Hoodless L, Bhatia R, Cong D, Cubie H, Busby-Earle C, Williams A, McLoughlin V, Campbell JD, Cuschieri K and Howie S. Increased cycling cell numbers and stem cell associated proteins as potential biomarkers for high grade human papillomavirus+ve pre-neoplastic cervical disease. PloS one. 2014; 9(12):e115379.

23. Liu XF, Yang WT, Xu R, Liu JT and Zheng PS. Cervical cancer cells with positive Sox2 expression exhibit the properties of cancer stem cells. PloS one. 2014; 9(1):e87092.

24. Shen L, Huang X, Xie X, Su J, Yuan J and Chen X. High Expression of SOX2 and OCT4 Indicates Radiation Resistance and an Independent Negative Prognosis in Cervical Squamous Cell Carcinoma. The journal of histochemistry and cytochemistry : official journal of the Histochemistry Society. 2014; 62(7):499-509.

25. Organista-Nava J, Gomez-Gomez Y, Ocadiz-Delgado R, Garcia-Villa E, Bonilla-Delgado J, Lagunas-Martinez A, Tapia JS, Lambert PF, Garcia-Carranca A and Gariglio P. The HPV16 E7 oncoprotein increases the expression of Oct3/4 and stemness-related genes and augments cell self-renewal. Virology. 2016; 499:230-242.

26. Ye F, Zhou C, Cheng Q, Shen J and Chen H. Stem-cell-abundant proteins Nanog, Nucleostemin and Musashi1 are highly expressed in malignant cervical epithelial cells. BMC cancer. 2008; 8:108.

27. Samarut E and Rochette-Egly C. Nuclear retinoic acid receptors: conductors of the retinoic acid symphony during development. Molecular and cellular endocrinology. 2012; 348(2):348-360.

28. Kam RK, Deng Y, Chen Y and Zhao H. Retinoic acid synthesis and functions in early embryonic development. Cell & bioscience. 2012; 2(1):11.

29. Sima A, Parisotto M, Mader S and Bhat PV. Kinetic characterization of recombinant mouse retinal dehydrogenase types 3 and 4 for retinal substrates. Biochimica et biophysica acta. 2009; 1790(12):1660-1664.

30. Kedishvili NY. Enzymology of retinoic acid biosynthesis and degradation. Journal of lipid research. 2013; 54(7):1744-1760.

31. Storms RW, Trujillo AP, Springer JB, Shah L, Colvin OM, Ludeman SM and Smith C. Isolation of primitive human hematopoietic progenitors on the basis of aldehyde dehydrogenase activity. Proceedings of the National Academy of Sciences of the United States of America. 1999; 96(16):9118-9123.

32. Zhou P, Wirthlin L, McGee J, Annett G and Nolta J. Contribution of human hematopoietic stem cells to liver repair. Seminars in immunopathology. 2009; 31(3):411-419.

33. Perin EC, Silva G, Gahremanpour A, Canales J, Zheng Y, Cabreira-Hansen MG, Mendelsohn F, Chronos N, Haley R, Willerson JT and Annex BH. A randomized, controlled study of autologous therapy with bone marrow-derived

aldehyde dehydrogenase bright cells in patients with critical limb ischemia. Catheterization and cardiovascular interventions : official journal of the Society for Cardiac Angiography & Interventions. 2011; 78(7):1060-1067.
34. Kitahara O, Katagiri T, Tsunoda T, Harima Y and Nakamura Y. Classification of sensitivity or resistance of cervical cancers to ionizing radiation according to expression profiles of 62 genes selected by cDNA microarray analysis. Neoplasia. 2002; 4(4):295-303.
35. Moreb JS, Ucar-Bilyeu DA and Khan A. Use of retinoic acid/aldehyde dehydrogenase pathway as potential targeted therapy against cancer stem cells. Cancer chemotherapy and pharmacology. 2017; 79(2):295-301.
36. Darwiche N, Celli G, Sly L, Lancillotti F and De Luca LM. Retinoid status controls the appearance of reserve cells and keratin expression in mouse cervical epithelium. Cancer research. 1993; 53(10 Suppl):2287-2299.
37. Guo JM, Xiao BX, Kang GZ, Liu DH, Chen H, Zhang S and Zhang XN. Suppression of telomerase activity and arrest at G1 phase in human cervical cancer HeLa cells by all-trans retinoic acid. International journal of gynecological cancer : official journal of the International Gynecological Cancer Society. 2006; 16(1):341-346.
38. Faluhelyi Z, Rodler I, Csejtey A, Tyring SK, Ember IA and Arany I. All-trans retinoic acid (ATRA) suppresses transcription of human papillomavirus type 16 (HPV16) in a dose-dependent manner. Anticancer research. 2004; 24(2B):807-809.
39. Berlin Grace VM, Niranjali Devaraj S, Radhakrishnan Pillai M and Devaraj H. HPV-induced carcinogenesis of the uterine cervix is associated with reduced serum ATRA level. Gynecologic oncology. 2006; 103(1):113-119.
40. Liu SY and Zheng PS. High aldehyde dehydrogenase activity identifies cancer stem cells in human cervical cancer. Oncotarget. 2013; 4(12):2462-2475.
41. Wang W, Li Y, Liu N, Gao Y and Li L. MiR-23b controls ALDH1A1 expression in cervical cancer stem cells. BMC cancer. 2017; 17(1):292.
42. Orywal K, Jelski W, Zdrodowski M and Szmitkowski M. The Diagnostic Value of Alcohol Dehydrogenase Isoenzymes and Aldehyde Dehydrogenase Measurement Sera of Cervical Cancer Patients. Anticancer research. 2016; 36(5):2265-2269.
43. Ortiz-Sanchez E, Santiago-Lopez L, Cruz-Dominguez VB, Toledo-Guzman ME, Hernandez-Cueto D, Muniz-Hernandez S, Garrido E, Cantu De Leon D and Garcia-Carranca A. Characterization of cervical cancer stem cell-like cells: phenotyping, stemness, and human papilloma virus co-receptor expression. Oncotarget. 2016; 7(22):31943-31954.
44. Sato M, Kawana K, Fujimoto A, Yoshida M, Nakamura H, Nishida H, Inoue T, Taguchi A, Takahashi J, Adachi K, Nagasaka K, Matsumoto Y, Wada-Hiraike O, Oda K, Osuga Y and Fujii T. Clinical significance of Gremlin 1 in cervical cancer and its effects on cancer stem cell maintenance. Oncology reports. 2016; 35(1):391-397.
45. Kwon T, Bak Y, Ham SY, Yu DY and Yoon DY. A1E reduces stemness and self-renewal in HPV 16-positive cervical cancer stem cells. BMC complementary and alternative medicine. 2016; 16:42.
46. Lv Y, Yang L and Wang F. Chemoradiation therapy reduces aldehyde dehydrogenase 1 expression in cervical cancer but does not improve patient survival. Medical oncology. 2015; 32(5):155.
47. Liu H, Wang H, Li C, Zhang T, Meng X, Zhang Y and Qian H. Spheres from cervical cancer cells display stemness and cancer drug resistance. Oncology letters. 2016; 12(3):2184-2188.
48. Yao T, Wu Z, Liu Y, Rao Q and Lin Z. Aldehyde dehydrogenase 1 (ALDH1) positivity correlates with poor prognosis in cervical cancer. The Journal of international medical research. 2014; 42(4):1038-1042.
49. Liao T, Kaufmann AM, Qian X, Sangvatanakul V, Chen C, Kube T, Zhang G and Albers AE. Susceptibility to cytotoxic T cell lysis of cancer stem cells derived from cervical and head and neck tumor cell lines. Journal of cancer research and clinical oncology. 2013; 139(1):159-170.
50. Casagrande N, De Paoli M, Celegato M, Borghese C, Mongiat M, Colombatti A and Aldinucci D. Preclinical

evaluation of a new liposomal formulation of cisplatin, lipoplatin, to treat cisplatin-resistant cervical cancer. Gynecologic oncology. 2013; 131(3):744-752.
51. Yao T, Chen Q, Zhang B, Zhou H and Lin Z. The expression of ALDH1 in cervical carcinoma. Medical science monitor : international medical journal of experimental and clinical research. 2011; 17(8):HY21-26.
52. Bortolomai I, Canevari S, Facetti I, De Cecco L, Castellano G, Zacchetti A, Alison MR and Miotti S. Tumor initiating cells: development and critical characterization of a model derived from the A431 carcinoma cell line forming spheres in suspension. Cell cycle. 2010; 9(6):1194-1206.
53. Schnier JB, Kaur G, Kaiser A, Stinson SF, Sausville EA, Gardner J, Nishi K, Bradbury EM and Senderowicz AM. Identification of cytosolic aldehyde dehydrogenase 1 from non-small cell lung carcinomas as a flavopiridol-binding protein. FEBS letters. 1999; 454(1-2):100-104.
54. Roque DR, Wysham WZ and Soper JT. The surgical management of cervical cancer: an overview and literature review. Obstetrical & gynecological survey. 2014; 69(7):426-441.
55. Green JA, Kirwan JM, Tierney JF, Symonds P, Fresco L, Collingwood M and Williams CJ. Survival and recurrence after concomitant chemotherapy and radiotherapy for cancer of the uterine cervix: a systematic review and meta-analysis. Lancet. 2001; 358(9284):781-786.
56. Li X, Huang K, Zhang Q, Shen J, Zhou H, Yang R, Wang L, Liu J, Zhang J, Sun H, Jia Y, Du X, Wang H, Deng S, Ding T, Jiang J, Lu Y, Li S, Wang S and Ma D. Early response to neoadjuvant chemotherapy can help predict long-term survival in patients with cervical cancer. Oncotarget. 2016; 7(52):87485-87495.
57. Luvero D, Plotti F, Aloisi A, Capriglione S, Ricciardi R, Miranda A, Lopez S, Scaletta G, De Luca G, Benedetti-Panici P and Angioli R. Patients treated with neoadjuvant chemotherapy + radical surgery + adjuvant chemotherapy in locally advanced cervical cancer: long-term outcomes, survival and prognostic factors in a single-center 10-year follow-up. Medical oncology. 2016; 33(10):110.
58. Castanon A and Sasieni P. Is the recent increase in cervical cancer in women aged 20-24years in England a cause for concern? Preventive medicine. 2018; 107:21-28.
59. Foley G, Alston R, Geraci M, Brabin L, Kitchener H and Birch J. Increasing rates of cervical cancer in young women in England: an analysis of national data 1982-2006. British journal of cancer. 2011; 105(1):177-184.
60. Sonoda Y, Abu-Rustum NR, Gemignani ML, Chi DS, Brown CL, Poynor EA and Barakat RR. A fertility-sparing alternative to radical hysterectomy: how many patients may be eligible? Gynecologic oncology. 2004; 95(3):534-538.
61. Duenas-Gonzalez A, Cetina L, Coronel J and Gonzalez-Fierro A. The safety of drug treatments for cervical cancer. Expert opinion on drug safety. 2016; 15(2):169-180.
62. Lapresa M, Parma G, Portuesi R and Colombo N. Neoadjuvant chemotherapy in cervical cancer: an update. Expert review of anticancer therapy. 2015; 15(10):1171-1181.
63. Quinn MA, Benedet JL, Odicino F, Maisonneuve P, Beller U, Creasman WT, Heintz AP, Ngan HY and Pecorelli S. Carcinoma of the cervix uteri. FIGO 26th Annual Report on the Results of Treatment in Gynecological Cancer. International journal of gynaecology and obstetrics: the official organ of the International Federation of Gynaecology and Obstetrics. 2006; 95 Suppl 1:S43-103.
64. Boussios S, Seraj E, Zarkavelis G, Petrakis D, Kollas A, Kafantari A, Assi A, Tatsi K, Pavlidis N and Pentheroudakis G. Management of patients with recurrent/advanced cervical cancer beyond first line platinum regimens: Where do we stand? A literature review. Critical reviews in oncology/hematology. 2016; 108:164-174.
65. Tayama S, Motohara T, Narantuya D, Li C, Fujimoto K, Sakaguchi I, Tashiro H, Saya H, Nagano O and Katabuchi H. The impact of EpCAM expression on response to chemotherapy and clinical outcomes in patients with epithelial ovarian cancer. Oncotarget. 2017; 8(27):44312-44325.

66. Fanali C, Lucchetti D, Farina M, Corbi M, Cufino V, Cittadini A and Sgambato A. Cancer stem cells in colorectal cancer from pathogenesis to therapy: controversies and perspectives. World journal of gastroenterology. 2014; 20(4):923-942.
67. Huang R and Rofstad EK. Cancer stem cells (CSCs), cervical CSCs and targeted therapies. Oncotarget. 2017; 8(21):35351-35367.
68. Rich JN. Cancer stem cells: understanding tumor hierarchy and heterogeneity. Medicine. 2016; 95(1 Suppl 1):S2-7.
69. Prasetyanti PR and Medema JP. Intra-tumor heterogeneity from a cancer stem cell perspective. Molecular cancer. 2017; 16(1):41.
70. Srivastava AK, Han C, Zhao R, Cui T, Dai Y, Mao C, Zhao W, Zhang X, Yu J and Wang QE. Enhanced expression of DNA polymerase eta contributes to cisplatin resistance of ovarian cancer stem cells. Proceedings of the National Academy of Sciences of the United States of America. 2015; 112(14):4411-4416.
71. Levina V, Marrangoni A, Wang T, Parikh S, Su Y, Herberman R, Lokshin A and Gorelik E. Elimination of human lung cancer stem cells through targeting of the stem cell factor-c-kit autocrine signaling loop. Cancer research. 2010; 70(1):338-346.
72. Galluzzi L, Senovilla L, Vitale I, Michels J, Martins I, Kepp O, Castedo M and Kroemer G. Molecular mechanisms of cisplatin resistance. Oncogene. 2012; 31(15):1869-1883.
73. Auffinger B, Tobias AL, Han Y, Lee G, Guo D, Dey M, Lesniak MS and Ahmed AU. Conversion of differentiated cancer cells into cancer stem-like cells in a glioblastoma model after primary chemotherapy. Cell death and differentiation. 2014; 21(7):1119-1131.
74. Wiechert A, Saygin C, Thiagarajan PS, Rao VS, Hale JS, Gupta N, Hitomi M, Nagaraj AB, DiFeo A, Lathia JD and Reizes O. Cisplatin induces stemness in ovarian cancer. Oncotarget. 2016; 7(21):30511-30522.
75. Wang L, Liu X, Ren Y, Zhang J, Chen J, Zhou W, Guo W, Wang X, Chen H, Li M, Yuan X, Zhang X, Yang J and Wu C. Cisplatin-enriching cancer stem cells confer multidrug resistance in non-small cell lung cancer via enhancing TRIB1/HDAC activity. Cell death & disease. 2017; 8(4):e2746.
76. Cheung-Ong K, Giaever G and Nislow C. DNA-damaging agents in cancer chemotherapy: serendipity and chemical biology. Chemistry & biology. 2013; 20(5):648-659.
77. Lathia JD and Liu H. Overview of Cancer Stem Cells and Stemness for Community Oncologists. Targeted oncology. 2017; 12(4):387-399.
78. Tang XH and Gudas LJ. Retinoids, retinoic acid receptors, and cancer. Annual review of pathology. 2011; 6:345-364.
79. Fang Y and Eglen RM. Three-Dimensional Cell Cultures in Drug Discovery and Development. SLAS discovery. 2017:2472555217696795.
80. Matthay KK, Reynolds CP, Seeger RC, Shimada H, Adkins ES, Haas-Kogan D, Gerbing RB, London WB and Villablanca JG. Long-term results for children with high-risk neuroblastoma treated on a randomized trial of myeloablative therapy followed by 13-cis-retinoic acid: a children's oncology group study. Journal of clinical oncology : official journal of the American Society of Clinical Oncology. 2009; 27(7):1007-1013.
81. Vainstein V, Kirnasovsky OU, Kogan Y and Agur Z. Strategies for cancer stem cell elimination: insights from mathematical modeling. Journal of theoretical biology. 2012; 298:32-41.
82. Smart CE, Morrison BJ, Saunus JM, Vargas AC, Keith P, Reid L, Wockner L, Askarian-Amiri M, Sarkar D, Simpson PT, Clarke C, Schmidt CW, Reynolds BA, Lakhani SR and Lopez JA. In vitro analysis of breast cancer cell line tumourspheres and primary human breast epithelia mammospheres demonstrates inter- and intrasphere heterogeneity. PloS one. 2013; 8(6):e64388.

83. Lopez-Lazaro M. Two preclinical tests to evaluate anticancer activity and to help validate drug candidates for clinical trials. Oncoscience. 2015; 2(2):91-98.
84. Phung YT, Barbone D, Broaddus VC and Ho M. Rapid generation of in vitro multicellular spheroids for the study of monoclonal antibody therapy. Journal of Cancer. 2011; 2:507-514.
85. Pampaloni F, Reynaud EG and Stelzer EH. The third dimension bridges the gap between cell culture and live tissue. Nature reviews Molecular cell biology. 2007; 8(10):839-845.
86. Karlsson H, Fryknas M, Larsson R and Nygren P. Loss of cancer drug activity in colon cancer HCT-116 cells during spheroid formation in a new 3-D spheroid cell culture system. Experimental cell research. 2012; 318(13):1577-1585.
87. Lee CH, Yu CC, Wang BY and Chang WW. Tumorsphere as an effective in vitro platform for screening anti-cancer stem cell drugs. Oncotarget. 2016; 7(2):1215-1226.
88. Hagemann J, Jacobi C, Hahn M, Schmid V, Welz C, Schwenk-Zieger S, Stauber R, Baumeister P and Becker S. Spheroid-based 3D Cell Cultures Enable Personalized Therapy Testing and Drug Discovery in Head and Neck Cancer. Anticancer research. 2017; 37(5):2201-2210.
89. Nakahata K, Uehara S, Nishikawa S, Kawatsu M, Zenitani M, Oue T and Okuyama H. Aldehyde Dehydrogenase 1 (ALDH1) Is a Potential Marker for Cancer Stem Cells in Embryonal Rhabdomyosarcoma. PloS one. 2015; 10(4):e0125454.
90. Chen C, Wei Y, Hummel M, Hoffmann TK, Gross M, Kaufmann AM and Albers AE. Evidence for epithelial-mesenchymal transition in cancer stem cells of head and neck squamous cell carcinoma. PloS one. 2011; 6(1):e16466.
91. Michaelis L, Menten ML, Johnson KA and Goody RS. The original Michaelis constant: translation of the 1913 Michaelis-Menten paper. Biochemistry. 2011; 50(39):8264-8269.
92. Tomczak JM and Weglarz-Tomczak E. Estimating kinetic constants in the Michaelis-Menten model from one enzymatic assay using Approximate Bayesian Computation. FEBS letters. 2019.
93. Duan JJ, Cai J, Guo YF, Bian XW and Yu SC. ALDH1A3, a metabolic target for cancer diagnosis and therapy. International journal of cancer. 2016; 139(5):965-975.
94. Szot CS, Buchanan CF, Freeman JW and Rylander MN. 3D in vitro bioengineered tumors based on collagen I hydrogels. Biomaterials. 2011; 32(31):7905-7912.
95. Xu X, Chai S, Wang P, Zhang C, Yang Y, Yang Y and Wang K. Aldehyde dehydrogenases and cancer stem cells. Cancer letters. 2015; 369(1):50-57.
96. Rodriguez-Torres M and Allan AL. Aldehyde dehydrogenase as a marker and functional mediator of metastasis in solid tumors. Clinical & experimental metastasis. 2016; 33(1):97-113.
97. Zhao J. Cancer stem cells and chemoresistance: The smartest survives the raid. Pharmacology & therapeutics. 2016; 160:145-158.
98. Jackson BC, Thompson DC, Charkoftaki G and Vasiliou V. Dead enzymes in the aldehyde dehydrogenase gene family: role in drug metabolism and toxicology. Expert opinion on drug metabolism & toxicology. 2015; 11(12):1839-1847.
99. Marcato P, Dean CA, Giacomantonio CA and Lee PW. Aldehyde dehydrogenase: its role as a cancer stem cell marker comes down to the specific isoform. Cell cycle. 2011; 10(9):1378-1384.
100. Cantz T, Key G, Bleidissel M, Gentile L, Han DW, Brenne A and Scholer HR. Absence of OCT4 expression in somatic tumor cell lines. Stem cells. 2008; 26(3):692-697.
101. Black WJ, Stagos D, Marchitti SA, Nebert DW, Tipton KF, Bairoch A and Vasiliou V. Human aldehyde dehydrogenase genes: alternatively spliced transcriptional variants and their suggested nomenclature. Pharmacogenetics and genomics. 2009; 19(11):893-902.

102. Tomita H, Tanaka K, Tanaka T and Hara A. Aldehyde dehydrogenase 1A1 in stem cells and cancer. Oncotarget. 2016; 7(10):11018-11032.
103. Matsumoto A, Arcaroli J, Chen Y, Gasparetto M, Neumeister V, Thompson DC, Singh S, Smith C, Messersmith W and Vasiliou V. Aldehyde dehydrogenase 1B1: a novel immunohistological marker for colorectal cancer. British journal of cancer. 2017; 117(10):1537-1543.
104. Miyo M, Konno M, Colvin H, Nishida N, Koseki J, Kawamoto K, Tsunekuni K, Nishimura J, Hata T, Takemasa I, Mizushima T, Doki Y, Mori M and Ishii H. The importance of mitochondrial folate enzymes in human colorectal cancer. Oncology reports. 2017; 37(1):417-425.
105. Zhou L, Sheng D, Wang D, Ma W, Deng Q, Deng L and Liu S. Identification of cancer-type specific expression patterns for active aldehyde dehydrogenase (ALDH) isoforms in ALDEFLUOR assay. Cell Biol Toxicol. 2019; 35(2):161-177.
106. Chang PM, Chen CH, Yeh CC, Lu HJ, Liu TT, Chen MH, Liu CY, Wu ATH, Yang MH, Tai SK, Mochly-Rosen D and Huang CF. Transcriptome analysis and prognosis of ALDH isoforms in human cancer. Sci Rep. 2018; 8(1):2713.
107. Krupenko NI, Dubard ME, Strickland KC, Moxley KM, Oleinik NV and Krupenko SA. ALDH1L2 is the mitochondrial homolog of 10-formyltetrahydrofolate dehydrogenase. J Biol Chem. 2010; 285(30):23056-23063.
108. Kurth I, Hein L, Mabert K, Peitzsch C, Koi L, Cojoc M, Kunz-Schughart L, Baumann M and Dubrovska A. Cancer stem cell related markers of radioresistance in head and neck squamous cell carcinoma. Oncotarget. 2015; 6(33):34494-34509.
109. Seidensaal K, Nollert A, Feige AH, Muller M, Fleming T, Gunkel N, Zaoui K, Grabe N, Weichert W, Weber KJ, Plinkert P, Simon C and Hess J. Impaired aldehyde dehydrogenase 1 subfamily member 2A-dependent retinoic acid signaling is related with a mesenchymal-like phenotype and an unfavorable prognosis of head and neck squamous cell carcinoma. Molecular cancer. 2015; 14:204.
110. Qian X, Coordes A, Kaufmann AM and Albers AE. Expression of aldehyde dehydrogenase family 1 member A1 and high mobility group box 1 in oropharyngeal squamous cell carcinoma in association with survival time. Oncology letters. 2016; 12(5):3429-3434.
111.Gonzalez VM, Fuertes MA, Alonso C and Perez JM. Is cisplatin-induced cell death always produced by apoptosis? Molecular pharmacology. 2001; 59(4):657-663.
112. Pinto AL and Lippard SJ. Binding of the antitumor drug cis-diamminedichloroplatinum(II) (cisplatin) to DNA. Biochimica et biophysica acta. 1985; 780(3):167-180.
113. Abubaker K, Latifi A, Luwor R, Nazaretian S, Zhu H, Quinn MA, Thompson EW, Findlay JK and Ahmed N. Short-term single treatment of chemotherapy results in the enrichment of ovarian cancer stem cell-like cells leading to an increased tumor burden. Molecular cancer. 2013; 12:24.
114. Latifi A, Abubaker K, Castrechini N, Ward AC, Liongue C, Dobill F, Kumar J, Thompson EW, Quinn MA, Findlay JK and Ahmed N. Cisplatin treatment of primary and metastatic epithelial ovarian carcinomas generates residual cells with mesenchymal stem cell-like profile. Journal of cellular biochemistry. 2011; 112(10):2850-2864.
115. Ikeda K, Terashima M, Kawamura H, Takiyama I, Koeda K, Takagane A, Sato N, Ishida K, Iwaya T, Maesawa C, Yoshinari H and Saito K. Pharmacokinetics of cisplatin in combined cisplatin and 5-fluorouracil therapy: a comparative study of three different schedules of cisplatin administration. Japanese journal of clinical oncology. 1998; 28(3):168-175.
116. Margaret Lois Thomas KMC, Mohammad Sultan, Ahmad Vaghar-Kashani1 and Paola Marcato. Chemoresistance in Cancer Stem Cells and Strategies to Overcome Resistance. Chemotherapy. 2014 3(1).
117. Lapidot T, Sirard C, Vormoor J, Murdoch B, Hoang T, Caceres-Cortes J, Minden M, Paterson B, Caligiuri MA and Dick JE. A cell initiating human acute myeloid leukaemia after transplantation into SCID mice. Nature. 1994;

367(6464):645-648.
118. Naveen SV and Kalaivani K. Cancer stem cells and evolving novel therapies: a paradigm shift. Stem cell investigation. 2018; 5:4.
119. Lo-Coco F, Cicconi L and Breccia M. Current standard treatment of adult acute promyelocytic leukaemia. British journal of haematology. 2016; 172(6):841-854.
120. Forghieri F, Bigliardi S, Quadrelli C, Morselli M, Potenza L, Paolini A, Colaci E, Barozzi P, Zucchini P, Riva G, Vallerini D, Lagreca I, Marasca R, Narni F, Venditti A, Martelli MP, Falini B, Lo Coco F, Amadori S and Luppi M. All-trans retinoic acid (ATRA) in non-promyelocytic acute myeloid leukemia (AML): results of combination of ATRA with low-dose Ara-C in three elderly patients with NPM1-mutated AML unfit for intensive chemotherapy and review of the literature. Clinical case reports. 2016; 4(12):1138-1146.
121. Young MJ, Wu YH, Chiu WT, Weng TY, Huang YF and Chou CY. All-trans retinoic acid downregulates ALDH1-mediated stemness and inhibits tumour formation in ovarian cancer cells. Carcinogenesis. 2015; 36(4):498-507.
122. Nguyen PH, Giraud J, Staedel C, Chambonnier L, Dubus P, Chevret E, Boeuf H, Gauthereau X, Rousseau B, Fevre M, Soubeyran I, Belleannee G, Evrard S, Collet D, Megraud F and Varon C. All-trans retinoic acid targets gastric cancer stem cells and inhibits patient-derived gastric carcinoma tumor growth. Oncogene. 2016; 35(43):5619-5628.
123. Stockhausen MT, Kristoffersen K, Stobbe L and Poulsen HS. Differentiation of glioblastoma multiforme stem-like cells leads to downregulation of EGFR and EGFRvIII and decreased tumorigenic and stem-like cell potential. Cancer biology & therapy. 2014; 15(2):216-224.
124. Ying M, Wang S, Sang Y, Sun P, Lal B, Goodwin CR, Guerrero-Cazares H, Quinones-Hinojosa A, Laterra J and Xia S. Regulation of glioblastoma stem cells by retinoic acid: role for Notch pathway inhibition. Oncogene. 2011; 30(31):3454-3467.
125. Wu W, Schecker J, Wurstle S, Schneider F, Schonfelder M and Schlegel J. Aldehyde dehydrogenase 1A3 (ALDH1A3) is regulated by autophagy in human glioblastoma cells. Cancer letters. 2018; 417:112-123.
126. Koenig U, Amatschek S, Mildner M, Eckhart L and Tschachler E. Aldehyde dehydrogenase 1A3 is transcriptionally activated by all-trans-retinoic acid in human epidermal keratinocytes. Biochemical and biophysical research communications. 2010; 400(2):207-211.
127. Darmochwal-Kolarz D, Gasowska-Giszczak U, Paduch R, Kolarz B, Wilcinski P, Oleszczuk J and Kwasniewska A. Apoptosis of HeLa and CaSki cell lines incubated with All-trans retinoid acid. Folia histochemica et cytobiologica. 2009; 47(4):599-603.
128. Feng D, Cao Z, Li C, Zhang L, Zhou Y, Ma J, Liu R, Zhou H, Zhao W, Wei H and Ling B. Combination of valproic acid and ATRA restores RARbeta2 expression and induces differentiation in cervical cancer through the PI3K/Akt pathway. Current molecular medicine. 2012; 12(3):342-354.
129. Skaga E, Skaga IO, Grieg Z, Sandberg CJ, Langmoen IA and Vik-Mo EO. The efficacy of a coordinated pharmacological blockade in glioblastoma stem cells with nine repurposed drugs using the CUSP9 strategy. Journal of cancer research and clinical oncology. 2019; 145(6):1495-1507.
130. Serafin MB, Bottega A, da Rosa TF, Machado CS, Foletto VS, Coelho SS, da Mota AD and Horner R. Drug Repositioning in Oncology. Am J Ther. 2019.
131. Kast RE, Karpel-Massler G and Halatsch ME. CUSP9* treatment protocol for recurrent glioblastoma: aprepitant, artesunate, auranofin, captopril, celecoxib, disulfiram, itraconazole, ritonavir, sertraline augmenting continuous low dose temozolomide. Oncotarget. 2014; 5(18):8052-8082.
132. Loessner D, Stok KS, Lutolf MP, Hutmacher DW, Clements JA and Rizzi SC. Bioengineered 3D platform to explore cell-ECM interactions and drug resistance of epithelial ovarian cancer cells. Biomaterials. 2010; 31(32):8494-8506.
133. Edmondson R, Broglie JJ, Adcock AF and Yang L. Three-dimensional cell culture systems and their applications

in drug discovery and cell-based biosensors. Assay and drug development technologies. 2014; 12(4):207-218.
134. Riedl A, Schlederer M, Pudelko K, Stadler M, Walter S, Unterleuthner D, Unger C, Kramer N, Hengstschlager M, Kenner L, Pfeiffer D, Krupitza G and Dolznig H. Comparison of cancer cells in 2D vs 3D culture reveals differences in AKT-mTOR-S6K signaling and drug responses. Journal of cell science. 2017; 130(1):203-218.
135. Luca AC, Mersch S, Deenen R, Schmidt S, Messner I, Schafer KL, Baldus SE, Huckenbeck W, Piekorz RP, Knoefel WT, Krieg A and Stoecklein NH. Impact of the 3D microenvironment on phenotype, gene expression, and EGFR inhibition of colorectal cancer cell lines. PloS one. 2013; 8(3):e59689.
136. Thakur A, Huang M and Lum LG. Bispecific antibody based therapeutics: Strengths and challenges. Blood reviews. 2018.
137. Huang H, Ding Y, Sun XS and Nguyen TA. Peptide hydrogelation and cell encapsulation for 3D culture of MCF-7 breast cancer cells. PloS one. 2013; 8(3):e59482.
138. Xu X, Gurski LA, Zhang C, Harrington DA, Farach-Carson MC and Jia X. Recreating the tumor microenvironment in a bilayer, hyaluronic acid hydrogel construct for the growth of prostate cancer spheroids. Biomaterials. 2012; 33(35):9049-9060.
139. Yip D and Cho CH. A multicellular 3D heterospheroid model of liver tumor and stromal cells in collagen gel for anti-cancer drug testing. Biochemical and biophysical research communications. 2013; 433(3):327-332.
140. Hongisto V, Jernstrom S, Fey V, Mpindi JP, Kleivi Sahlberg K, Kallioniemi O and Perala M. High-throughput 3D screening reveals differences in drug sensitivities between culture models of JIMT1 breast cancer cells. PloS one. 2013; 8(10):e77232.

8. Affidavit

“I, [Xu, Jinfeng], certify under penalty of perjury by my own signature that I have submitted the thesis on the topic [Investigation of ALDH^{bright} Cancer Stem (-like) Cell-targeted Treatment by Cisplatin and all-trans Retinoic Acid in Cervical Cancer Cell Lines]. I wrote this thesis independently and without assistance from third parties, I used no other aids than the listed sources and resources.

All points based literally or in spirit on publications or presentations of other authors are, as such, in proper citations (see "uniform requirements for manuscripts (URM)" the ICMJE www.icmje.org) indicated. The sections on methodology (in particular practical work, laboratory requirements, statistical processing) and results (in particular images, graphics and tables) correspond to the URM (s.o) and are answered by me. My interest in any publications to this dissertation correspond to those that are specified in the following joint declaration with the responsible person and supervisor. All publications resulting from this thesis and which I am author correspond to the URM (see above) and I am solely responsible.

The importance of this affidavit and the criminal consequences of a false affidavit (section 156,161 of the Criminal Code) are known to me and I understand the rights and responsibilities stated therein.

Date Signature

9. Curriculum Vitae and Publications

My curriculum vitae is not shown in the electronic version of my thesis for reasons of private data protection.

Publications

1. New Developments in Therapeutic HPV Vaccines. *Jiaying Lin, **Jinfeng Xu**, Andreas E. Albers, Andreas M. Kaufmann*. Current obstetrics and gynecology reports. (2012) 1:106-115

2. MicroRNA-34a regulates epithelial-mesenchymal transition and cancer stem cell phenotype of head and neck squamous cell carcinoma in vitro. *Zhifeng Sun, Weiming Hu, **Jinfeng Xu**, Andreas M. Kaufmann, Andreas E. Albers*. International Journal of Oncology. (2015) 47: 1339-1350

Posters in conference

1. Response of ALDH after ATRA and cisplatin treatment in cervical cancer cell line-derived spheroids. ***Jinfeng Xu**, Fang Guo, Weiming Hu, Andreas M. Kaufmann.* 8th International Charite-Mayo conference. Berlin, April 16th-18th 2015

2. Disulfiram inhibits cell proliferation and synergizes apoptosis induced by cisplatin in cervical cancer cells. ***Jinfeng Xu**, Fang Guo, Andreas E. Albers, Andreas M. Kaufmann.* Poster number 121, HPV 2017 - 31st International Papillomavirus Conference. South Africa, Cape Town, February 28th - March 4th, 2017 (Presented by Dr. Andreas M. Kaufmann)

3. Synergistic cytotoxic effects of disulfiram and cisplatin on human cervical cancer cells. ***Jinfeng Xu**, Kube Tina, Andreas E. Albers, Andreas M. Kaufmann*. 9th International Charite-Mayo conference. May 3rd-6th 2017

4. Response of Aldehyde Dehydrogenase (ALDH) after Cisplatin and All-Trans Retinoic Acid (ATRA) treatment of Spheroid-derived Cells (SDCs) from cervical cancer cell lines. ***Jinfeng Xu**, Jalid Sehouli, Andreas M. Kaufmann.* 62. Kongress der Deutschen Gesellschaft für Gynäkologie und Geburtshilfe – DGGG'18 Berlin, October 7th-10th 2018

10. Acknowledgements

I would like to express my sincere gratitude to my supervisor Dr. Andreas M. Kaufmann, for offering the precious opportunity and providing kindly support from the first day in the lab 'Gynäkologische Tumorimmunologie' at Charité-Universitätsmedizin Berlin, Campus Benjamin Franklin, and for his warm welcome with enthusiasms, continuous guidance with patience, his good care with kind throughout the entire period of study. His advice and support will always be appreciated and remembered lifelong.

I am also grateful to Dana Schiller, Tina Kube, Amrei Krings, Aleksandra Pesic, Sophia Ossmann, Sarah Thies, and Anna Skof for their technical and languish support. I also have very much appreciation to my siblings, Dr Jiaying Lin, Dr Zhifeng Sun, Dr Weiming Hu, Dr Fang Guo, Dr Zhi Yang, Wenhao Yao, Sarina, and Lili Liang for their friendship brings me great power to finish this study.

I own my sincere gratitude to my wife, my parents, and my family for their love, encouragement and support throughout my study in Germany.